

https://dspace.org/

Identification of conditionally essential genes in Mycobacterium tuberculosis DD- carboxypeptidase mutant strains exposed to Augmentin

Jacobs, Olivia

2022
https://hdl.handle.net/10539/34407

Downloaded from a DSpace repository. https://dspace.org/

Identification of conditionally essential genes in *Mycobacterium tuberculosis* DD-carboxypeptidase mutant strains exposed to Augmentin



School of Pathology, Faculty of Health Sciences, University of the Witwatersrand, Johannesburg, South Africa

Name: Olivia Jacobs

Student number: 1347720

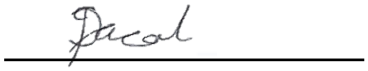
Degree: MSc (Molecular Medicine and Haematology)

Supervisor(s): Dr. Christopher Ealand & Dr Nikki Gentle

Department(s): DST/NRF Centre of Excellence for Biomedical TB Research (CBTBR), University of the Witwatersrand, National Health Laboratory Services (NHLS) & School of Molecular and Cell Biology, Faculty of Science.

Declaration

I, Olivia Jacobs, declare that this Master's dissertation is of my own work. It is being submitted for the degree of Master of Science in Medicine (Molecular Medicine and Haematology) to the University of the Witwatersrand. It has not been submitted for any other degree at this institution or another.



Olivia Jacobs

23 June 2022

Dedication

This dissertation is dedicated to my father,

This is the one degree he had the privilege of watching me start but never finish. I am who I am today because of the man he was.

“I am so proud of you my lucky packet.”

-Ignatius Patrick Jacobs (31st July 1963-1st April 2020)

Presentations arising from this study

Conference: Molecular Biosciences Research Trust (MBRT)

Presentation: GradFlash

Venue and year: Online, 2021.

Abstract

Mycobacterium tuberculosis (*Mtb*) is the causative agent of tuberculosis (TB), one of the most successful human pathogens to date. TB is the top ten leading cause of death worldwide despite the fact that it is curable. This is partially due to the emergence of multi-drug and extensively drug resistant TB. There is thus a need for new drugs and/or targets. The mycobacterial cell wall is a complex structure composed of various inner and outer layers providing a rich environment for potential drug targets. Of particular interest to this study is the peptidoglycan (PG) layer. PG is composed of glycan chains linked to short peptides. The PG layer is essential for cell stability, ensuring rigidity and resistance to internal turgor pressure. PG is consistently remodelled to allow for cell growth and division. One class of proteins involved in the biosynthetic and remodelling processes are penicillin binding proteins (PBPs). PBPs are divided into two categories, namely high molecular weight (HMW) and low molecular weight (LMW). The focus of this study was on LMW PBPs, specifically DD-carboxypeptidases (DD-CPases) which cleave the terminal D-amino acid from stem peptides. There are three identified DD-CPase homologues in *Mtb* (Rv3330 (*dacB1*), Rv2911 (*dacB2*) and Rv3627c). Only Rv3627c is annotated as essential for *in vitro* growth. In *Mycobacterium smegmatis* (*Msmeg*), of the four homologues (MSMEG_1661, MSMEG_2432, MSMEG_2433 and MSMEG_6113 (*dacB*)), only *dacB* is essential. The aim of this project was to determine if LMW PBPs with DD-Cpase activity plays a role in response to antibiotic exposure either via direct peptidoglycan remodelling or as antibiotic sensors to recruit other proteins. Experiments were conducted in two mycobacterial species, namely *Mtb* and *Msmeg*. Mutant strains lacking DD-CPase homologues were assessed for changes in drug susceptibility, morphology, and PG biosynthesis. We observed an increased susceptibility of *Msmeg* mutant strains to RIF, the presence of bulging in *Msmeg* mutant cells when probed with fluorescent vancomycin as well as a shortening of the double mutant strain in *Mtb* relative to wild type. No other major phenotypes were observed suggesting that these proteins may only play minor roles in response to antibiotics, if any. We also sought to identify conditionally essential genes in an *Mtb* DD-Cpase mutant background exposed to Augmentin (β-lactam antibiotic plus β-lactamase inhibitor). We constructed MycoMarT7 transposon mutagenesis libraries in the *Mtb* strains but consistently noted that high mycobacteriophage titres (PFU/ml $>10^{12}$) were associated with low library/genome coverage (maximum of $1x10^4$ CFU/ml). As the project initially aimed to identify conditionally essential genes in *Mtb*, the low coverage was deemed inadequate to proceed further. In order to remedy this and improve library coverage, we sought to identify a

novel mycobacteriophage and identified one from soil, subsequently named øIPJ3107. Phenotypic and genomic analysis of this mycobacteriophage suggested that is part of the *Siphoviridae* family and is classified under sub-cluster A1. Further modifications are required to make this a novel molecular tool for transposon mutagenesis libraries.

Acknowledgements

Firstly, I would like to thank my family. You have all supported, loved, encouraged, and prayed for me through all the years of my education. I am incredibly grateful to you all. This degree would not have been possible without you. To my loving boyfriend, thank you for being my rock and biggest cheerleader. You are simply amazing.

To the friends I have made throughout all my years at the CBTBR, thank you for always offering a helping hand, for taking the time to listen and encourage me. Your support and guidance means a great deal to me. We have shared many laughs and intriguing conversations throughout the years, and I hope our paths may one day cross again.

To my amazing supervisors, Dr Christopher Ealand and Dr Nikki Gentle, thank you for all your help, guidance, support, and dedication this project. You both encouraged and pushed me to always do my best. Working with you both has been a great honour.

To Professor Bavesh Kana, thank you for allowing me the great privilege of being a student in your laboratory. You have always been a helping hand in times of great struggle, and I am incredibly humbled by the opportunities you have provided me with.

Lastly, I would also like to thank the financial contributors, the National Research Foundation (NRF) and the DST/NRF Centre of Excellence for Biomedical Tuberculosis Research, without whom, this project would not have been possible.

Table of Contents

Dedication iii
Presentations arising from this study iv
Abstract v
Acknowledgements vii
List of Figures xi
List of Tables: xii
List of Abbreviations xiii
1. Introduction 1
1.1 Tuberculosis 1
1.2 Infection and disease 2
1.3 Treatment and drug resistance 3
1.4 The Mycobacterial Cell Wall 4
1.5 Mycobacterial growth and division 5
1.6. Peptidoglycan biosynthesis 7
1.7 PG remodeling 7
1.8 Penicillin-Binding Proteins (PBPs) 8
1.8.1 High Molecular Weight Penicillin-Binding Proteins 9
1.8.2 Low Molecular Weight Penicillin-Binding Proteins 10
1.8.2.1 Endopeptidases 10
1.8.2.2 DD-Carboxypeptidases 10
1.9 LD-Transpeptidases 12
1.10 Identification of essential genes in mycobacteria 13
1.10.1 Mycobacteriophages 14
1.10.2 Transposon mutagenesis 15
1.11 Hypothesis 16
1.12 Aim and Objectives 17
1.12.1 Aim 17
1.12.2 Objectives 17
2. Methods and Materials 18
2.1 DNA extraction 18
2.1.1 Small scale genomic DNA extraction 18
2.1.2 Large scale genomic DNA extraction 18
2.2. Visualization of nucleic acids 19
2.3 Confirmation of mutant strains by Polymerase Chain Reaction (PCR) 19
2.4 Generation of *Mycobacterium smegmatis* complementation strains 21
2.4.1 Plasmid DNA purification 21

2.4.2 Confirmation of plasmid DNA (used for complementation) by restriction digest analysis....22
2.4.3 Ethanol precipitation of plasmid DNA....23
2.4.4 Preparation of electro-competent *Mycobacterium smegmatis* cells....23
2.4.5 Transformation of *Mycobacterium smegmatis* cells by electroporation....24
2.4.6 Confirmation of complementation by PCR....24
2.5 Phenotypic characterization of strains....25
2.5.1 Determination of minimum inhibitory concentration (MIC90) of first line and other cell-wall-targeting drugs in wild-type and mutant strains using the micro-broth dilution assay....25
2.5.2 Determination of change in peptidoglycan side wall and polar labelling in mycobacterial strains exposed to Augmentin using FDAA staining....26
2.5.3 Determination of change in peptidoglycan side wall and polar labelling in *Mycobacterial smegmatis* strains using BODIPY Vancomycin staining....28
2.6 Materials and methods of mycobacteriophage work....29
2.6.1 Reagents for mycobacterial experiments....29
2.6.2 Construction of transposon mutagenesis libraries....29
2.7 Identification of novel mycobacterial phage from soil....33
2.7.1 Isolation of mycobacterial phage from soil....33
2.7.2 Mycobacterial phage plaque formation at various temperatures....34
2.7.3 Isolation of novel mycobacterial phage genomic DNA....34
2.7.4 Next generation sequencing analysis....35
3. Results: Characterization of DD-CPases strains in *Msmeg* and *Mtb*....37
3.1 Confirmation of Δ*1661*Δ*2432*Δ*2433* in *Msmeg* by PCR....37
3.2 Confirmation of Δ*dacB1*Δ*dacB2* in *Mtb* by PCR....39
3.3 There is a difference in the MICs of first line drug treatment and cell wall targeting antibiotics between wild type and the triple mutant in *Msmeg*....42
3.4 There is no difference in the MICs of first line drug treatment and cell wall targeting antibiotics between wild type and the double mutant in *Mtb*. 43
3.5 Complementation of the Δ*1661*Δ*2432*Δ*2433* mutant in *Msmeg*....43
3.5.1 Restriction digest analysis of the *1661pmv306H*, *2432pmv306H* and *2433pmv306H* plasmids....44
3.5.2 Confirmation of complemented derivatives by PCR....45
3.6 There was no significant difference in the MIC values for Rifampicin, Vancomycin and Meropenem between wild type, the triple mutant and complement strains in *Msmeg*....47
3.7 There was no significant difference in the PG biosynthesis or cross-linking patterns, as observed by fluorescent vancomycin, between the wild type, triple mutant strains as well as the complement derivative strains in *Msmeg*....48
3.8 There was no difference between the MICs of Augmentin in the wild type and mutant strains in *Msmeg* and *Mtb*....50

3.9 There was no significant difference in the cell length and PG biosynthesis between wild type and the triple mutant in *Msmeg* when exposed to Augmentin....51
3.10 There was a significant difference in the cell length between *H37Rv* and Δ*dacB1*Δ*dacB2* in *Mtb* but no difference in staining pattern was noted....53
3.11 Bulking up of øMycoMarT7 mycobacteriophage stock for maximal viral titre (PFU/ml) and library construction....55
3.12 Transposon mutagenesis library in *Mtb* strains was deemed to have inadequate library/genome coverage....56
3.13 Mycobacterial phage isolation from soil....58
3.14 øIPJ3107 forms larger plaques and is shorter in length and diameter compared to øMycoMarT7....59
3.15 Next generation sequencing analysis....60
3.15.1 The sequence data of øIPJ3107 was of a high quality....60
3.15.2 øIPJ3107 is a novel mycobacterial phage that is classified under subcluster A1....60
4. Discussion....61
5. Conclusion, limitations, and future studies....69
5.1 Conclusion....69
5.2 Limitations of this study....70
5.3 Future studies....70
6. References....72

List of Figures

Figure 1. 1: Global estimated TB incidence in 2020, for countries with at least 100 000 incident cases.. 2
Figure 1. 2: Schematic representation of the mycobacterial cell wall 4
Figure 1. 3: Schematic representation of the two models of mycobacterial cell division and growth. 6
Figure 1. 4: Schematic representation of the composition of the peptidoglycan layer.....7
Figure 1. 5: Schematic representation of the sites of actions of enzymes involved in the remodeling of PG.....8
Figure 1. 6: Schematic diagram illustrating the lytic and lysogenic cycle of bacteriophages. 15
Figure 1. 7: A schematic representation of sites of insertion of a transposon mutagenesis library......16
Figure 2. 1: Schematic representation of genomic maps of wild type and mutant alleles for *Mtb* and *Msmeg*.…… 21
Figure 2. 2: Schematic representation to determine the Minimum Inhibitory Concentration (MIC) of first line and cell wall targeting antibiotics using the micro-broth dilution assay.. .26
Figure 2. 3: A schematic representation of FDAA staining workflow.....28
Figure 2. 4: Schematic representation of mycobacterial phage stock preparation. 31
Figure 2. 5: Schematic representation of transposon mutagenesis using two different methods 33
Figure 2. 6: Schematic representation of the computational workflow used to analyze the genomic sequencing data. 35

Figure 3. 1: Confirmation of DD-Cpase tripe mutant in *Mycobacterium smegmatis*.....38
Figure 3. 2: Confirmation of double mutant in *Mtb* using *dacB1* and *dacB2* primers. 40
Figure 3. 3: Confirmation of DD-Cpase double mutant in *Mycobacterium tuberculosis* 41
Figure 3. 4: Restriction digest analysis of *pmv306H* plasmids.....45
Figure 3. 5:Confirmation of complement strains in *Msmeg* by PCR.....47
Figure 3. 6: BODIPY Vancomycin staining of wild type, triple mutant, and the complement strains in *Msmeg* 50
Figure 3. 7: Cell length and staining pattern of *Msmeg* cells observed under a fluorescent microscope. 52
Figure 3. 8: Cell length and staining pattern of *Mtb* cells observed under a fluorescent microscope 54
Figure 3. 9: High titer øMycoMarT7 phage stock 55
Figure 3. 10: Mycobacterial phage transductions in *Msmeg* 57
Figure 3. 11: Mycobacterial phage isolation from soil.....58
Figure 3. 12: øIPJ3107 plaque formation and TEM analysis in comparison to øMycoMarT7 59

List of Tables:

Table 1. 1: Summary of the characteristics of DD-Carboxypeptidases in *Mycobacterium smegmatis* and *Mycobacterium tuberculosis*. 12
Table 2. 3: PCR primers used for confirmation of strains……...20
Table 2. 4: List of restriction enzymes used in restriction digests, appropriate buffers, and the expected DNA fragment sizes for each plasmid. 23
Table 2. 5: Primers used in confirmation of compliment strains by PCR 25
Table 3. 1: Minimum inhibitory concentration of antibiotics in *Msmeg*.……...42
Table 3. 2: Minimum inhibitory concentration of antibiotics in *Mtb* 43
Table 3. 3: Minimum inhibitory concentration of antibiotics in *Msmeg* derivative strains.....48
Table 3. 4: Minimum inhibitory concentration of Augmentin in *Msmeg*.....51
Table 3. 5: Minimum inhibitory concentration of Augmentin in *Mtb*.....51
Table 3. 6: CFU/ml of transposon mutagenesis libraries in *Mtb* and the methods used.....56
Table 3. 7: Top ten mycobacterial phages that are similar to the hypothetical proteins of øIPJ3107 61

List of Abbreviations

TB	Tuberculosis
Mtb	*Mycobacterium tuberculosis*
WHO	World health organization
UN	United Nations
INH	Isoniazid
PZA	Pyrazinamide
EMB	Ethambutol
RIF	Rifampicin
MDR	Multi-drug resistant
XDR	Extensively drug resistant
PG	Peptidoglycan
CW	Cell wall
AG	Arabinogalactan
MA	Mycolic acids
PBPs	Penicillin binding proteins
NAG	*N*-acetylglucosamine
NAM	*N*-acetylmuramic acid
Rpfs	Resuscitation promoting factors
HMW	High molecular weight
LMW	Low molecular weight
E. coli	*Escherichia coli*
Msmeg	*Mycobacterium smegmatis*
DD-Cpases	DD-carboxypeptidases
Ldts	LD-Transpeptidases
WGS	Whole genome sequencing
DNA	Deoxyribonucleic acid
TraSH	Transposon site hybridization
NGS	Next generation sequencing
PCR	Polymerase Chain Reaction
MIC	Minimum inhibitory concentration

CTAB	Cetyltrimethyl Ammonium Bromide
dH_2O	Distilled water
EDTA	Ethylenediaminetetraacetic acid
Tris	Trisaminomethane
HCl	Hydrochloric acid
NaOH	Sodium hydroxide
TE	Tris-EDTA
TAE	Tris-acetate-EDTA
SDS	Sodium dodecyl sulfate
gDNA	Genomic DNA
NaCl	Sodium chloride
UV	Ultraviolet light
µ	Micro
ß	Beta
rpm	Revolutions per minute
xg	Relative centrifugal force
min	Minutes
sec	Seconds
NEB	New England Biolabs
U	Unit
TEM	Transmission Electron Microscopy
V	Voltage
F	Farads
TY	Yeast extract tryptone
dNTPs	Deoxyribonucleotide triphosphate
hrs	Hours
FDAA	Fluorescent D-amino acid
PBS	Phosphate buffered saline
$MgSO_4$	Magnesium sulfate
$CaCl_2$	Calcium chloride
Tn-seq	Transposon insertion sequencing
PFU/ml	Plaque forming units per milliliter
CFU/ml	Colony forming units per milliliter
OD_{600}	Optical density measured at a wavelength of 600 nm

1. Introduction

1.1 Tuberculosis

Tuberculosis (TB) is one of the most successful human pathogens. According to the latest statistics, it remains one of the top ten causes of death globally (WHO, 2021). TB is caused by *Mycobacterium tuberculosis (Mtb)* and transmission is facilitated via aerosols spread through the air when an infected person coughs or sneezes. The World Health Organization (WHO) estimates that one fourth of the global population is infected with latent TB (Sotgiu, *et al*., 2019), which is characterized by a lack of clinical symptoms (Cohen, *et al*., 2019). The United Nations' (UN) Sustainable Development Goals and the WHO's End TB Strategy aimed to reduce the number of annual TB deaths by 35% and incidence by 20% by 2020. However, in 2017 there was only a 1.8% and 3.9% reduction in deaths and incidence rate, respectively (MacNeil, *et al*., 2019). Moreover, this goal was not reached at the end of 2020, as globally, an estimated 9.9 million people were infected with active TB, with most of these infections occurring in Africa, Southeast Asia, and Western Pacific (Figure 1.1) (WHO, 2021). Coincidentally, there was a decrease in the number of TB infections in 2020 compared to previous years; this was largely due to the COVID-19 pandemic, which disrupted diagnosis and treatment TB services (WHO, 2021). South Africa accounts for approximately 3.3% of TB infections globally (Figure 1.1) (WHO, 2021). Of these, nearly 50% are co-infected with HIV-1. HIV-1 infection increases the TB burden in countries by increasing the risk for active disease and reactivation of latent TB (Onyebujoh, *et al*., 2005). People who are co-infected are also more likely to die as a result of TB. The high co-infection rate along with the emergence of multi-drug and extensively drug resistant TB poses a significant health threat and necessitates the identification of novel drug targets.

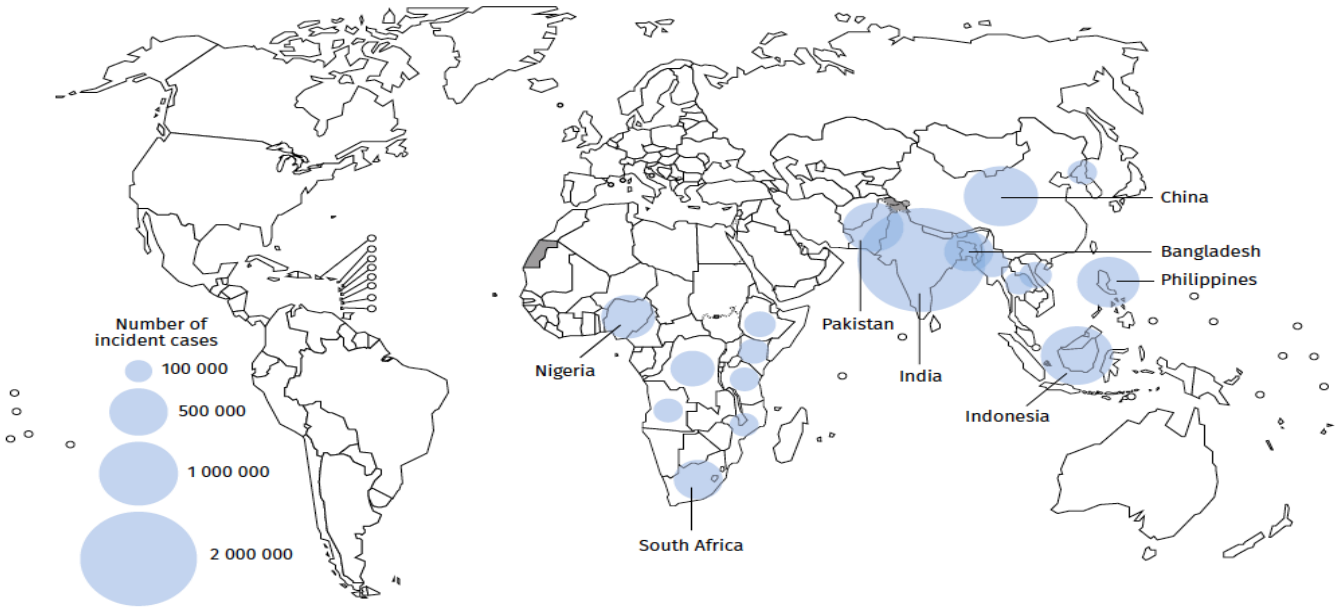


Figure 1. 1: Global estimated TB incidence in 2020, for countries with at least 100 000 incident cases. TB incidences are predominantly reported in Africa, Southeast Asia, and Western Pacific (figure reproduced from Global Tuberculosis Report 2021 (WHO, 2021).

1.2 Infection and disease

Robert Koch identified *Mtb* as the causative agent of TB almost 130 years ago (Philips & Ernst, 2012). Since then, numerous advances have been made in understanding the disease etiology. *Mtb* enters the alveolar passages of exposed individuals as respiratory droplets and encounters alveolar macrophages (Smith, 2003). It is speculated that other phagocytic cells such as neutrophils and dendritic cells engulf mycobacteria as well but there is little evidence to support this (Philips & Ernst, 2012). Instead, the primary focus has been on the macrophage-*Mtb* interaction. Macrophages phagocytize bacteria via contact with C-type lectin receptors, scavenger receptors and complement receptors (Philips & Ernst, 2012; Smith, 2003). Upon entry, bacteria (including *Mtb*) are housed in an endocytic vacuole known as the phagosome. During the course of infection, the phagosome fuses with the lysosome, producing an acidic environment that contains reactive oxygen intermediates, lysosomal enzymes, and toxic peptides, which are all aimed at killing the bacteria (Smith, 2003). However, *Mtb* is able to mediate this response and avoid the phagosome-lysozyme fusion (McDonough, *et al*., 1993). The exact mechanism of lysozyme evasion is poorly understood.

The infected macrophages produce chemokines that attract inactivated monocytes, lymphocytes, and neutrophils (Smith, 2003). Granuloma lesions, composed of macrophages

and lymphocytes, begin to form in the lungs (Philips & Ernst, 2012). These granulomas then attempt to contain the spread of infection. As cellular immunity develops, the infected macrophages are successfully killed, resulting in a caseous center in the granulomas (Smith, 2003). The caseous center is surrounded by fibroblasts and lymphocytes. *Mtb* is unable to replicate during this stage but can remain dormant for years (Smith, 2003). The status of the host's immune system will dictate whether the infected person will develop active or latent TB. In active TB, the immune system is weakened (this weakening could be the result of HIV-1 infection, immunosuppressive drugs, malnutrition, or other factors), which results in the granuloma becoming liquefied and serving as a rich nutrient source in which the bacteria can replicate rapidly, possibly spreading to other areas outside of the lungs (known as extrapulmonary TB) (Smith, 2003). A person with active TB is infectious and will require antibiotic intervention to treat the disease.

1.3 Treatment and drug resistance

The treatment for active drug susceptible TB is a six-month course of chemotherapy consisting of a combination of Isoniazid (INH), Pyrazinamide (PZA), Ethambutol (EMB) and Rifampicin (RIF) (Zhang, *et al.*, 2013). During the initial two months (intensive treatment phase), all four antibiotics are administered, but thereafter only RIF and INH are given for the remaining duration of treatment (continuation phase) (Onyebujoh, *et al*., 2005). PZA specifically targets the population of *Mtb* persisters (a population of *Mtb* cells that resist initial stages of treatment) that are not targeted by other drugs by inhibiting energy production, translation, and coenzyme A (Zhang, *et al*., 2013; Mitchison, 1985). INH is highly active against replicating bacilli and ethambutol increases the activity of anti-TB drugs by increasing the permeability of the mycobacterial cell wall (i.e., by inhibiting the transfer of arabinogalactan into the cell wall) (Onyebujoh, *et al*., 2005; Sreevatsan, *et al*., 1997). RIF inhibits transcription by targeting and binding to RNA polymerase (Somoskovi, *et al*., 2001). Although chemotherapy has proven to be an effective treatment, poor patient adherence and the occurrence of adverse side effects can be limiting (Onyebujoh, *et al*., 2005).

In South Africa, 67 044 cases of people infected have drug resistant TB (WHO, 2021). Multi-drug resistant (MDR) TB is characterized by resistance to first line drug treatment, namely INH and RIF (Caminero, et al., 2010). Extensively drug resistant (XDR) TB occurs when the strain is resistant to INH, RIF, any fluoroquinolone and at least one of the anti-tuberculosis injectable drugs (Caminero, *et al*., 2010). Resistance may also develop under conditions of

poor compliance with drug treatment (Caminero, *et al*., 2010). Fluoroquinolones (ciprofloxacin, ofloxacin, levofloxacin and moxifloxacin) as well as injectable anti-tuberculosis drugs (streptomycin, kanamycin, amikacin, capreomycin and viomycin) are used to treat MDR and XDR TB (Caminero, *et al*., 2010). These high rates of resistance led to a need for new drug development and a subsequent search for new drug targets. A rich source of novel drug targets is the peptidoglycan (PG) layer, a component of the cell wall.

1.4 The Mycobacterial Cell Wall

The mycobacterial cell wall (CW) is a complex structure, composed of an inner and outer layer, which surrounds the plasma membrane (Hett & Rubin, 2008). Due to this complexity, the CW is impermeable to a number of compounds and inherently resistant to various antibiotics. This aids in the success of *Mtb* in the host environment (Griffin, *et al*., 2011). The outer layer consists of proteins and lipids, which are thought to be effector molecules essential for cell signaling (Hett & Rubin, 2008). The inner layer surrounds the plasma membrane and consists of a layer of PG, arabinogalactan (AG) and mycolic acids (MA) (Figure 1.2). PG is a rigid layer that maintains cell shape but is versatile, in that it allows for bacterial growth and division (Hett & Rubin, 2008). AG is essential for maintaining cell wall integrity and serves as an anchor for the MA layer, which is the primary determinant of cell permeability. The outer layer attaches to the MA layer. (Hett & Rubin, 2008).

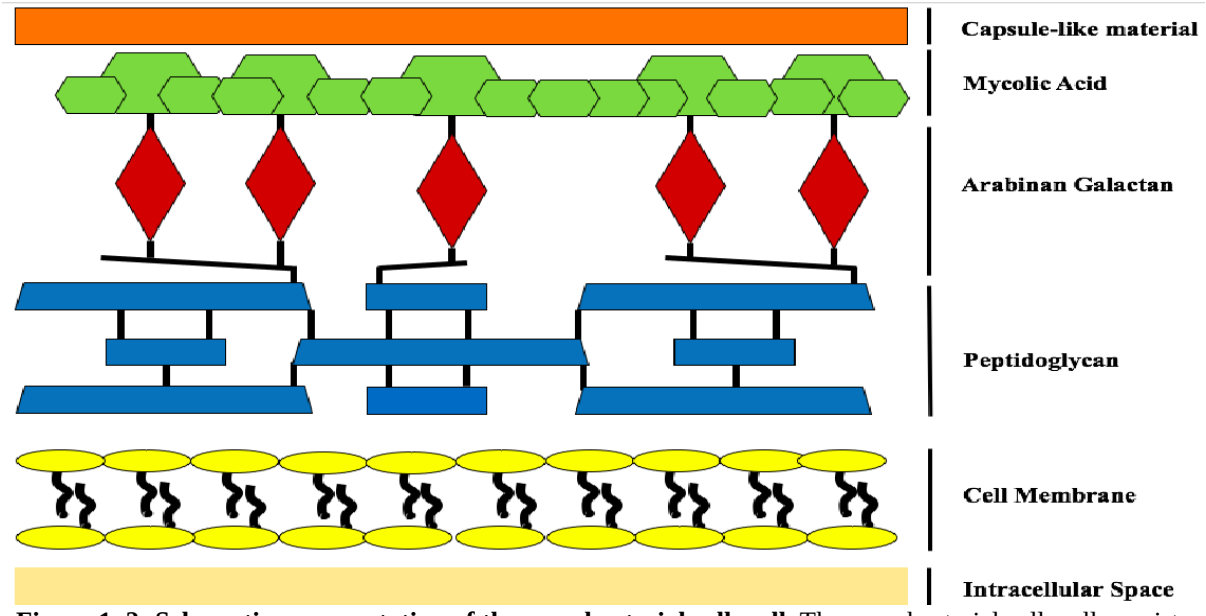


Figure 1. 2: Schematic representation of the mycobacterial cell wall. The mycobacterial cell wall consists of an inner layer that is composed of mycolic acids, arabinogalactan and peptidoglycan surrounding the cell membrane and intracellular space. The inner layer is surrounded by a capsule-like material known as the outer layer (figure adapted from Hett & Rubin (2008)).

The mycobacterial cell wall is a rich source of drug targets (Hett & Rubin, 2008). Many anti-tuberculosis drugs that are being developed or are in current clinical use target the cell wall, e.g., EMB. A widely used class of antibiotics to treat gram positive bacteria is the ß-lactams (Hugonnet & Blanchard, 2007, Waxman, 1983, Faikong, *et al*., 2009). ß-lactams inhibit bacterial DD-transpeptidases, which catalyze PG cross linking (Hugonnet & Blanchard, 2007). ß-lactam antibiotics are ineffective against mycobacteria because the bacteria are inherently resistant; this is due to the presence of ß-lactamases. (Chambers, *et al*., 1995). ß-lactamases have a similar shape to and share conserved active site residues with the DD-transpeptidase domains of penicillin-binding proteins (PBPs). Some PBPs also have ß-lactamases activity (Hugonnet & Blanchard, 2007). It is therefore thought that ß-lactamases have evolved from PBPs (Hugonnet & Blanchard, 2007). ß-lactamases are inhibited by chemical compounds such as clavulanate, which reacts with BlaC to produce a hydrolytically stable, inactive form of the enzyme (Hugonnet & Blanchard, 2007). These inhibitors, in combination with ß-lactam antibiotics, have shown robust bactericidal effects against *Mtb in vivo*, making the PG layer of the cell wall an attractive site for development of new anti-TB drugs (Chambers, *et a*l., 1995). In order to develop new drugs, an in-depth understanding of PG biosynthesis and remodeling is crucial.

1.5 Mycobacterial growth and division

Bacterial growth and division are essential processes for life and contribute to morphological diversity (Joyce, *et al*., 2012). An essential component to bacterial growth and shape is PG synthesis, which is controlled by site-specific insertion. In general, bacterial proliferation can be divided into two stages: elongation and division. In model bacterial organisms, such as *Escherichia coli* and *Bacillus subtilis*, PG is synthesized and incorporated along the length of the cell, and is regulated by MreB proteins (Joyce, *et al*., 2012). MreB proteins form mobile fragmented elongation complexes that insert new PG. Mycobacteria differ from other bacterial species in that they do not have a homologue of MreB and instead grow by incorporating PG at the poles (Joyce, *et al*., 2012, Odermatt, et al., 2020, Hett & Rubin, 2008). The lack of coordinated elongation means that mycobacteria are unable to divide into two daughter cells that are symmetrical. Instead, mycobacteria divide asymmetrically (Kieser & Rubin, 2014). All rod-shaped bacteria contain two poles: one that is inherited from the mother cell and a new pole that is synthesized during division. There are currently two models to explain the asymmetrical growth and division of mycobacteria (Kieser & Rubin, 2014). In the first model, cell poles are thought to grow symmetrically until cytokinesis, where the inherited pole will

grow at a faster rate until separation, resulting in two unequally sized daughter cells (Figure 1.3A). The second model suggests that the old pole elongates at a faster rate throughout cell growth, as seen in Figure 1.3B (Aldridge, *et al.*, 2012). It is clear from both models that asymmetrical division produces heterogeneous daughter cells that have different growth rates that could potentially have survival advantages in the host environment and/or be a possible cause of latency.

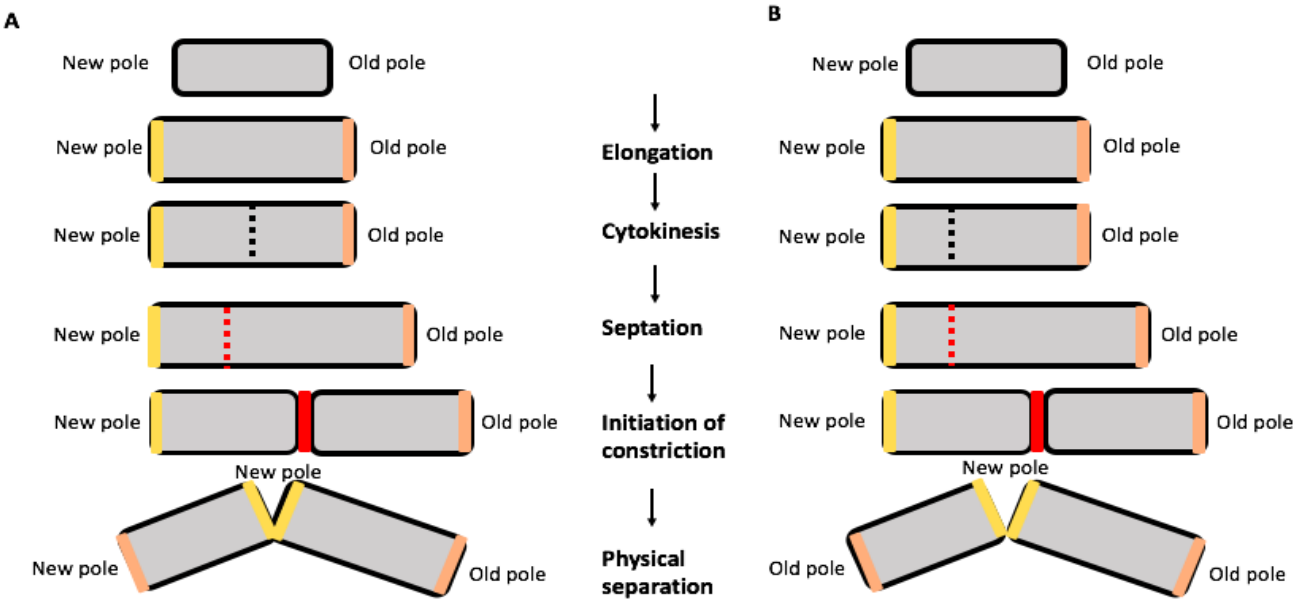


Figure 1. 3: Schematic representation of the two models of mycobacterial cell division and growth. (A) In the first model, the poles grow symmetrically until cytokinesis, where it is believed that the old pole (orange) will grow at a faster rate until separation. (B) In the second model, it is thought that the old pole will grow at a faster rate than the new pole (yellow) throughout cell growth (figure adapted from Kieser & Rubin (2014)).

Mycobacterial cell division is initiated with the assembly of the divisome in the middle of the cell (Hett & Rubin, 2008). This complex of proteins generates a septum that will divide the cell into two daughter cells following separation. These proteins include cytoskeletal-like proteins, structural factors, and PG synthases and hydrolases that coordinate synthesis and splitting of the septum (Kieser & Rubin, 2014). FtsZ is the first of the complex of proteins to assemble in the middle of the cell (Hett & Rubin, 2008). It forms a ring under the plasma membrane known as the Z-ring. The localization of FtsZ initiates septal formation (Hett & Rubin, 2008). This process is controlled by DivIVA (Joyce, *et al*., 2012, Meniche, *et al*., 2014). Eventually the PG will be hydrolyzed allowing the two daughter cells to separate. When the daughter cells begin to separate, mycobacteria exhibit a v-snapping phenotype, a possible result of asymmetrical elongation (Kieser & Rubin, 2014).

1.6. Peptidoglycan biosynthesis

The peptidoglycan layer (PG) is composed of glycan chains, *N*-acetylglucosamine (NAG) and *N*-acetylmuramic acid (NAM), crosslinked by short peptides (Siegrist, *et al*., 2013; Murphy, *et al*., 2019; Figure 1.4). Synthesis is initiated when a UDP is linked to an NAG, forming the UDP-NAG complex (Hett & Rubin, 2008). MurA adds aenoyl pyruvate to the 3' position of NAG, initiating MurB to reduce the UDP-NAG complex into UDP-NAM. A pentapeptide consisting of L-alanine, D-glutamine, DAP, and D-alanyl-D-alanine (in that order) is added to the reduced UDP-NAM complex (Hett & Rubin, 2008). MurX transfers UDP-NAM pentapeptide to decaprenyl phosphate to generate a functional Lipid I protein. Lipid I Is linked to NAG by MurG synthesizing Lipid II (Hett & Rubin, 2008). Lipid II will be transported across the plasma membrane possibly by a flipping mechanism. Transglycolase proteins are linked to the Lipid II, the PG monomer and to the existing PG strands. Transpeptidase proteins create between DAP molecules or between DAP and D-alanine of the existing PG (Crick, *et al*., 2001; Hett & Rubin, 2008). The processes of transglycosylation and transpeptidation are mediated by PBPs (Hett & Rubin, 2008; Sauvage, *et al*., 2008).

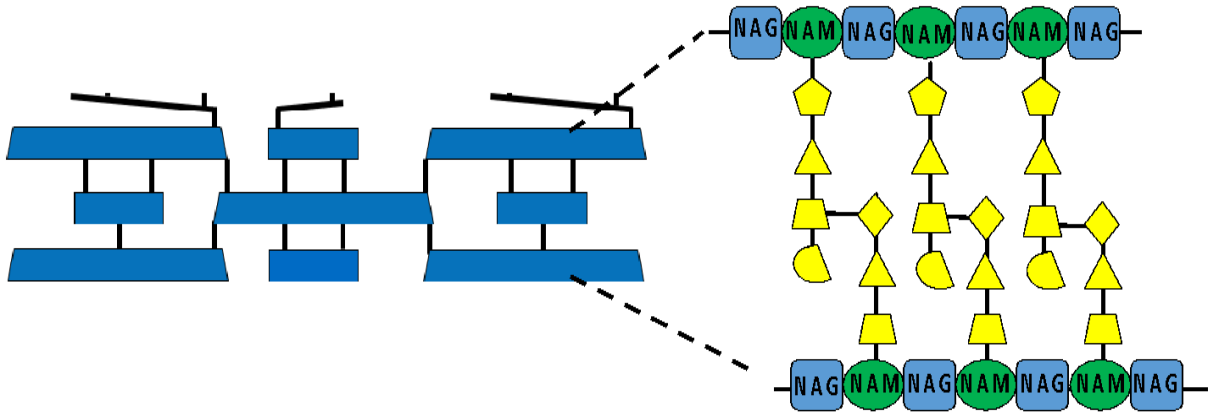


Figure 1. 4: Schematic representation of the composition of the peptidoglycan layer. The PG layer consists of alternating chains of N-acetylglucosamine (NAG) and N-acetylmuramic acid (NAG) residues. A pentapeptide is attached to NAM and crosslinks will be generated by the action of PBPs to connect adjacent glycan strands (figure adapted from Botella, *et al*. (2017)).

1.7 PG remodeling

The PG layer in mycobacteria is constantly evolving and changing (Machowski, *et al*., 2014) to accommodate the insertion of new PG subunits as the bacterium grows and undergoes cell division. PG remodeling is mediated via the actions of PG hydrolyses, (Egan, *et al*., 2020; Figure 1.5). The catalytic activity of these proteins is carefully regulated at multiple levels to ensure that PG growth is synchronized with the cell cycle and the growth rate of the cell. The

remodeling proteins belong to five classes, namely lytic transglycosylases, penicillin-binding proteins, endopeptidases, LD-transpeptidases and amidases (Raghavendra, *et al*., 2018). Resuscitation promoting factors (Rpfs) and endopeptidases belong to the class of lytic transglycosylases. *Mtb* encodes five Rpfs, namely *rpfA-rpfE*, which have been shown to play a role in the reactivation of disease in individuals that are latently infected with TB (Machowski, *et al*., 2014). All the Rpfs are dispensable for growth but are needed to establish and re-activate TB infection. Rpfs act together with endopeptidases to hydrolyze PG (Egan, *et al*., 2020). *N*-acetylyglucosaminidases such as *N*-acetyl-β-d-glucosaminidases and *N*-acetyl-β-d-muramidases cleave the bonds between NAM and NAG residues, while *N*-acetylmuramyl-l-Ala amidases cleave the bond between the MurNAc and L-Ala of the stem peptide (Maitra, *et al*., 2019).

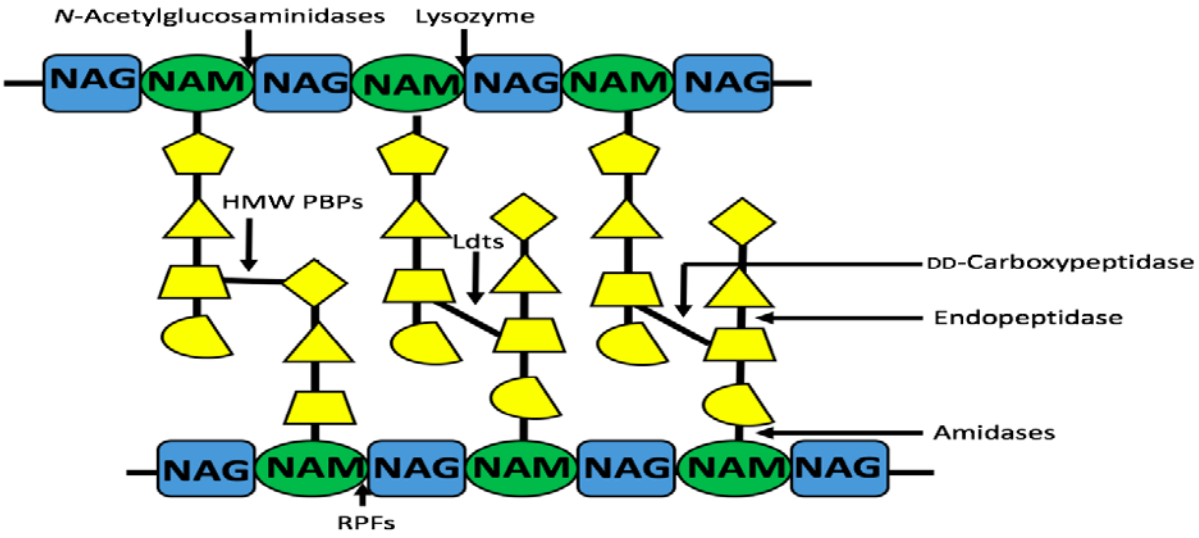


Figure 1. 5: Schematic representation of the sites of actions of enzymes involved in the remodeling of PG. The sites of action are indicated by the black arrows. The pentapepetide chain is indicated by the yellow shapes and the black lines between the shapes are representative of the various crosslinks formed between the proteins (figure adapted from Botella, *et al*. (2017)).

1.8 Penicillin-Binding Proteins (PBPs)

PBPs are membrane-bound enzymes involved in the remodeling and biosynthesis of PG to allow for bacterial cell growth and division (Chambers, *et al*., 1995; Nelson & Young, 2000). PBPs incorporate newly synthesized PG into the existing layer via two chemical reactions, namely transglycosylation (polymerization of the glycan strand) and transpeptidation (cross linking between glycan chains) (Nelson & Young, 2000; Sauvage, *et al*., 2008). The transpeptidase domain of PBPs is the binding site of penicillin, while the transglycosylase

domain is insensitive to currently available antibiotics (Hett & Rubin, 2008). PBPs are classified according to their molecular weight, i.e., high molecular weight (HMW) or low molecular weight (LMW). The latter can further be broken down into Class A, Class B or Class C (Machowski, *et al*., 2014). Class A PBPs are typically bifunctional enzymes containing both transglycosylation and transpeptidation activity. Class B enzymes only possess transpeptidation activity and class C are either endopeptidases or carboxypeptidases (Sharifzadeh, *et al*., 2020).

1.8.1 High Molecular Weight Penicillin-Binding Proteins

High Molecular Weight (HMW) PBPs are responsible for PG polymerization and incorporation into the existing PG layer (Sauvage, *et al*., 2008; Figure 1.5). The structure of these enzymes consists of a cytoplasmic tail, a transmembrane anchor and two linked domains (Sauvage, *et al*., 2008). These domains confer bi-functionality to HMW PBPs, in which the N-terminal domain and C-terminal domain have transglycosylase and transpeptidase activity, respectively (Popham & Setlow, 1996). Some HMW PBPs have been found to be essential for bacterial survival (Patru & Pavelka, 2010). In *Escherichia coli* (*E. coli*) the HMW PBPs are PBP1a, PBP1b, PBP1c, PBP2 and PBP3, which are integral for cell viability (Ghosh, *et al*., 2008). *Bacillus subtilis*, a spore generating gram positive bacterium, encodes three HMW PBPs, PBP1, 2c and 4 (Popham & Setlow, 1996). Following single deletion of PBPs 2c or 4, no cell division phenotype was observed. In contrast, morphological defects including increased cell length, the appearance of kinks and a decline in the growth rate in normal (2XSG), rich (2XYT) and minimal media (Spizizen) were observed when PBP1 was deleted from the genome (Popham & Setlow, 1996). Moreover, these phenotypes were exacerbated when coupled with the simultaneous loss of PBPs 2c and 4 (Popham & Setlow, 1996).

Two HMW PBP homologues have been identified in the genome of *Mtb*, namely Rv005 (PonA1) and Rv3682 (PonA2). These enzymes generate 4-3 crosslinks in the PG component of the CW (Kieser, *et al*., 2015). *Mycobacterium smegmatis* (*Msmeg*), a homologue of Mtb, encodes three HMW PBPs, namely PonA1, PonA2, PonA3 (Patru & Pavelka, 2010). In *Msmeg*, PonA1 is required for growth in minimal media, while in *Mtb*, it is only essential during hypoxia (Kieser, *et al*., 2015). In both *Mtb* and *Msmeg*, PonA2 is dispensable, but mutant strains lacking the gene were associated with an increased susceptibility to ß-lactam antibiotics (Kieser, *et al*.,2015; Patru & Pavelka, 2010).

1.8.2 Low Molecular Weight Penicillin-Binding Proteins

1.8.2.1 Endopeptidases

Endopeptidases cleave the amide bond between two amino acids in the peptide chain, typically allowing for the incorporation of newly synthesized PG and cell separation during division (Frirdich and Gaynor, 2013; Figure 1.5). Two endopeptidases are characterized in *E. coli* namely, PBP4 (*dacB*) and PBP7 (Ghosh, *et al*., 2008; Romeis & Holtje, 1994; Meberg, *et al*., 2004). PBP4 was thought to have dual endopeptidase and DD-carboxypeptidase activity, but this has since been disputed (Ghosh, *et al*., 2008). PBP4 is dispensable for growth and its overexpression is not lethal. However, in combination with PBP5 its deletion results in morphological defects such as altered diameters, contours, and topological features (Ghosh, *et al*., 2008, Neslon & Young, 2000). PBP7 has not been extensively characterized but it is known that like PBP4, it is not essential for *in vitro* growth and is a known target for ß-lactam antibiotics. This was determined by the binding of Benzyl[^{14}C] penicillin to *E. coli* membranes (Henderson, *et al*., 1995; Tuomanen & Schwartz, 1987; Spratt, 1977). In *Vibrio cholera,* two of the three endopeptidases encoded in the genome (*ShyA* and *ShyC*) are essential for bacterial growth and division, while the third (*ShyB*) is not expressed under standard laboratory conditions (LB media) but rather under zinc starvation (Murphy, *et al*., 2019). A transposon screen to investigate the activity of *ShyB* revealed that it is induced as part of a Zur-mediated zinc starvation response that has not been reported for any other bacterial PBPs.

The genome of *Mtb* encodes four endopeptidases, namely Rv1477 (*ripA*), Rv1478 (*ripB*), Rv2190c (*ripC*), and Rv1566c (*ripD*) (Cole, *et al*., 393). RipA interacts with RpfB, which stimulates the growth of dormant *Mtb* during infection (Martinelli & Pavelka, 2016; Hett, *et al*., 2007). RipA and RipB are essential for growth in *Mtb* (Frirdich & Gaynor, 2013). *Msmeg*, encodes five endopeptidases, namely MSMEG_3145 (*ripA*), MSMEG_3146 (*ripB*), MSMEG_4256 (*ripC*), MSMEG_3477 (*ripD*) and MSMEG_1686 (*Rv0024*) (Martinelli & Pavelka, 2016). Unlike the genetic homologues in *Mtb*, *ripA* and *ripB* are non-essential in *Msmeg* (Martinelli & Pavelka, 2016).

1.8.2.2 DD-Carboxypeptidases

DD-Carboxypeptidases (DD-Cpases) cleave the terminal D-amino acid from stem peptides (Hett & Rubin, 2008; Ghosh *et. al*, 2008; Figure 1.5). This allows for PG remodeling by altering the type of crosslinking that can occur between glycan chains (Neslon & Young, 2000). PBPs with transpeptidase activity will typically generate 4-3 crosslinks, while LD-transpeptidases will

create 3-3 crosslinks, which are more abundant in mycobacteria. In *E. coli*, there are three characterized DD-Cpases, namely, PBP5 (*dacA*), PBP6 (*dacC*) and DacD (*dacD*) (Neslon & Young, 2000). The LMW PBPs of *E. coli* have overlapping functions and none are essential for growth. Of these, PBP5 is the most well characterized homologue (Neslon & Young, 2000). Deletion of PBP5, in combination with multiple other PBP deletions, can cause alteration; in cellular morphology, such as the appearance of branching and kinks (Neslon & Young, 2000; Mallick, *et al*., 2019).

In *Bacillus subtilis,* six LMW PBPs have been identified in the genome (Sharifzadeh, *et al*., 2020). These PBPs are involved in cell wall growth and division, as well as synthesis of the spore PG (Sharifzadeh, *et al*., 2020). There is little known about the individual functions of these PBPs (Sharifzadeh, *et al*., 2020). Of the six LMW PBPs, four are characterized DD-Cpases, namely PBP4a (*dacC*), PBP5 (*dacA*), PBP5* (*dacB*) and DacF (Ghosh, *et al*., 2008). PBP4a is not essential for growth, but similar to *E. coli* PBP5, over-expression is toxic (Pedersen, *et al*., 1998). PBP5 is expressed in the mid-log phase of growth and plays a role in the maturation of PG (newly inserted PG has a different muropeptide composition in comparison to old PG and the layer is thought to age or mature before the two materials become indistinguishable) (Ghosh, *et al*., 2008; Vollmer, *et al*., 2008). PBP5* is involved in endospore formation while DacF is thought to be involved in PG modification during sporulation (Ghosh, *et al*., 2008).

In *Msmeg*, four DD-Cpases have been identified, namely MSMEG_1661, MSMEG_2432, MSMEG_244 and MSMEG_6113 (*dacB*). Of the four, MSMEG_6113 (*dacB*) has been shown to be essential for growth (Ealand *et al*., 2019). In addition to DD-carboxypeptidase activity, MSMEG_2432 has *ß*-lactamase activity (Pandey, *et al*., 2020). The genome of *Mtb* encodes three DD-carboxypeptidases, namely Rv3330 (*dacB1*), Rv2911 (*dacB2*) and Rv3627c. Rv3627c is the only gene annotated as essential for growth *in vitro* (Bourai, *et al*., 2012; Machowski, *et al*., 2014). Overexpression of *dacB2* in *Msmeg* resulted in several growth phenotypes: a decreased growth rate, altered colony formation, and abnormal sliding motility and biofilm formation (Bourai, *et al*., 2012). A summary of the characteristics of DD-Cpases in *Msmeg* and *Mtb* is provided in Table 1.1.

Table 1. 1: **Summary of the characteristics of DD-Carboxypeptidases in *Mycobacterium smegmatis* and *Mycobacterium tuberculosis*.**

DD-Carboxypeptidases	Characteristics
Mycobacterium smegmatis	
MSMEG_1661	Non-essential for growth.
MSMEG_2432	Non-essential for growth. ß-lactamase activity.
MSMEG_2433	Non-essential for growth.
MSMEG_6113 (*dacB*)	Essential for growth.
Mycobacterium tuberculosis	
Rv3330 (*dacB1*)	Non-essential for growth. Increased expression in response to Augmentin.
Rv2911 (*dacB2*)	Non-essential for growth Overexpression in *Msmeg* results in altered colony formation, decreased growth rate, abnormal sliding motility and biofilm formation. Decreased expression in response to Augmentin.
Rv3627c	Essential for growth. Increased expression in response to Augmentin.

A microarray analysis of the transcriptome of *Mtb* cells exposed to Augmentin (amoxicillin and clavulanate) suggested that a cytoplasmic redox potential and intracellular redox sensor, WhiB4, played an essential role in antibiotic resistance. Redox potential was specifically linked to β-lactamase resistance via the differential expression of various genes involved in cell-envelope associated pathways – including all three DD-CPase homologues (Mishra, *et al*., 2017). Our previous findings, together with the current literature, suggest that non-essential LMW PBPs may therefore have auxiliary roles, particularly under specific environmental stress conditions.

1.9 LD-Transpeptidases

LD-Transpeptidases (Ldts) form 3-3 crosslinks in the PG layer of mycobacteria (Machowski, *et al*., 2014; Figure 1.5). These 3-3 crosslinks replace the 4-3 crosslink generated by HMW PBPs as maturation occurs and are approximately 60% more abundant than 4-3 crosslinks in mycobacteria (Garcia-Heredia, *et al*., 2018; Machowski, *et al*., 2014). In contrast, the PG of *E. coli* and *Bacillus subtilis* is made up predominantly of 4-3 crosslinks (Gupta, *et al*., 2010). Ldts are therefore thought to play a role in the resistance of mycobacteria to ß-lactam antibiotics - 4-3 crosslinks are targeted by ß-lactam antibiotics (Gupta, *et al*., 2010; Schoomaker, *et al*., 2014). *Mtb* encodes five Ldts, namely Ldt_{Mt1} (Rv0116c), Ldt_{Mt2} (Rv2518c), Ldt_{Mt3} (Rv1433), Ldt_{Mt4} (Rv0192) and Ldt_{Mt5} (Rv0483) (Basta, *et al*., 2015). All five-share sequence homology

(Basta, *et al*., 2015). The reason for this redundancy is unclear. Ldt_{Mt2} is the dominant Ldt as it is highly expressed during growth in comparison to other Ldts (Gupta, *et al*., 2010). Loss of Ldt_{Mt2} results in altered cell size, growth, and virulence, as well as the loss of ability to express LMW PBPs and an increased susceptibility to amoxicillin (Gupta, *et al*., 2010). In a recent study conducted by Basta *et al.* (2015), it was reported that, although structurally similar to Ldt_{Mt2}, Ldt_{Mt5} has a distinctly different active site. Ldt_{Mt5} is thought to have a role in PG metabolism and is perhaps interacting with other cell wall proteins (Basta, *et al*., 2015. When Ldt_{Mt5} is deleted from the genome of *Mtb,* there is an associated decrease in bacterial growth rate and an increase in the permeability of the mycobacteria to crystal violet, osmotic shock and susceptibility to select carbapenem antibiotics (Basta, *et al*., 2015). Many of the PBPs discussed are not essential for growth, however, may have an auxiliary role that could potentially become essential under specific stress conditions. It is, therefore, important to identify conditionally essential genes.

1.10 Identification of essential genes in mycobacteria

Whole genome sequencing (WGS) has revolutionized genetics in the last twenty years, allowing for a greater understanding of the complex interplay between genes (Griffin, *et al*., 2011). Despite this, a large proportion (~ 40%) of the genes in *Mtb* have no known function (Sassetti, *et al*., 2001). Determining the essentiality of these genes may aid in developing an understanding of their physiological roles in the *Mtb* genome and could potentially lead to the identification of novel drug targets (Sassetti, *et al*., 2001). Essential genes are defined as genes that are required for bacterial growth and division. The identification of essential genes in *Mtb* is complex (Sassetti, *et al*., 2001). During the course of infection, the bacterium must be able to adapt to various host microenvironments, therefore the essentiality of genes could change depending on the environmental stress faced by the organism. The genes that undergo these changes in essentiality are known as conditionally essential genes. Previously, controlled gene expression systems have been used to determine the essentiality of genes in bacteria (Ji, *et al*., 2001). This allows for the expression of selected genes to be increased or decreased. This has been successfully applied to *E. coli* and *Bacillus subtilis* (Guzman, *et al*., 1995; Geissendorfer & Hillen, 1990). In *Staphylococcus aureus,* conditionally lethal phenotypes were identified using antisense technology in a regulated gene expression system (Ji, *et al*., 2001). Essential genes were identified in *Haemophillus influenza* by the use of a plasmid containing mariner transposon genes (Akerley, *et al*., 2002) Sites of insertion were then identified using a polymerase chain reaction mapping approach. One type of a genome-wide approach to identify

essential genes in mycobacteria is the use of mycobacterial phages to generate transposon mutagenesis libraries (Sassetti & Rubin, 2003; Sassetti, *et al*., 2001).

1.10.1 Mycobacteriophages

Mycobacterial phages are viruses that only infect mycobacteria. Infection can result in two different types of replication cycles, namely lytic and lysogenic (Maurice, *et al*., 2013). Bacteriophages attach to the cell wall of the host organism and release enzymes that degrade the CW to allow for the entry of viral deoxyribonucleic acid (DNA) and virion associated proteins (Wilson, *et al*., 2009). The viral DNA then translocases to the nucleus and initiates transcription using host cell replication machinery. In the lytic cycle, the DNA of the host will be reprogrammed to transcribe viral RNAs to produce more mycobacteriophages (Wilson, *et al*., 2009; Figure 1.6). In the late stages of infection, the progeny viral particles assemble and are released by lysing the host cell. In contrast, during the lysogenic cycle, the genomic material of the bacteriophage is incorporated and will remain dormant until the formation of reproductive cells in the hosts (Wilson, *et al*., 2009; Figure 1.6). The viral DNA will then be replicated in the gametangia, or sporangia and the virion will be assembled and released from these cells. In the creation of a mycobacterial transposon mutagenesis library, the mycobacterial phage used is temperature sensitive and makes use of both the lytic and lysogenic life cycles of the bacteriophage. At 30º, the lytic cycle of the bacteriophage is activated and used to generate a mycobacterial phage stock (Figure 1.6). The generation of a mycobacterial phage stock allows for the replication of the mycobacteriophage, as a high titer stock is needed to generate a transposon mutagenesis library. At 37ºC, in the presence of an antibiotic (used as a selectable marker), the lysogenic cycle will be activated, and the transposon inserted randomly into the genome of the mycobacteria (Figure 1.6).

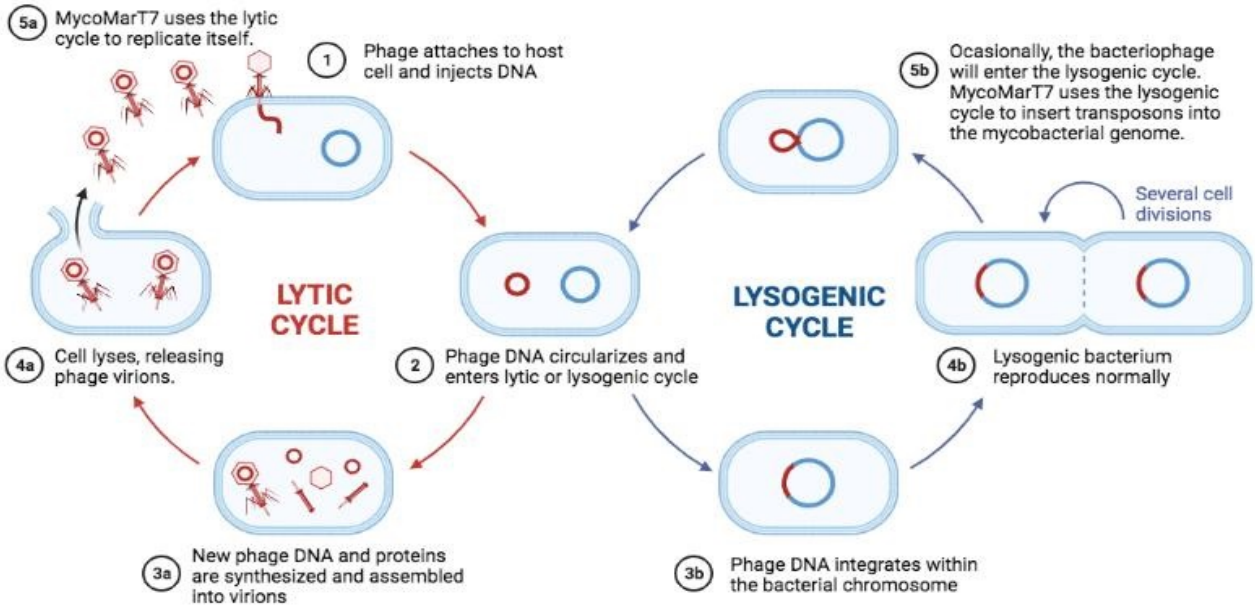


Figure 1. 6: Schematic diagram illustrating the lytic and lysogenic cycle of bacteriophages. During the lytic cycle viral DNA is replicated, and proteins are synthesized. Virions will be assembled and released from the cell. The lysogenic cycle results in the insertion of bacteriophage genes into the bacterial genome (figure drawn using Biorender.com).

1.10.2 Transposon mutagenesis

A transposon mutagenesis library is created through the use of a temperature-sensitive mycobacterial phage, øMycoMarT7. øMycoMarT7 contains the *Himar1* mariner gene (an insect-derived transposon) that inserts transposons randomly at TA dinucleotides in the genome of mycobacteria (Sassetti, *et al*., 2003). øMycoMarT7 also contains a kanamycin resistance gene (which is used as a selectable marker), as well as a T7 promoter (to promote transcription into the adjacent chromosomal DNA) (Rubin, *et al*., 1999). The use of a transposon mutagenesis library has been successfully used to identify essential genes related to the cholesterol pathway and mycobacterial metabolism, as well as virulence (Griffin, *et al*., 2011; Sassetti & Rubin, 2003; Sassetti, *et al*., 2003). Insertions in essential genes will result in mycobacterial cell death. Initially, essential genes were identified by microarray hybridization or conventional sequencing analysis of transposon site hybridization (TraSH) libraries (Sassetti & Rubin, 2003). There are limitations to both methods as they are not able to precisely map sites of insertions (Griffin, *et al*., 2011). This resulted in confusion of the precise location of essential genes. To combat this, next generation sequencing (NGS) has become the method of choice in identifying conditionally essential genes (Griffin, *et al*., 2011). An insertion in the site of an essential gene is lethal and the population of genomic DNA sequenced will be those

that lack transposon insertions in these essential sites. Therefore, there will be spaces at specific gene regions in the analysis of the sequencing reads and these will be deemed conditionally essential (Figure 1.7). Those that have an abundance of insertions are characterized as non-essential (Figure 1.7).

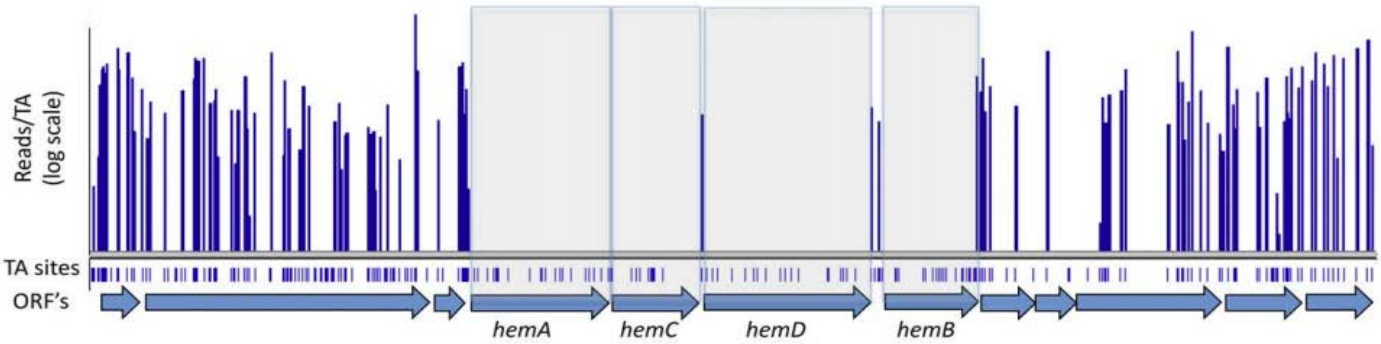


Figure 1. 7: A schematic representation of sites of insertion of a transposon mutagenesis library. Insertions are shown as blue bars. Essential genes are those that lack insertions while non-essential genes are those that have an abundance of insertions (figure extracted from Griffen *et. al* (2011)).

1.11 Hypothesis

The DD-CPase homologues, *dacB1* and *dacB2* in *Mtb*, despite being dispensable for *in vitro* growth, become conditionally essential in the presence of Augmentin. The LMW PBPs, *dacB1* and *dacB2* of *Mtb*, are dispensable for growth under standard conditions but when the organism is exposed to β-lactam antibiotics, these proteins become conditionally essential either by acting as sensors or by recruiting other PG-associated enzymes for an adaptive response.

1.12 Aim and Objectives

1.12.1 Aim

The aim of this study is to determine if LMW PBPs with DD-CPase/endopeptidase activity play a role in exposure to antibiotic stress via direct peptidoglycan remodeling.

1.12.2 Objectives

1. Genetic confirmation of previously constructed DD-CPase mutant and complement strains by polymerase chain reaction (PCR).
2. Determination of the minimum inhibitory concentration (MIC) of first line and other cell-wall-targeting drugs in wild-type and DD-CPase mutant strains using the micro-broth dilution assay.
3. Using *Msmeg* to multiply mycobacterial phage (øMycoMarT7) harboring the *Himar1* mariner gene.
4. Generation of transposon mutagenesis libraries in both wild-type *Mtb* and double deletion mutant strain lacking *dacB1* and *dacb2*.
5. Exposure of mutant libraries to Augmentin for 6 hours, isolation of the genomic DNA from surviving clones, and sequencing using NGS to identify conditionally essential genes.

2. Methods and Materials

2.1 DNA extraction

2.1.1 Small scale genomic DNA extraction

The recipes for chemical reagents as well as bacterial strains and plasmids used in this study are listed in Supplementary information A. Small scale genomic DNA extraction is a simple, time efficient method used to extract genomic DNA (gDNA) using chloroform, for PCR screening. One loop full of each mycobacterial strain, growing on solid media, was re-suspended in 100 µl dH_2O. The cells were then heat-killed at 95 °C for 5 min before 100 µl of chloroform was added and mixed vigorously. Cell suspensions were centrifuged at 12 470 *xg* for 5 min and the top aqueous layer transferred to a sterile tube for use in downstream applications.

2.1.2 Large scale genomic DNA extraction

Mtb and *Msmeg* strains were grown on solid media at 37°C, until a bacterial lawn was evident. Five loop-fulls of bacteria were re-suspended in 500 µl of TE buffer and heat-killed at 75°C for 30 min, before being cooled on ice for 5 min. Alternatively, 5 to 10 ml of liquid culture at an OD_{600nm} of 1 were pelleted by centrifugation for 10 min at 4000 rpm and re-suspended in 500 µl of TE buffer before heat killing. The cells were lysed by treating with 50 µl of Sigma lysozyme (10 mg/ml) and incubated at 37°C for 1 hr. Proteins were degraded by treating with 6 µl of Sigma Proteinase K (10 mg/ml) and 70 µl of 10% SDS at 65°C for 2 hrs. Proteins were precipitated out of solution by the addition of 100 µl of 5 M sodium chloride (NaCl). About 80 µl of pre-warmed (65°C) Cetyltrimethyl Ammonium Bromide (CTAB) was added to each sample, mixed briefly and then incubated at 65°C for 10 min. An equal volume of chloroform and isoamyl alcohol (24:1) was added and mixed vigorously before centrifugation at 12 000 *xg* for 20 min. The supernatant (i.e., upper aqueous phase) was transferred to a sterile Eppendorf tube and the gDNA precipitated by the addition of 450 µl of isopropanol. After mixing by brief vortexing, samples were centrifuged at 12 470 *xg* for 20 min. The supernatant was discarded and the gDNA pellet washed in 500 µl of 70% ethanol, before a brief centrifugation (5 min). The ethanol was then discarded, and the pellet dried at 60°C in a SpeedVac (Eppendorf Concentrator 5301) for 10 min. The gDNA pellet was dissolved in 150 µl of pre-warmed (65°C) nuclease-free water and further incubated at 65°C for 10 min. The gDNA was quantitated on a Nanodrop ND-100 Spectrophotometer (Nanodrop Technologies) and its integrity checked on a 0.8% agarose gel before storage at -20°C.

2.2. Visualization of nucleic acids

Agarose gel electrophoresis is a technique used to resolve DNA on the basis of molecular weight (DeFlaun & Paul, 1996). Larger molecules will migrate faster through a gel matrix than smaller molecules. Following the addition of a DNA intercalating agent, such as ethidium bromide or Syber safe (Sigma) exposure to ultraviolet light (UV) will enable visualization of the DNA fragments (DeFlaun & Paul, 1996).

All PCR products and gDNA preparations were visualized on a 0.8% agarose gel. Gels were prepared by dissolving 0.4 g of agarose powder (SeaKem) in 50 ml of 1x tris-acetate-EDTA (TAE) buffer. The solution was boiled for 2 min to dissolve the agarose before the final volume was re-adjusted back to 50 ml with 1x TAE buffer (to account for volume lost due to steam generation). SYBR safe (or ethidium bromide at 0.5 µg/ml) was then added to enable later visualization using UV-light (SYNGENE G-Box BIO-RAD system). A 6 µl aliquot of each gDNA sample was added to 5 µl loading dye and the entire mixture was loaded into its respective well in the agarose gel. All agarose gels were run at 90 V for 45 min to 2 hours. An appropriate molecular weight marker was used for gDNA sizing.

2.3 Confirmation of mutant strains by Polymerase Chain Reaction (PCR)

PCR enables the amplification of specific regions of gDNA using gene-specific DNA primers. PCR typically involves three steps: denaturation, annealing and extension (Mohini & Deshpande, 2010). Deletions in the genomes of *Mtb* and *Msmeg* strains were confirmed by PCR. The gDNA isolated from strains were used as the template in the PCR reactions. All primers (Table 3.2) were synthesized by Inqaba Biotech. Primers were designed to flank the regions of interest (Figure 3.1). A master mix was prepared using the following reagents: 10x Buffer, 5x GC rich, 1.25 mM dNTPs, 10 µM of forward and reverse gene-specific primers, 5 U/µl Taq polymerase (FastStart, Roche) and dH_2O. About 22 µl of the master mix was added to a PCR Eppendorf tube and 3 µl of template DNA was added to a final volume of 25 µl. The BIO-RAD PCR thermocycler was set up as follows; an initial denaturation step at 95ºC for 3 min; 40x cycles of denaturation at 95ºC for 30 sec, 55ºC for 30 sec, extension at 72ºC for 1 min; and a final extension at 72ºC for 5 min. A 0.8% agarose gel and PCR amplicons were prepared for visualization. An image of the gel was captured using a SYNGENE G-Box BIO-RAD system.

Table 2. 1: PCR primers used for confirmation of strains

Gene	Primer sequence	Expected sizes	
		H37RvS	**Mutant Strain**
Rv3330 (*dacB1*) F	5’ – CCG ACA CCG GAC GCA AAT –3’	700 bp 1 698 bp	548 bp
Rv3330(*dacB1*) R1	5’ – CAG ATT GAT TTT CTC CAG – 3’		
Rv3330(*dacB1*) R2	5' – GGT GGT CAG CAA CTC CTG – 3’		
Rv2911 (*dacB2*) F	5’ – CCA CGC TCA ACA TGC TCC – 3’	764 bp 1 392 bp	564 bp
Rv2911(*dacB2*) R1	5’ – AGC AGC TCG TCC TGG TTG – 3’		
Rv2911 (*dacB2*) R2	5’ – CGA AAT ACC GGC CGA TCG – 3’		
		mc^2155	**Mutant strain**
MSMEG_1661 F	5’ CAC ACG AGT CAC AAC TGT 3’	1 569 bp	417 bp
MSMEG_1661 R	5’ ACG GTG TTC ACC ACG TGC 3’		
MSMEG_2432 F	5’ CGC GAT GAT GTA CGG CCT 3’	1 194 bp	414 bp
MSMEG_2432 R	5’ TCA AAC GTA TCG GCA TGA 3’		
MSMEG_2433 F	5’ GCA GTC GAA TAG TCC ACC 3’	1 327 bp	485 bp
MSMEG_2433 R	5’ GTT GTC GGG GCG CAG ATG 3’		
MSMEG_2433 F	5’ GCA GTC GAA TAG TCC ACC 3’	2 154 bp	462 bp
MSMEG_2432 R	5’ TCA AAC GTA TCG GCA TGA 3’		

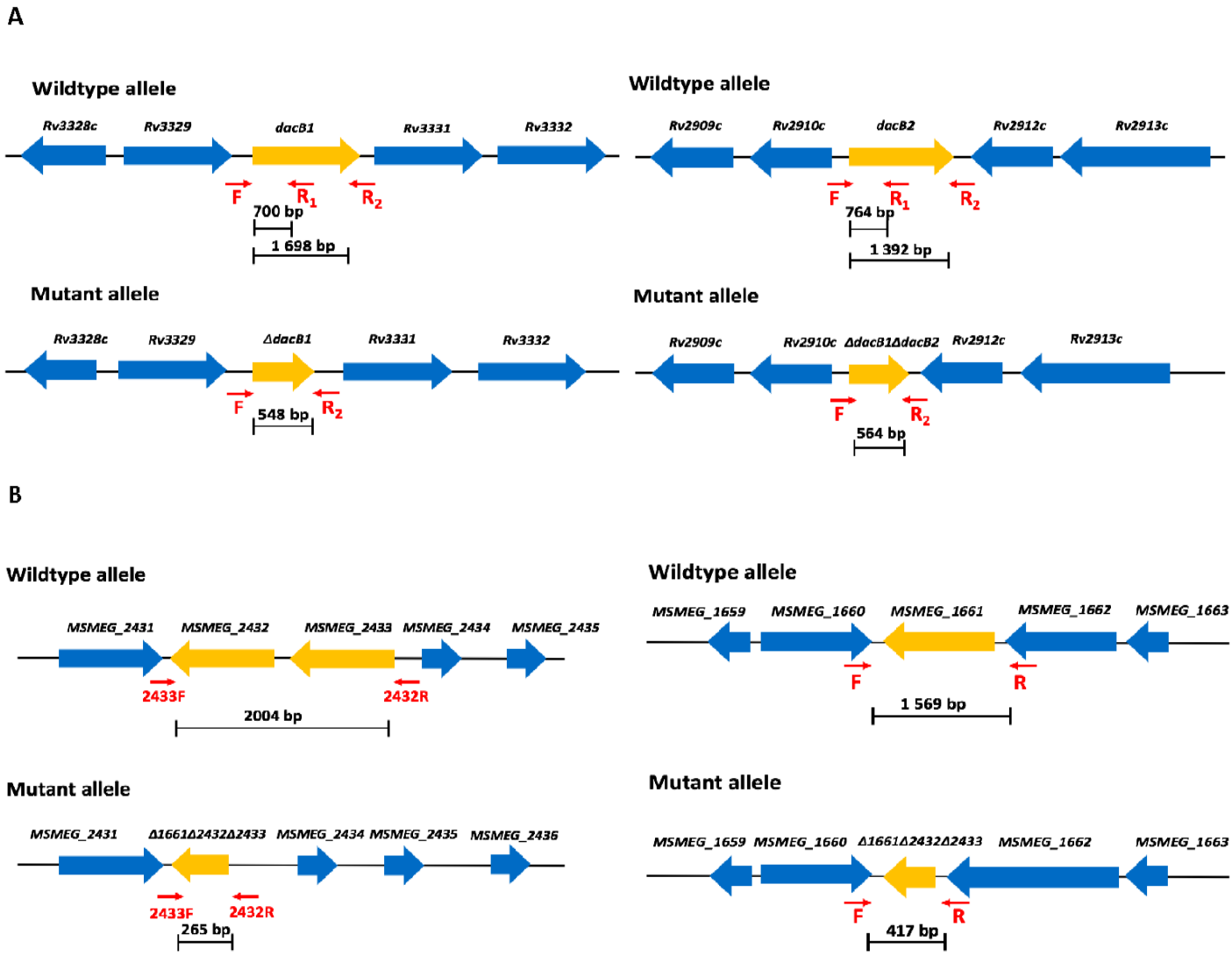


Figure 2. 1: Schematic representation of genomic maps of wild type and mutant alleles for *Mtb* and *Msmeg*. The genomic maps are shown for *Mtb* (A) and *Msmeg* (B)Flanking genes are shown in blue (arrows), and the targeted genes are shown in yellow (arrows). Primers flanking each gene (in red) were used to confirm gene deletion in the mutant strains. The expected gene sizes are indicated.

2.4 Generation of *Mycobacterium smegmatis* complementation strains

2.4.1 Plasmid DNA purification

Plasmid DNA was extracted using the NucleoBond Xtra plasmid purification kit (Macherey-Nagel) as per the manufacturer's instructions. Briefly, 1 ml of an *E. coli* freezer stock containing *1661pmv306H, 2432pmv306H* or *2433pmv306H* plasmids were added to 5 ml of LB media supplemented with hygromycin (final concentration of 50 µg/ml) and grown for approximately 8 hours at 37°C, with shaking at 70 rpm. This starter culture was then used to inoculate a larger volume (100 ml) of LB media (with hygromycin) by diluting the strain

1/1000. This larger culture was further incubated overnight at 37°C, with shaking at 70 rpm. The cells were then harvested by centrifugation (4 500 *xg* for 10 min at 4°C). The supernatant was discarded, and the cell pellet re-suspended in 8 ml of Resuspension Buffer RES + Rnase A. Cells were lysed by the addition of 8 ml of cell lysis buffer and gentle inversion. The mixture was incubated at room temperature for 5 min. Equilibration buffer (12 ml) was added to the rim of the NucleoBond Xtra Column. Eight milliliters of neutralization buffer were added to the sample mixture and tubes were inverted until they turned from blue to completely colourless. The lysate was directly applied to the column and then bound DNA washed using 5 ml of Equilibration buffer. The filter was removed, and the column washed again using 8 ml of Wash Buffer. The plasmid DNA was eluted by the addition of 5 ml of Elution buffer and collected in a 50 ml conical tube. Plasmid DNA was precipitated using 3.5 ml Isopropanol. The mixture was briefly vortexed and then aliquoted in equal proportion into 2 ml Eppendorf tubes and centrifuged for 15 min at 15 000 *xg*. The resulting pellet was washed in 2 ml 70% ethanol and centrifuged at 15 000 *xg* for 5 min. The ethanol was completely removed by aspiration and the pellet air-dried at room temperature. Finally, the pellet was dissolved in 100 µl of sterile dH_2O. The concentration and purity of plasmid DNA was quantitated using a Nanodrop Spectrophotometry. Plasmid DNA was stored at –20°C until use.

2.4.2 Confirmation of plasmid DNA (used for complementation) by restriction digest analysis

A list of the restriction enzymes used, their appropriate buffers and expected band size is provided in Table 3.3. Restriction enzymes and buffers were provided by either Roche Applied Science (Roche) or New England Biolabs (NEB). Plasmid DNA was extracted according to section 3.8.1. The restriction digest was set up as follows: 2.5 µl of 10x appropriate buffer, 10 U/µl of enzyme, 1 µg of plasmid DNA and dH_2O to a final volume of 25 µl. DNA digests were incubated at 37°C for a minimum of one hour and then checked on a 0.8% TAE agarose gel.

Table 2. 2: List of restriction enzymes used in restriction digests, appropriate buffers, and the expected DNA fragment sizes for each plasmid.

Plasmid	Enzyme	Buffer	Expected size (bp)
1661pmv306H	*SmaI*	Cutsmart	5 621
	NotI	Cutsmart	4 850 and 771
	MluI	Cutsmart	4 271 and 1 350
	PvuI	Cutsmart	4 859, 585 and 447
	EcoRI	Cutsmart	2 858 and 2 763
2432pmv306H	*ApaI*	Cutsmart	6 251
	NotI	Cutsmart	5 023 and 955
	MluI	Red	4 755 and 1 460
	HindIII	Cutsmart	4 271 and 1944
	PvuI	Cutsmart	4 670 and 1 545
2433pmv306H	*XhoI*	Cutsmart	5 318
	HindIII	Cutsmart	4 271 and 1047
	NcoI	Cutsmart	4 564 and 754
	NotI	Cutsmart	4 363 and 955
	MscI	Cutsmart	3 974 and 1 344

2.4.3 Ethanol precipitation of plasmid DNA

Plasmids were precipitated by adding 1/10th of the volume of 3 M sodium acetate and 2.5 volumes of ethanol (100%) to each sample. Mixtures were then chilled on ice for 30 min, followed by centrifugation at 12 470 *xg* for 5 min. The supernatants were discarded, and pellets washed twice in 70% ethanol followed by drying in a SpeedVac at 65°C for 10 min. Finally, the pellet was re-suspended in 75 µl of nuclease-free dH_2O and quantitated using a Nanodrop Spectrophotometer. All plasmids were stored at -20°C until use.

2.4.4 Preparation of electro-competent *Mycobacterium smegmatis* cells

Msmeg cells were prepared for electroporation by washing in ice cold 10% glycerol. A starter culture was prepared by inoculating 5 ml of 7H9 with 1 ml of freezer stock of Δ*1661*Δ*2432*Δ*2433* and grown overnight at 37°C. The starter culture was used to inoculate 100 ml of 7H9. The sub-culture was grown overnight at 37°C to mid-log phase. The culture was dispensed into 50 ml conical tubes that were pre-chilled and then incubated on ice for 30 min. The cells were harvested by centrifugation at 4 000 rpm at 4°C for 10 min. The supernatant was discarded, and the pellet re-suspended in 10 ml of ice cold 10% glycerol. The volume of the cell suspension was made up to 40 ml with ice cold 10% glycerol and centrifuged at 4 000

rpm at 4°C for 10 min. This wash step was repeated two more times and then the pellet was re-suspended in 4 ml of ice cold 10% glycerol. The cells were kept on ice until use.

2.4.5 Transformation of *Mycobacterium smegmatis* cells by electroporation

The *Msmeg* strain Δ*1661*Δ*2432*Δ*2433* was used as the parental background to generate complimented derivatives using electroporation. During electroporation, an electric field generates pores in the membrane of a desired organism and charged molecules, such as DNA, can enter the cell (Nakamura & Funahashi, 2013). The DNA from the various plasmids used was added to sterile 1.5 ml Eppendorf tubes at 1 and 3 µg. Plasmid *pvaB300*, a positive control, was added at 1 µg. Electro-competent *Msmeg* was prepared according to section 3.8.3 and 400 µl added to each of the respective plasmid DNA samples, followed by gentle mixing. The entire cell suspension was transferred to an electroporation cuvette and then placed on ice. The BIO-RAD Gene Pulser XCell system was set to the following parameters: voltage = 2 500 V, time constant = 25 µF, resistance = 1 000 Ω, path length = 2 mm. The time constant and voltage were noted after each pulse and then 800 µl of 2x TY (Yeast extract tryptone) was added to the cuvette and placed back on ice. The cell suspensions were aliquoted into sterile 2 ml Eppendorf tubes and incubated overnight at 37°C to allow recovery. Cells were harvested by centrifugation at 4 000 rpm for 5 min and re-suspended in 400 µl of 7H9. A 1:10 dilution series was performed, of which 100 µl of dilution was plated on to 7H10 supplemented with hygromycin (final concentration of 50 µg/ml). The plates were incubated at 37°C for 7 days and the transformation efficiency calculated.

$$\text{Transformation efficiency} = \frac{\textit{The number of colonies} \times \textit{Dilution factor}}{\textit{micro-grams of plasmid DNA used}}$$

2.4.6 Confirmation of complementation by PCR

Genomic DNA was isolated from each of the complementation derivatives as per section 3.3.1 and used as template DNA in the PCR reactions. All primers (Table 3.4) were synthesized by Inqaba Biotech. A master mix was prepared using the following reagents: 10x Buffer, 5x GC rich, 1.25 mM dNTPs, 10 µM of forward and reverse primers, 5 U/µl fast start Taq polymerase and dH_2O. Twenty-eight microliters of the master mix was added to sterile PCR Eppendorf tubes and the final volume was made up to 30 µl by adding 2 µl of template DNA. The PCR cycling profile was programmed as follows; an initial denaturation step at 94ºC for 3 min, 40 cycles of denaturation at 94ºC for 30 sec, 58ºC for 30 sec, extension at 72ºC for 30 sec and a

final extension at 72ºC for 7 min. A 0.8% agarose gel was prepared, and amplicons were separated at 90 V for 1 hour. DNA fragments were sized with an appropriate molecular weight marker. An image of the gel was captured using a SYNGENE G-Box BIO-RAD system

Table 2. 3: Primers used in confirmation of compliment strains by PCR

Gene	Primer sequence	Expected size (bp)
ATTP_L2	5'– ACG TGG CGG TCC CTA CCG–3'	282
ATTB_BSI	5'–CTT GGA TCC CGC TGC GC–3'	
ATTB_BS2	5'–ACA GGA TTT GAA CCT GCG GC–3'	320
ATTP_L4	5'–AAT TCT TGC AGA CCC TGG A–3'	

2.5 Phenotypic characterization of strains

2.5.1 Determination of minimum inhibitory concentration (MIC90) of first line and other cell-wall-targeting drugs in wild-type and mutant strains using the micro-broth dilution assay

The microbroth dilution method was used to determine the MIC90 for first-line, anti-TB drugs and select CW-targeting ß-lactams (vancomycin, meropenem, clavulante and amoxicillin). Mycobacterial strains were grown in liquid (i.e., 7H9 media) to an exponential growth phase (OD_{600nm} of ~ 0.5). Dilutions (1:10 and 1:500) of these cultures were performed in order to adjust the OD_{600nm} to 0.05 and 0.001 for *Msmeg* and *Mtb*, respectively. Fifty microliters of 7H9 media were added to each well of a 96 well plate, except for the first row (Figure 3.2). In the first well of the first row, 7H9 media was added followed by water and antibiotic, at a concentration of 1 mg/ml or calculated from the expected MIC found in the literature. A two-fold dilution was performed until the last row in the 96-well plate. Fifty microliters of the adjusted, diluted cultures for each strain were then added to all wells except Row 1. Plates were incubated at 37ºC overnight or for two weeks (*Msmeg* and *Mtb*, respectively). Ten microliters of Alamar Blue (Thermofisher) were added to every well and the plates further incubated at 37°C for a minimum of 16 hours in *Mtb* or three hours in *Msmeg*.

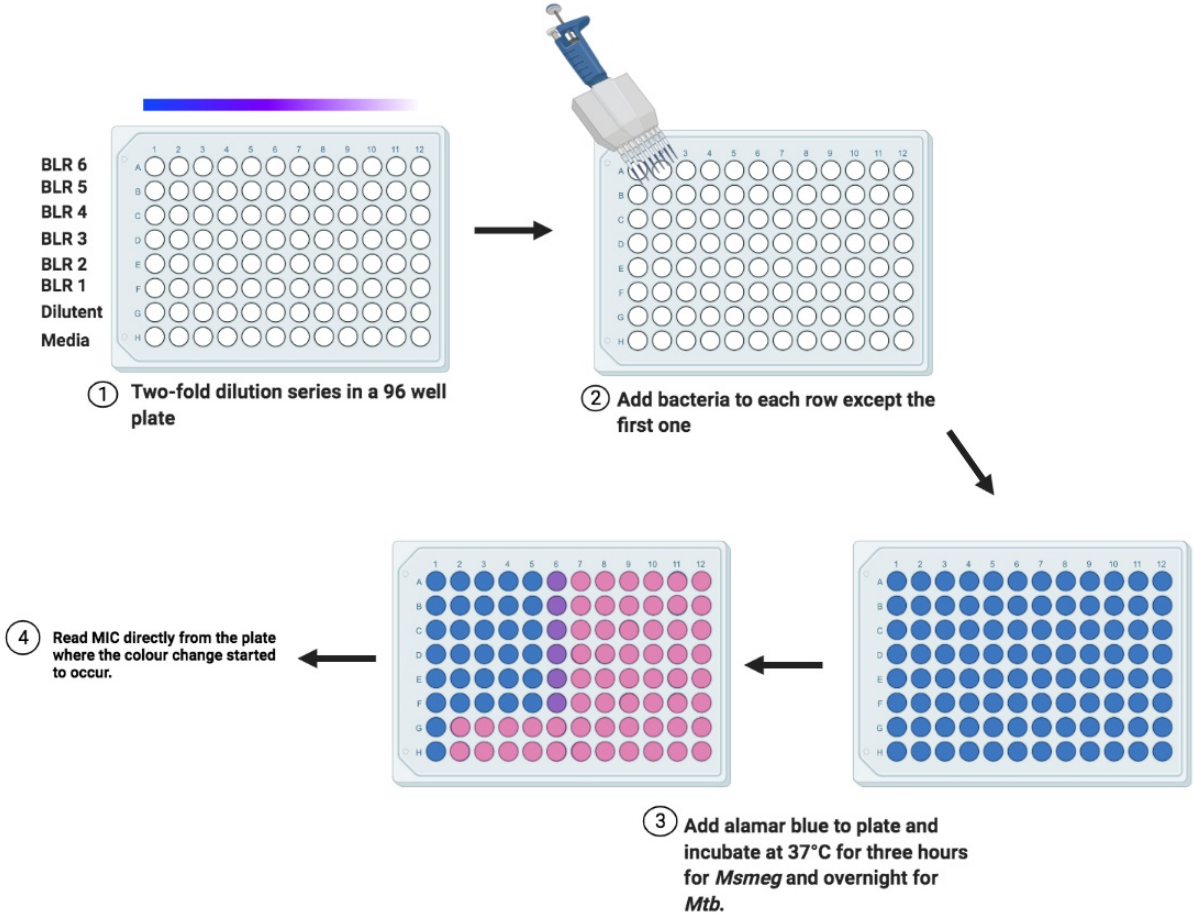


Figure 2. 2: Schematic representation to determine the Minimum Inhibitory Concentration (MIC) of first line and cell wall targeting antibiotics using the micro-broth dilution assay. A two-fold dilution series was performed in a 96 well plate before the addition of bacterial cells. The plates were incubated at 37°C overnight and two weeks for *Msmeg* and *Mtb*, respectively. Thereafter, 10 µl of alamar blue was added to quantify the number of viable cells Plates were incubated for 3 hrs and overnight for *Msmeg* and *Mt*b respectively (figure drawn using BioRender.com).

2.5.2 Determination of change in peptidoglycan side wall and polar labelling in mycobacterial strains exposed to Augmentin using FDAA staining

Fluorescent D-amino acid (FDAA) probes are fluorescently labelled probes that are used to study PG synthesis in numerous bacterial species (Alam, *et al*., 2018). These probes are incorporated into extracellular and intracellular pathways for PG biosynthesis in various bacteria. These probes are composed of fluorescently labelled D-amino acids, which are unique to PG (Alam, *et al*., 2018). These D-amino acid probes (monopeptide e.g., TADA and dipeptide e.g., AlkDada) incorporate into PG and label both the poles and sidewall of mycobacteria. Monopeptide probes are thought to be incorporated into the peptidoglycan by Ldts (Alam, *et al*., 2018). TADA, a monopeptide FDAA probe, was used to determine if there was a change in the remodeling of peptidoglycan by Ldts in *Mtb* and *Msmeg* strains exposed to Augmentin.

Bacterial strains were grown to an OD_{600nm} of 0.5 in liquid media. About 500 µl of each culture was added to a sterile 1.5 ml Eppendorf tube. *Msmeg* was exposed to Augmentin for four hours at sub-MIC (0.5xMIC as determined by Section 3.7.1 above), before incubating with 2.5 µl of TADA for 30 min (Figure 2.3). In *Mtb*, incorporation of TADA and exposure to Augmentin occurred simultaneously for 24 hours. The parameters were changed to account for the slower growth rate of *Mtb*. A portion (3 ml) of the cultures was not exposed to Augmentin and immediately stained with TADA for the same duration (Figure 2. 3). Cells were pelleted at 13 000 rpm for 1 min at room temperature and then fixed in 100 µl of 2.5% glutaraldehyde and incubated at room temperature for 30 min and 3 hrs for *Msmeg* and *Mtb*, respectively, before being centrifuged at 13 000 rpm for 5 min. Cell pellets were re-suspended in 100 µl of 1X PBS. Thereafter, 10 µl of cell suspensions were spotted onto 2% agarose pads and then viewed using a Nikon Eclipse T12 AND PE4000 LED light source fluorescent microscope. Images were captured in bright field (Phase, 200 msec exposure) and pre-configured TADA channels (excitation 550 nm, 50% power; emission 598 nm; 2 s exposure). This microscope was used as it has built-in analysis tools that can be used to determine cell length. The software used is NIC Elements version 5.02 and the objective used is 100x magnification with oil immersion. The experiment was performed in triplicate.

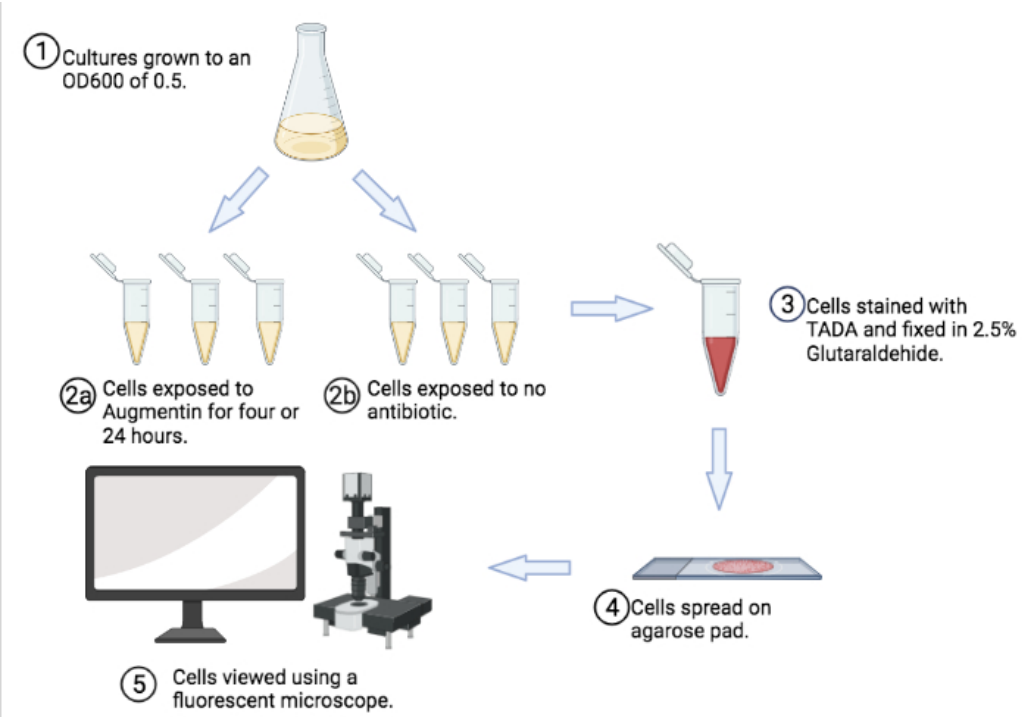


Figure 2. 3: **A schematic representation of FDAA staining workflow.** *Mtb* and *Msmeg* strains were grown up to an OD_{600} of 0.5. Cells were exposed to Augmentin for 4 hrs and 24 hrs for *Msmeg* and *Mtb*, respectively. Those that were not exposed to Augmentin were stained immediately. TADA was incorporated into the cells and cells were fixed in 2.5% glutaraldehyde and washed with PBS. The cells were spotted onto a 2% agarose pad and then viewed using a fluorescent microscope. The staining patterns, as well as cell lengths, were recorded for analysis (figure drawn using BioRender.com).

2.5.3 Determination of change in peptidoglycan side wall and polar labelling in *Mycobacterial smegmatis* strains using BODIPY Vancomycin staining

Vancomycin inhibits the action of PBPs by binding to D-Ala D-Ala residues, which are their substrates (Rice, 2006). BODIPY Vancomycin contains a fluorophore, which has been conjugated to its core to enable visualization (Stone, *et al*., 2018). One milliliter of a freezer stock, corresponding to each of the *Msmeg* strains, was used to inoculate 5 ml of 7H9. The pre-culture was then used to inoculate 10 ml of liquid media to a starting OD_{600} of 0.02 and strains were grown and adjusted to an OD_{600} of 0.6. About 1 ml of each culture was added to a sterile 1.5 ml Eppendorf tube. Vancomycin-BODIPY (100 µg/ml), supplied by Sigma, and unlabeled 1 mg/ml vancomycin (Sigma) were each added to a final concentration of 1 µg/ml. Samples were then incubated at 37ºC with shaking for 1.5 hrs. Cells were pelleted by centrifugation at 3 000 *xg* for 5 min, washed twice in 500 µl of 0.05% Tween-80 in PBS (phosphate buffered saline) and finally re-suspended in 50 µl of 0.05% Tween-80 in PBS. The addition of Tween-80 was to minimize bacterial clumping. Cell suspensions (10 µl) were spotted onto a 2%

agarose pad and viewed under the Zeiss Observer Z1 inverted fluorescence microscope. Images were taken in bright-field (DIC, 211.216 ms) and FITC (1 500 ms) channels using an AxioCam Hrm camera and using the Zen blue Version 5.1.2600 (Zeiss). The objective used was 100x magnification with oil immersion. The staining pattern of a hundred cells per biological repeat was manually noted as well as any abnormal phenotypes.

2.6 Materials and methods of mycobacteriophage work

2.6.1 Reagents for mycobacterial experiments

MP Buffer is typically used to harvest and store mycobacterial phages. This was prepared by adding 5 ml of 1 M Tris-HCl (pH 7.6), 3 ml of 5 M NaCl, 1 ml of 1 M Magnesium sulfate ($MgSO_4$), 0.2 ml of 1 M Calcium chloride ($CaCl_2$) and making up a final volume of 100 ml with sterile dH_2O. All reagents were autoclaved, unless otherwise stated, at 121°C for 20 min. Tris-HCl (pH 7.6) was prepared by dissolving 12.1 g of Tris powder (Sigma) in 80 ml of dH_2O and the pH adjusted by the addition of approximately 6 ml of concentrated HCl (Sigma). NaCl (Sigma) was prepared by dissolving 29.22 g of NaCl powder in 100 ml of dH_2O. 1 M $MgSO_4$ (Sigma) by dissolving 12 g of $MgSO_4$ powder in 100 ml of dH_2O. 1 M $CaCl_2$ (Sigma) was prepared by dissolving 14.7 g of $CaCl_2.2H_20$ powder in 100 ml of dH_20. Top agar was prepared by dissolving 0.71 g of 7H9 powder, 0.9 g of LB agar (Miller), 0.3 ml of glycerol in 147.9 ml of dH_2O and supplementing with 1.5 ml of 100x glucose salts after autoclaving.

2.6.2 Construction of transposon mutagenesis libraries

Essential genes are those that are necessary for growth under various environmental conditions (Sassetti & Rubin, 2001). Identification and then characterization of these genes are important for the discovery of potential new drug targets. *Himar 1* transposons insert randomly in the genome at TA dinucleotides, disrupting the function of the gene (Griffin, *et al*., 2011). Using these transposons enables the identification of non-essential genes via numerous insertion sites without affecting viability. In contrast, essential genes are those that cannot tolerate any disruptions and will therefore lack insertions. The transposon donor phagemid used in this study was øMycoMarT7, which includes the transposon *Himar1* gene with kanamycin resistance. T7 promoters are oriented to promote transcription of adjacent chromosomal DNA and flanked by inverted repeats. In this study, we aimed to use transposon insertion sequencing (Tn-seq) to identify conditionally essential and non-essential genes in *Mtb* strains exposed to Augmentin in the wild-type and double deletion mutant (lacking *dacB1* and *dacB2*) backgrounds. In order to achieve sufficient coverage of the genome, mycobacterial strains were

transfected with mycobacteriophage stock that had a minimum plaque forming units per milliliter (PFU/ml) of $5x10^{10}$. Resultant clones were then pooled to comprise a library for that strain (Griffin, *et al*., 2011; Sassetti & Rubin, 2001; Sassetti & Rubin, 2003). Mycobacterial phage stock preparation and mycobacterial transduction will be briefly explained below.

2.6.2.1 Mycobacterial phage stock preparation

øMycoMarT7 was obtained, via request, from Eric Rubin (Harvard) (Sassetti & Rubin (2001). Ten-fold dilutions were prepared from the original stock in 50 µl of MP Buffer (50 mM Tris, pH 7.5, 150 mM NaCl, 10 mM $MgSO_4$, 2 mM $CaCl_2$). Each dilution (from 10^{-1} to 10^{-9}) was added to 100 µl of wild-type *Msmeg* grown to stationary phase (OD_{600} 2.5) that had been washed twice in MP Buffer, by centrifugation at 4000 rpm and re-suspending the pellet in 20 ml of MP Buffer (Figure 4.1). The mixture of mycobacteriophage and *Msmeg* was incubated at 37°C for 30 min to allow for mycobacteriophage absorption. The mixture was then added to 3.5 ml of top agar (0.6% agar in 7H9 standard media) and poured on to 7H10 plates. Top agar has to be kept at 55°C until use to prevent solidification. The plates were incubated at 30ºC for two days (Figure 2.4). PFU/ml was determined by counting the number of plaques and mycobacteriophages were subsequently harvested by flooding the 'lacy' plates with MP buffer and rocking at 4ºC for three hours. It is important that the plates are lacy as this indicates a high volume of mycobactriophage. MP buffer containing the mycobacteriophage was removed from the plates and purified by filter sterilization (0.2 µm filter was used). The purification step removes any residual *Msmeg* that is present. This working stock of high titer mycobacteriophage was stored at 4ºC until use.

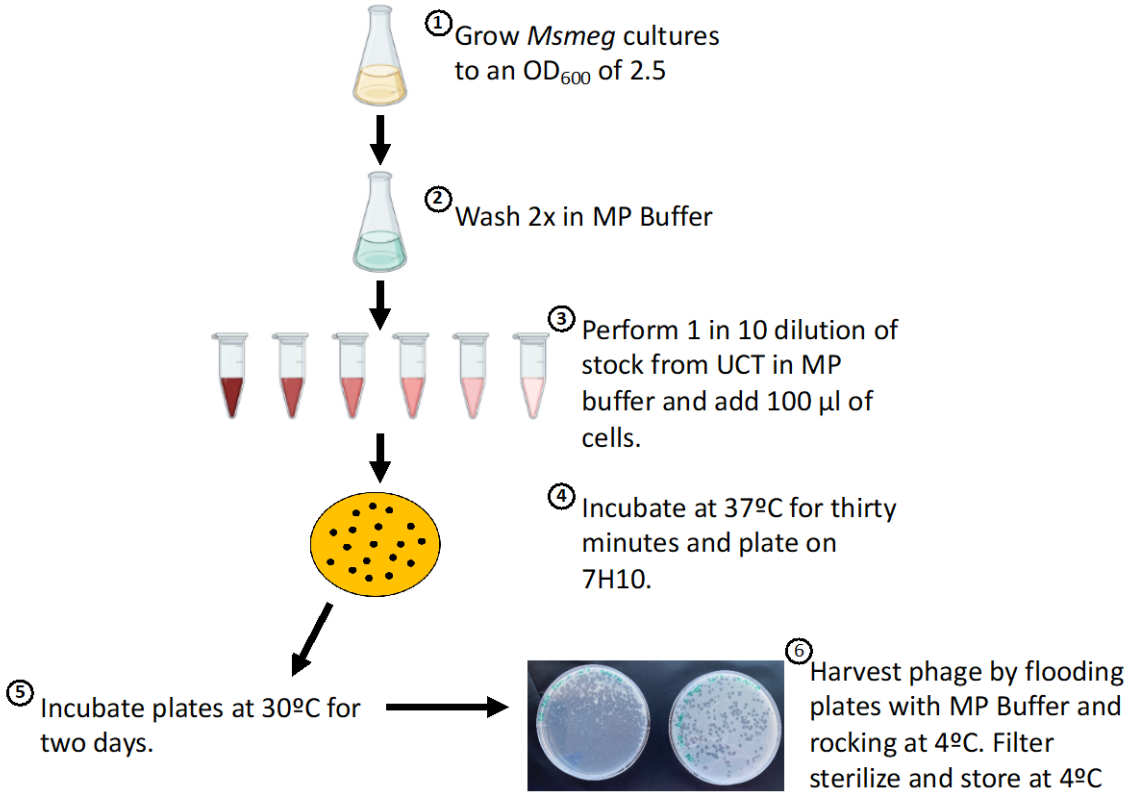


Figure 2. 4: Schematic representation of mycobacterial phage stock preparation. *Msmeg* was grown to stationary phase (OD_{600} 2.5) and washed twice in MP Buffer. A dilution series (from 10^{-1} to 10^{-9}) of the original phage stock was performed and the cells incubated at 37ºC for twenty to thirty minutes. Thereafter, the mycobacteriophage and bacterial cell mixtures were added to warm top agar (55°C) and poured on to 7H10 plates. The plates were incubated at 30ºC for two days.

2.6.2.2 Determination of PFU/ml of mycobacteriophage stock by spot test

The PFU/ml of mycobacterial phage stock was determined by a spot test. Spotting refers to the preparation of a dilution series of the mycobacterial phage stock and adding this to a plate containing solidified top agar and *Msmeg*. This method is a quick and relatively simple way to determine the PFU/ml of the mycobacterial phage stock in comparison to section 2.4.1. Wild type *Msmeg* was grown to stationary phase (OD_{600} 2.5) and 500 µl added to 3.5 ml of top agar and poured on to 7H10 plates. The plates were allowed to dry at room temperature for approximately an hour and 10 µl of phage stock spotted at various dilutions (from 10^{-1} to 10^{-12}). The plates were incubated at 30ºC for two days.

2.6.2.3 Transduction of *Mycobacterium tuberculosis*

For the transduction of *Mtb* H37Rvs and the mutant strain lacking *dacB1* and *dacB2*, two different methods were used, hereafter, referred to as the "old" and "new" methods. Mycobacterial cultures (100 ml) were grown to exponential phase (OD_{600nm} of between 0.8 and 1) (Figure 2.5). Cells were washed twice in MP buffer (by centrifugation at 4000 rpm and re-suspending the pellet in 20 ml of MP Buffer) and re-suspended in 1/10th of the original culture volume in MP buffer; 100 µl of the culture was removed to serve as a negative control for plating. The old and new method differed in the process of transduction. Cells were transfected, using the old method, by the addition of 1 to 2 ml of mycobacterial phage stock and incubating for 3 hrs at 37ºC and freezing cells overnight at -80ºC and plating on 7H10+Kan plates (Figure 2.5). The cells, using the new method, were transfected with 1 ml of mycobacterial phage stock (titer of1x10 11 PFU/ml) and incubated at 37ºC for 18 hrs (Figure 2.5).

In both cases, cells were pelleted by centrifugation and washed once in PBS supplemented with Tween80 (0.05%). The cells were re-suspended in 10 ml of PBS-Tween-80 and a 1:10 dilution performed in PBS-Tween-80. About 500 µl were plated on to 7H10 solid media (9 cm petri dish) supplemented with kanamycin (20 µg/ml), OADC and Tween80 (0.05%). The remaining cells were plated on 15 cm 7H10-OADC-Tween-80-Kanamycin plates. Plates, PBS-Tween-80, MP Buffer, phage stock and the centrifuge chamber were all pre-warmed at 37ºC. The wash step with PBS-Tween80 was included to remove any residual mycobacteriophage that had not entered bacterial cells. All plates were incubated at 37ºC for three to four weeks. The emergent colonies, representing the transposon insertions and mutagenesis libraries, were pooled by scraping off the plates and re-suspending in 7H9 supplemented with OADC, Tween80 (0.05%) and glycerol (60%). The CFU/ml of each library was then determined by the following formula:

$$CFU/ml = \frac{The\ number\ of\ colonies \times Dilution\ factor}{volume\ spread\ on\ the\ plate}$$

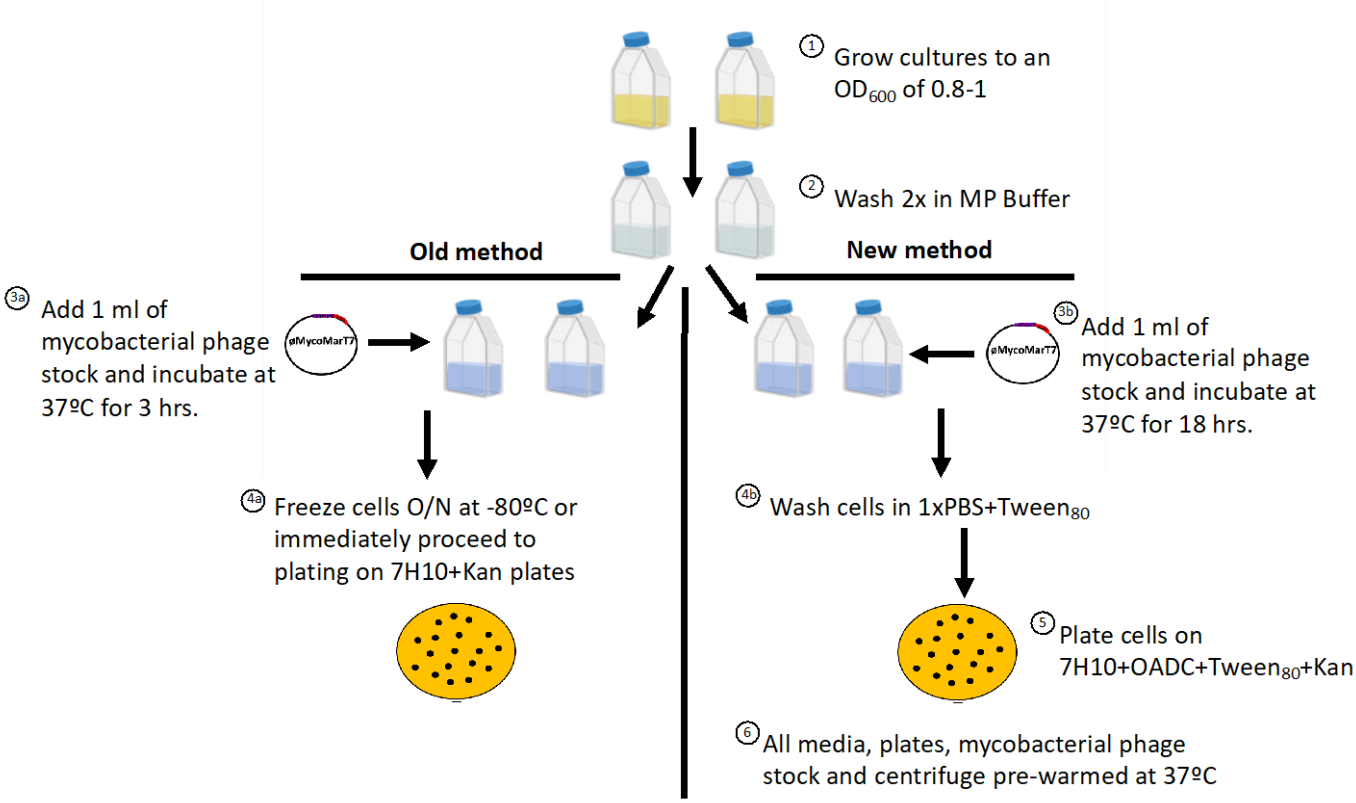


Figure 2. 5: Schematic representation of transposon mutagenesis using two different methods. Strains were grown to exponential phase (OD_{600} of between 0.8-1) and washed twice in MP Buffer. Thereafter, the methods of transfection differed. Cells were transfected with the ØMycoMarT7mycobacteriophage expressing the transposon to create libraries (a minimum of 10^{10} PFU/ml was used to ensure complete coverage in the genome).

2.7 Identification of novel mycobacterial phage from soil

2.7.1 Isolation of mycobacterial phage from soil

The CFU/ml of the mycobacterial phage libraries generated was consistently low (less than 10^5 CFU/ml) which implies a low genome coverage. To remedy this, we sought to identify a novel mycobacterial phage and introduce the *Himar5* mariner gene into to its genome, which has been shown to have an increased insertion rate compared to *Himar1*. Approximately 150 soil samples (between 15 to 50g of soil) were collected from various parts of the Gauteng province, South Africa. Soil samples were collected from damp areas, as this is thought to be the ideal habitat of mycobacterial phages (Bajpai, *et al*., 2018). Samples were re-suspended in MP buffer (15 to 50 ml, depending on the size of the soil sample collected) and filter sterilized using a 0.2 µm filter. The wild-type strain of *Msmeg* was grown to stationary phase (OD_{600} 2.5) and washed twice in MP buffer, by pelleting the cells at 4000 rpm and re-suspending in 20 ml of MP buffer. Fifty micro-liters of the purified soil sample was added to 500 µl of mycobacterial

cells, which was then incubated at room temperature for thirty minutes. Following this, mixtures were added to 3.5 ml of warm top agar and poured on to 7H10 plates supplemented with cycloheximide (final concentration of 10 µg/ml) to minimize bacterial contamination from the original soil sample. Plates were incubated at 37ºC for two days to promote plaque formation. The MycoMarT7 phage stock was prepared according to section 3.8.2.1 and then used to infect *Msmeg* as a positive control. If plaques formed, a sterile pipette tip was stuck in the middle of the plaque to retrieve mycobacteriophages which were then re-suspended in 200 µl of MP Buffer. All samples were stored at 4ºC until use. The morphology of mycobacteriophages was determined by transmission electron microscopy (TEM) which was performed at the University of Cape Town. Briefly, samples were stained with 1% uranyl acetate and images were taken at a magnification of 30 000x.

2.7.2 Mycobacterial phage plaque formation at various temperatures

The plaque formation at various temperatures was assessed for any newly isolated mycobacteriophages relative to the øMycoMarT7 mycobacteriphage previously used. This was done as described by section 4.2.1 and all plates were incubated at 30ºC, 37ºC and 42ºC for two days. Plaque size was measured with a ruler and recorded for each mycobacterial phage.

2.7.3 Isolation of novel mycobacterial phage genomic DNA

The gDNA of the novel mycobacterial phage was isolated using the Wizard Genomic DNA Purification Kit (Promega), according to the manufacturer's instructions. All reagents were provided with the kit. Briefly, 1 ml of phage stock (PFU/ml of ~ 10^{10}) was added to a sterile 1.5 ml Eppendorf tube and 600 µl of Nuclei Lysis solution was added. Cells were lysed by incubation at 80ºC for five minutes and allowed to cool to room temperature. Three microliters of RNAse solution were added to the cell lysate followed by an incubation at 37ºC for 1 hr. The sample was allowed to cool to room temperature before the addition of 200 µl of Protein Precipitation Solution, then vortexed vigorously and then incubated on ice for 5 min. Samples were centrifuged at 13 000 *xg* for 3 min and the supernatant transferred to sterile 1.5 ml Eppendorf tube containing 600 µl of isopropanol. Samples were gently inverted until thread-like strands of DNA were visible. The genomic DNA was pelleted by centrifugation at 13 000 for 2 min. The supernatant was discarded, and the pellet washed twice in 600 µl of 70% ethanol. The gDNA pellet was air dried in a vacuum concentrator (Eppendorf Concentrator 5301 SpeedVac) for 10 min at 60ºC. Finally, the gDNA pellet was re-suspended in 100 µl of DNA

Rehydration Solution and dissolved by incubation at 65ºC for 1 hr. The gDNA whole genome sequencing was performed by Inqaba Biotech using the PacBio® HiFi platform.

2.7.4 Next generation sequencing analysis

PacBio® HiFi is a relatively new technique that can be used to generate high quality *de novo* genome assemblies (Rhoads & Au, 2015). The reads produced are highly accurate and longer in length compared to those produced by Illumina sequencing. Several steps were taken to analyze the sequencing data (Figure 2.6). The first step involved library preparation by Inqaba Biotech followed by sequencing. The third step involved assembly of the genome by Inqaba Biotech and the quality of the assembly assessed using Quast (Gurevich, *et al*., 2013). The fourth step was to annotate the genome of the novel phage using Prokka (Seemann, 2014) which was available through Galaxy (https://usegalaxy.org/login). Hypothetical proteins were then identified through an NCBI Protein BLAST (Johnson, *et al*., 2008). Lastly, to identify which cluster the novel mycobacterial phage belonged to, a k-mer search was conducted using Kraken2 (Wood, *et al*., 2019).

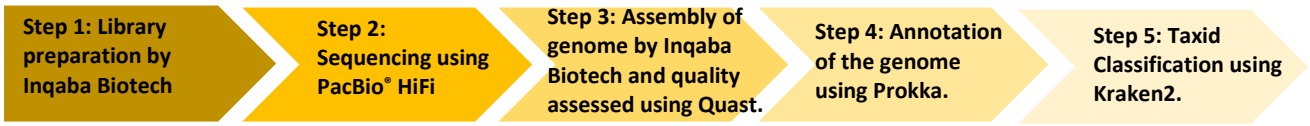


Figure 2. 6: Schematic representation of the computational workflow used to analyze the genomic sequencing data. Four steps were used to analyze the sequencing data received from Inqaba Biotech. The first step was library preparation by Inqaba Biotech, followed by sequencing. Thirdly, the genome was assembled by Inqaba Biotech and the quality of the assembly validated using Quast. The next step was to annotate the genome using Prokka. Lastly, the novel mycobacterial phage was classified using Kraken2.

2.7.4.1 Preparation of sequencing library and assessment of sequencing quality control.

The quality of the gDNA sent for sequencing was confirmed by agarose gel electrophoresis as per section 3.4. The preparation of the gDNA for sequencing was performed by Inqaba Biotech and consisted of a basic HiFi Library construction workflow. Firstly, the gDNA was sheared using Diagenode's Megaruptor 3 system and single-strand overhangs were removed. The damaged DNA was repaired followed by end-repair/A-tailing. The adaptors were then ligated onto the strands of DNA and the library purified using 1.0x AMPure®PB Beads. Damaged SMRTbell templates (a double stranded DNA template capped by hairpin loops at both ends) were removed by nuclease treatment followed by another purification step using 1.0x AMPure®PB Beads. SMRTBell templates that were less than 10 kb in size were removed using

the PippinHt System and then purified for a third time. The library was then ready for sequencing. The quality of the sequencing data produced was assessed by FastQC (Brown, *et al*., 2017). FastQC is a bioinformatics tool that summarizes the quality of reads by position and informs the user of adaptor content, tetramer frequencies and many other aspects. The FastQ file provided by Inqaba Biotech was run through the FastQC program. The per base sequence quality, quality scores, content, GC content, per base N content, length distribution, duplication levels, overrepresented sequences and adaptor content were assessed.

2.7.4.2 Genome assembly and assessment of assembly

The genome was assembled by Inqaba Biotech, and this was used for downstream applications. The quality of this genome assembly sequencing data was assessed using Quast (Gurevich, *et al*., 2013). Quast is an assessment tool for evaluating and comparing genome assemblies. This specific tool was chosen for its ability to evaluate assembly quality without a reference genome. The Quast report provides information on the largest contig in the assembly, total length of the genome, percentage of GC content, N50 (indicates if the assembly is balanced between long and short contigs) and lastly L50 (is the number of contigs equal to or longer than N50 length) (Gurevich, *et al*., 2013).

2.7.4.3 Genome annotation

The genome of *øIPJ3107* was annotated using Prokka (Seemann, 2014) and NCBI Protein BLAST (Johnson, *et al*., 2008). Prokka is a quick, effective tool for identifying and labelling potential features (i.e., genes, in the case of viral and bacterial genomes) in a genome sequence. The FASTA file provided by Inqaba Biotech was run through the online Prokka tool available on Galaxy (https://usegalaxy.org/login). Prokka provided a FASTA file of the protein sequences of all potential open reading frames in the genome assembly. The individual protein sequences were then run through an NCBI Protein BLAST. Basic Local Alignment Search Tool (BLAST) is a web interface search tool that allows similar sequences to be identified based on sequence identity matches to curated sequences in the NCBI-hosted primary sequence database.

2.7.4.4 Taxonomic classification

Kraken2 (Wood, *et al*., 2019) was used to identify other known mycobacterial phage strains that could potentially have a taxonomic relationship with the novel mycobacteriophage identified and characterized in this study. Kraken2 is a metagenomics analysis tool that provides fast taxonomic classification by using a memory-intensive algorithm that associates the genomic reads with a likely common ancestor. The FASTA file was run through the

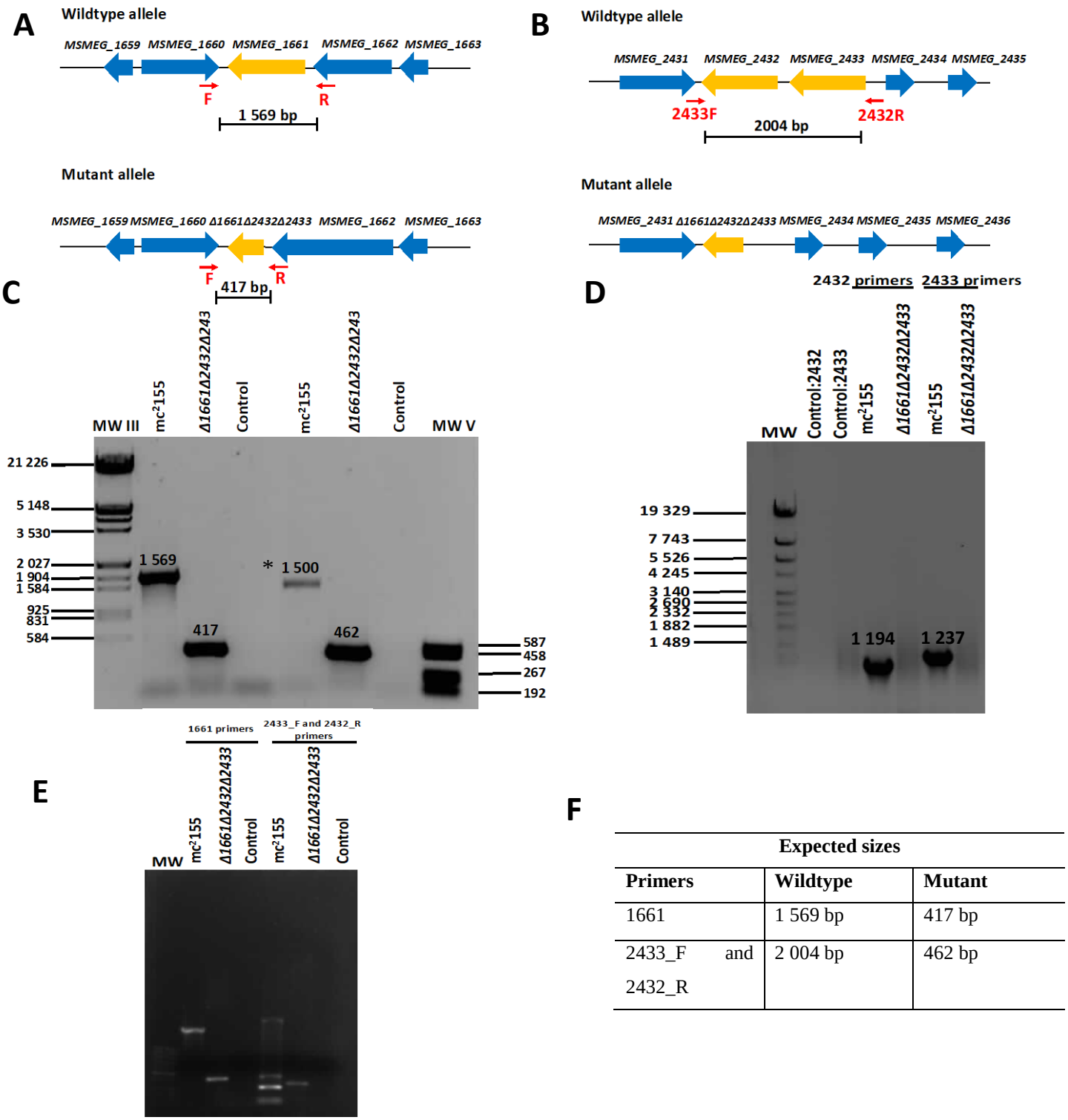
program and the identified organisms used to identify which cluster and sub-cluster the novel mycobacterial phage potentially belongs to.

3. Results: Characterization of DD-CPases strains in *Msmeg* and *Mtb*

3.1 Confirmation of Δ*1661*Δ*2432*Δ*2433* in *Msmeg* by PCR

The confirmation of the triple gene deletion in *Msmeg* was performed by PCR. Large scale gDNA extraction was performed to isolate the gDNA of the wild type and triple mutant strains. The optimal annealing temperature of the primer sets were determined by gradient PCR to be 55°C and 56.4°C, respectively, for 1661 and 2433_F and 2432_R primer sets. A genomic map is shown in Figure 3.1 to illustrate the binding sites of the primer pairs as well as the expected band sizes in the triple mutant and wild type strains. In the confirmation of the triple mutant using the 1661 primer set (Figure 3.1A), wild type template gDNA produced a band greater than the expected size of 1 569 bp while the triple mutant produced a band larger than the expected size of 417 bp (Figure 3.1C). These bands also appeared to be smeared. This is possibly due to excessive amounts of gDNA added either in the PCR run or on the gel. In the confirmation of the triple mutant using the 2433_F and 2432_R primer set (Figure 3.1B) wild type produced a band of approximately 1 500 bp while the triple mutant produced a band of 462 bp (Figure 3.1C). The wild type band produced was not of the expected size. This is due to the fact that Fast start taq polymerase can only extend at a rate of 1 kb per minute. The extension time was, therefore, increased and the expected band size produced along with multiple other bands. This due to non-specific binding of the primers as the extension time was too long (Supplementary Figure 1B).

Primer sets were previously designed to flank the genes *MSMEG_2432* and *MSMEG_2433* (Ealand, unpublished). The optimal annealing temperature of each primer set was previously determined to be 55°C and 64.3°C for the 2432 and 2433 primer sets respectively. The expected band sizes of 1 194 bp and 1 237 bp were produced in the wild type strain and the mutant did not produce any bands (Figure 3.1D). The appearance of no bands in the mutant was expected as the forward and reverse primers for 2432 and 2433 respectively bind in the regions where the deletions took place. All negative controls were clean. This confirms that *MSMEG_1661*, *MSEMG_2432* and *MSMEG_2433* were successfully deleted in the *Msmeg* triple mutant.



F

Expected sizes		
Primers	**Wildtype**	**Mutant**
1661	1 569 bp	417 bp
2433_F and 2432_R	2 004 bp	462 bp

Figure 3. 1: Confirmation of DD-Cpase tripe mutant in *Mycobacterium smegmatis*. Genomic map illustrating *MSMEG_1661* (A), and *MSMEG_2432* and *MSMEG_2433* (B) for the wild type and mutant alleles. Flanking primers are shown in red, while the yellow arrows represent the DD-Cpase genes. The expected fragment sizes are indicated. PCR was used to confirm the triple mutant (C). The 2432 and 2433 primer pairs further confirmed the wild type and triple mutant strains (D). The extention time was increased when 2432 and 2433 primer pair was used and the gel shown (F). The expected sizes for wild type and the DD-Cpase triple mutant using 1661

primer set and 2433_F and 2432_R primer set are indicated in the table (F). * The band observed was unexpected and possibly due to the limitations of Fast start taq polymerase.

3.2 Confirmation of Δ*dacB1*Δ*dacB2* in *Mtb* by PCR

The confirmation of the double mutant in *Mycobacterium tuberculosis* was performed by PCR. gDNA extraction was performed to isolate wild type and mutant gDNA. The optimal annealing temperature of each primer set was determined by a gradient PCR to be 55°C and 64.3°C for *dacB1* and *dacB2,* respectively. Three primers were used, a forward and an internal reverse primer (designed to bind in the region of the gene of interest), as well as an external reverse primer (designed to flank the gene of interest). The forward and internal reverse and external reverse primers were run separately PCRs for the *dacB1* and *dacB2* primer sets. The optimal annealing temperature for the primer pairs was determined by gradient PCR. For the confirmation of *dacB1,* the optimal annealing temperature for the forward and internal primer pair was 55°C, while the optimal annealing temperature for the forward and reverse two primer pair was 64.3°C. The forward and internal reverse primer pair produced a band of 1 698 bp in the wild type strain, while the double mutant strain produced no band (Figure 3.2A). The forward and external reverse primer pair produced a 700 bp band in the wild type and a 584 bp band in the mutant (Figure 3.2B).

For the confirmation of *dacB2,* the optimal annealing temperature for the forward and internal reverse primer pair was found to be 61.1°C while the optimal annealing temperature for the forward and external reverse primer pair was 56.9°C. For the forward and internal reverse primer pair the wild type strain produced a band of 1 392 bp, while the double mutant strain produced no band (Figure 3.2C). The forward and external primer pair produced a 764 bp band in the wild type strain and a 564 bp band in the double mutant strain (Figure 3.2D).

A genomic map is shown in Figure 3.2 to illustrate the binding sites of the primer pairs, as well as the expected band sizes in the double mutant and wild type strains. In the confirmation of the double mutant strain using the *dacB1* primer set (Figure 3.3A) wild type strain produced a band of 700 bp, while the double mutant strain produced a band of 548 bp (Figure 3.3C). The second band in the wild type strain was unexpected and is likely a result of non-specific binding of the primer pairs (Figure 3.3C). In the confirmation of the double mutant strain using the *dacB2* primer set (Figure 3.3B), the wild type strain produced a band of 764 bp, while the

double mutant strain produced a dark band of 564 bp (Figure 3.3C). *dacB1* and *dacB2* was successfully deleted in the double mutant strain.

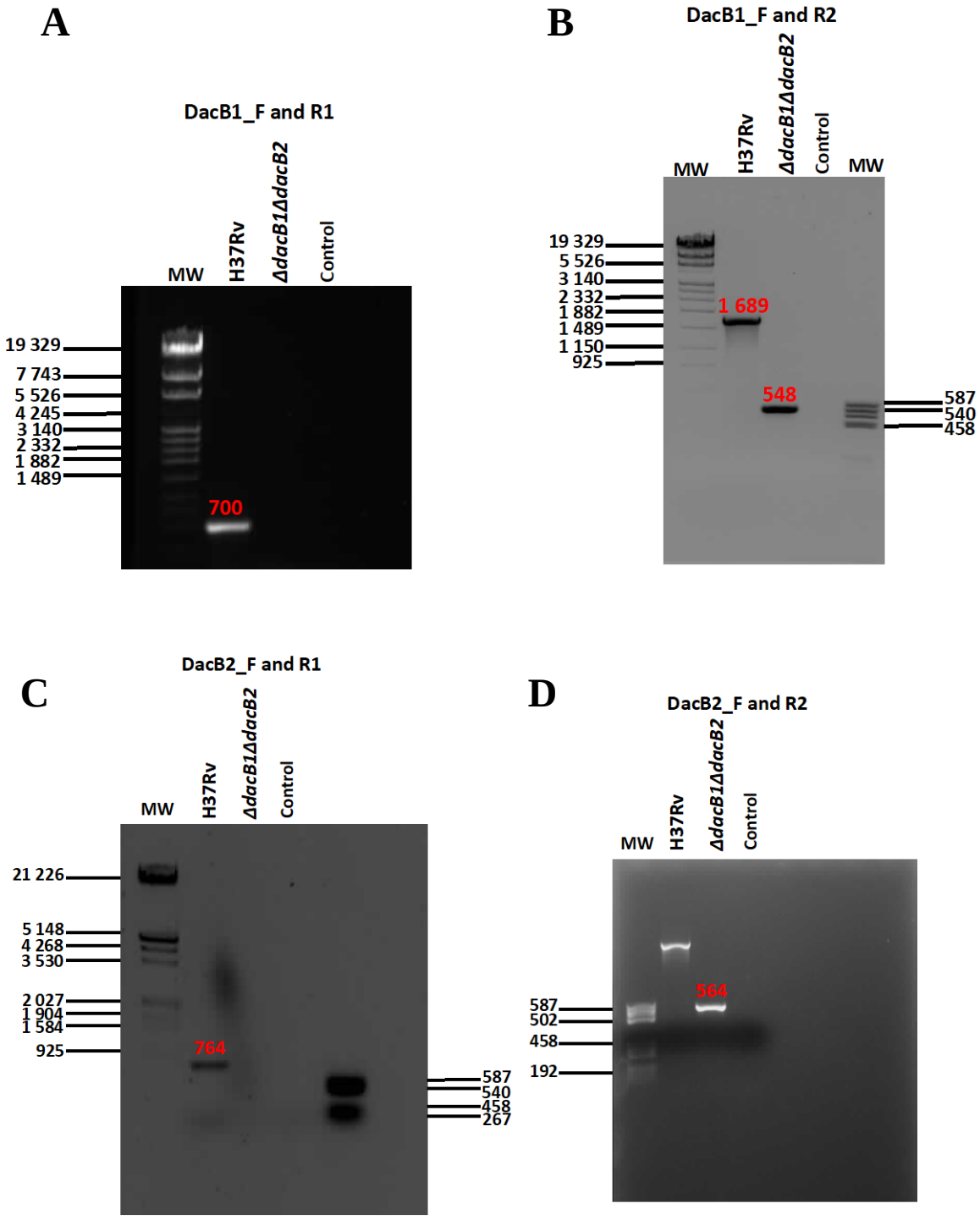
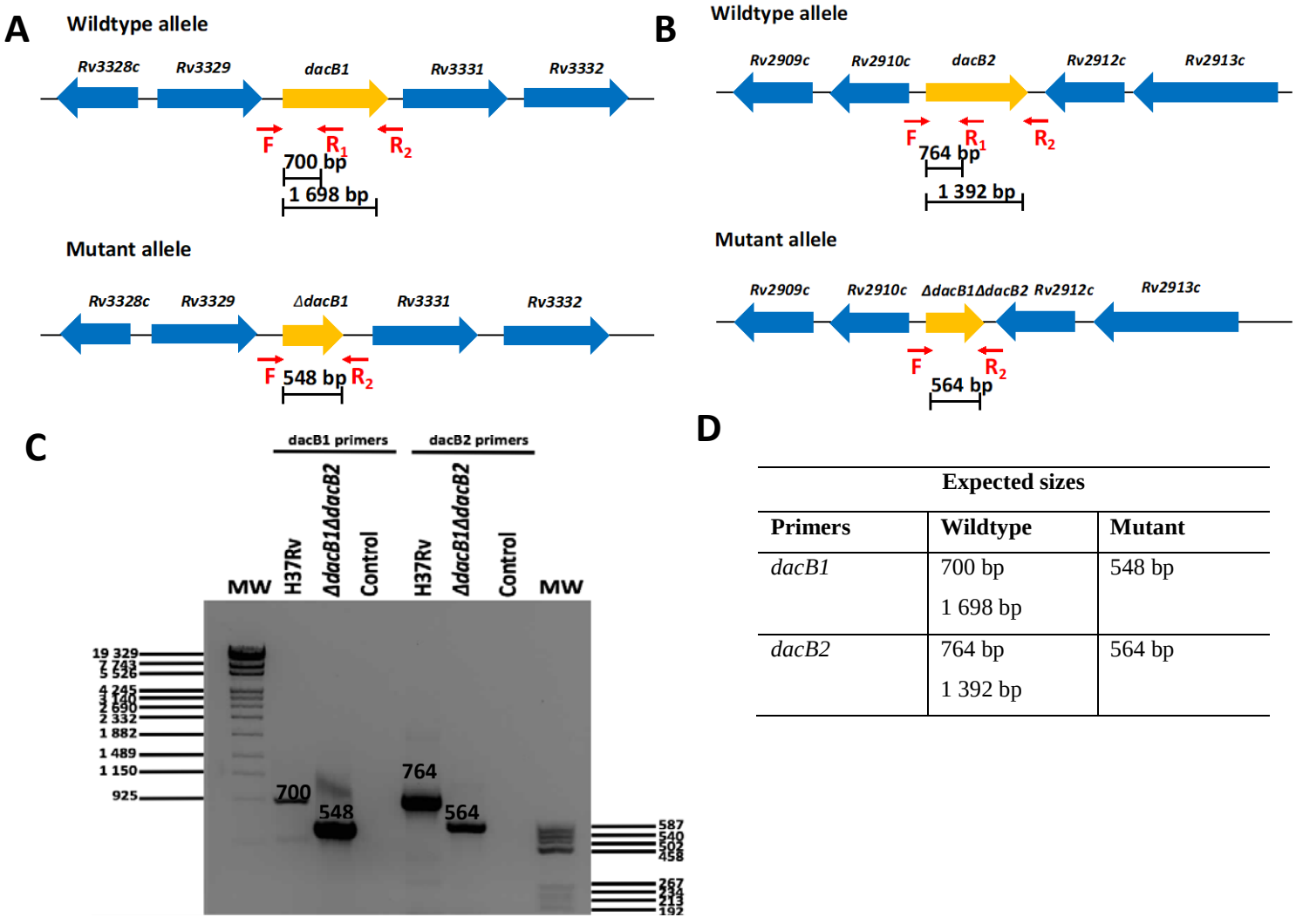


Figure 3. 2: Confirmation of double mutant in *Mtb* using *dacB1* and *dacB2* primers. PCR was used to confirm the deletion of *dacB1*(A and B) as well as the deletion of *dacB2* (C and D) with the forward and internal reverse primer (A and C) and forward and external reverse primer (B and D). The bands sizes are indicated in red.



Expected sizes		
Primers	**Wildtype**	**Mutant**
dacB1	700 bp 1 698 bp	548 bp
dacB2	764 bp 1 392 bp	564 bp

Figure 3. 3: Confirmation of DD-Cpase double mutant in *Mycobacterium tuberculosis*. Genomic map illustrating *dacB1* (A) and *dacB2* (B) for the wild type and mutant alleles. Flanking primers are shown in red while the yellow arrows represent the DD-Cpase genes. The expected fragment sizes are indicated. PCR was used to confirm the double mutant (C). The expected sizes for wild type and the DD-Cpase triple mutant using the *dacB1* primer set and *dacB2* primer set are indicated in the table (D).

3.3 There is a difference in the MICs of first line drug treatment and cell wall targeting antibiotics between wild type and the triple mutant in *Msmeg*

To determine if there was a difference in the susceptibility to first line drug and other cell wall targeting antibiotics treatment between the wild type and triple mutant strains in *Msmeg*, a micro-broth dilution assay was performed. All MICs were performed in triplicate with six biological repeats. Liquid media and DMSO were used as controls. The MIC_{90} values were read directly from the 96 well plates (Supplementary Figure 1B). An increase or decrease in the MIC_{90} value in comparison to wild type, is highlighted in green and red, respectively. For RIF, the wild type had an MIC_{90} of 2.5 µg/ml, while the triple mutant had an MIC_{90} of 1.03 µg/ml (Table 3.1). This was significantly different ($p < 0.01$). All replicates in the wild type were identical while there was a standard deviation of 0.4 between the replicates of the triple mutant strain. It was found that the *Msmeg* strains in the laboratory are resistant to INH (Table 3.1). The third replicate used RIF as a positive control to ensure that the set-up of the MICs was correct. For Meropenem, the MIC_{90} was found to be 4.5 µg/ml in wild type but 4 µg/ml in the triple mutant (Table 3.1). A standard deviation of 4.9 was observed in the wild type strain but all replicates were identical in the mutant. Vancomycin had an MIC_{90} of 1.95 µg/ml in the wild type and 1.215 µg/ml in the mutant (Table 3.1). All replicates were identical for wild type and a standard deviation of 1.04 was observed in the triple mutant strain. Several MICs were repeated using EMB, at varying concentrations, but no MIC_{90} was able to be determined (Supplementary Figure 1B). No alamar blue was added to these MIC plates as there was no clear MIC. There was no significant difference between the MIC_{90} values between wild type and the triple mutant strain for Vancomycin and Meropenem.

Table 3. 1: Minimum inhibitory concentration of antibiotics in *Msmeg*

Antibiotic	Expected MIC from literature	Reference	mc^2155	Δ1661Δ2432Δ2433
Rifampicin	8-25	Piddock, et al., 2000; Stephan, et al., 2004	2.5	1.03
Isoniazid	>40	Stephan, et al., 2004	Resistant	Resistant
Meropenem	4-8	Botella, et al., 2007	4.5	4
Vancomycin	5-8	Stephan, et al., 2004	1.95	1.215

*All MIC_{90} reported in µg/ml

3.4 There is no difference in the MICs of first line drug treatment and cell wall targeting antibiotics between wild type and the double mutant in *Mtb*.

An MIC_{90} determination using the micro-broth dilution assay was used to confirm if there was a difference in susceptibility to first line drug treatment and other cell wall targeting antibiotics between the wild type and double mutant strains in *Mtb*. All MICs were performed in triplicate with six biological repeats. Liquid media and DMSO were used as controls. The MIC_{90} values were read directly from the 96 well plates (Supplementary Figure 2B). For RIF the wild type and mutant strain had an MIC_{90} of 4 µg/ml and 3 µg/ml respectively (Table 3.2). For isoniazid the MIC_{90} was found to be 0.15 µg/ml (Table 3.2). The MIC_{90} for Meropenem was determined to be 1.17 and 1.67 µg/ml for the wild type and the mutant strains, respectively (Table 3.2). For Vancomycin the MIC_{90} was found to be 2.12 µg/ml (Table 3.2). The MIC_{90} for Ethambutol was observed to be 3.03 and 2.52 µg/ml for the wild type and mutant strains respectively (Table 5.2). There was no significant difference between the MIC_{90} for wild type and the double mutant for RIF, INH, Meropenem, Vancomycin and EMB.

Table 3. 2: Minimum inhibitory concentration of antibiotics in *Mtb*

Antibiotic	**Expected MIC from literature**	**Reference**	**H37Rv**	***ΔdacB1ΔdacB2***
Rifampicin	0.003-0.006	Kana, et al., 2010	4	3
Isoniazid	0.025	Kana, et al., 2010	0.15	0.15
Meropenem	1	Botella, et al., 2007	1.67	1.67
Vancomycin	6.25-12.5	Kana, et al., 2010	2.12	2.12
Ethambutol	1.6-3.1	Kana, et al., 2010	3.03	2.52

*All MICs reported in µg/ml

3.5 Complementation of the Δ*1661*Δ*2432*Δ*2433* mutant in *Msmeg*

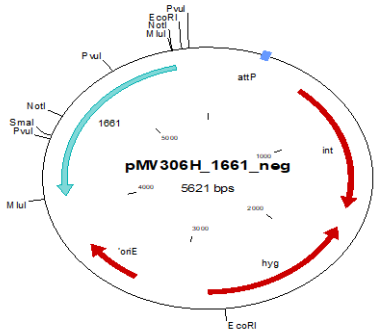
To interrogate whether each of the homologues had a difference in susceptibility to first line drugs and other cell wall targeting antibiotics similar to that seen between *mc²155* and Δ*1661*Δ*2432*Δ*2433*, complement strains were generated. The triple mutant was electrophoresed with full length *MSMEG_1661*, *MSMEG_2432* or *MSMEG_2433* as well as their respective native promoters. The plasmid was mapped before electroporation was performed.

3.5.1 Restriction digest analysis of the *1661pmv306H*, *2432pmv306H* and *2433pmv306H* plasmids

The *MSMEG_1661*, *MSMEG_2432* and *MSMEG_2433* genes were previously cloned into the pmV306H vector with a hygromycin selectable marker (Figure 3.4). For the complementation of the *MSMEG_1661*, *MSMEG_2432* and *MSMEG_2433* genes into the Δ*1661*Δ*2432*Δ*2433* mutant strain a restriction digest of the *1661pmv306H* (Figure 3.4A), *2432pmv306H* (Figure 3.4B) and *2433pmv306H* (Figure 3.4C) plasmids was performed. The restriction analysis produced the expected band sizes for all the restriction enzymes used. The plasmids were correct and could be used for electroporation.

A

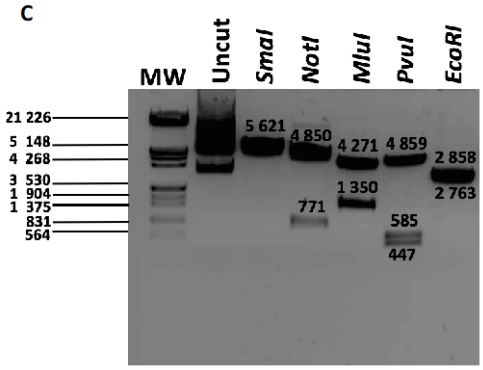
A



B

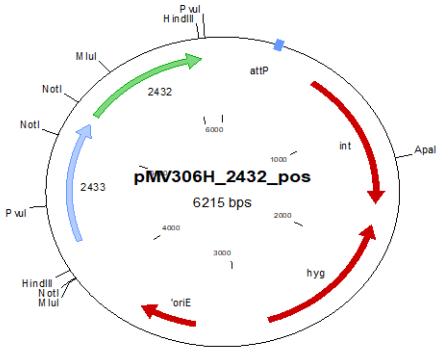
Expected sizes	
Restriction Enzyme	**Expected size (bp)**
SmaI	5 621
NotI	4 850 and 771
MluI	4 271 and 1 350
PvuI	4 859, 585 and 447
EcoRI	2 858 and 2 763

C



B

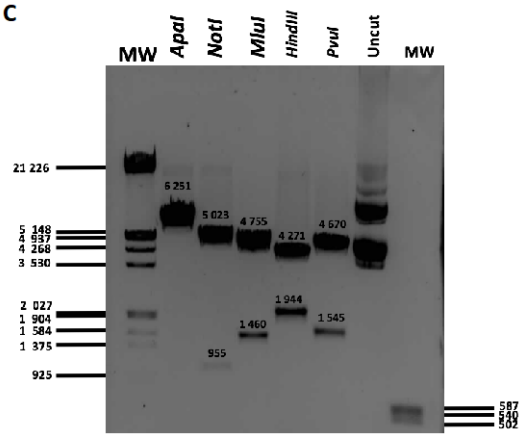
A



B

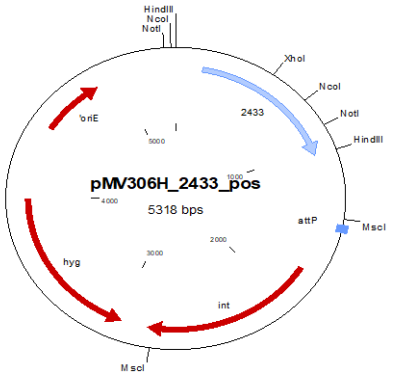
Expected sizes	
Restriction Enzyme	**Expected size (bp)**
ApaI	6 251
NotI	5 023 and 955
MluI	4 755 and 1 460
HindIII	4 271 and 1 944
PvuI	4 670 and 1 545

C



C

A



B

Expected sizes	
Restriction Enzyme	**Expected size (bp)**
XhoI	5 318
HindIII	4 271 and 1 047
NcoI	4 564 and 754
NotI	4 363 and 955
MscI	3 974 and 1 344

C

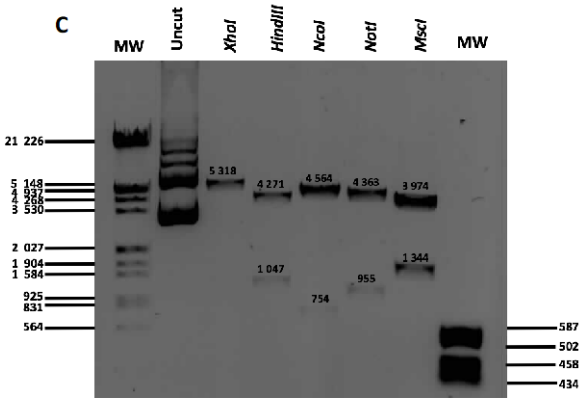


Figure 3. 4: Restriction digest analysis of *pmv306H* plasmids. Plasmid maps of *pmv306H1661* (A), *pmv306H2432* (B) and *pmv306H2433* (C) are provided. The restriction digest fragments were resolved on a 0.8% agarose gel and the expected band sizes are shown in the respective tables.

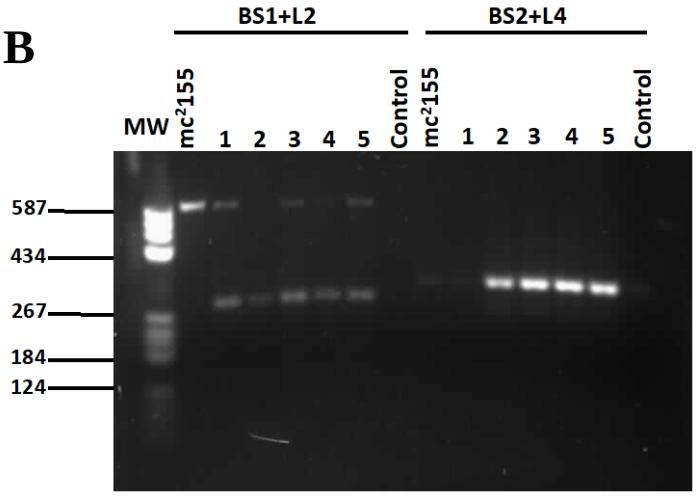
3.5.2 Confirmation of complemented derivatives by PCR

Integration of the complement vector was confirmed by PCR. The CFU/ml and transformation efficiency were determined for each of the complement strains at 1 µg and 3 µg of plasmid DNA, as well as for the positive control (Table 3.3). The plates are shown in the appendix

(Supplementary Figure 1C). Each of the strains had a high CFU/ml and transformation efficiency at 1 µg and 3 µg of plasmid DNA except for Δ*1661*Δ*2432*Δ*2433::2433* when 1 µg of plasmid DNA was electrophoresed (Supplementary Table 1C). The difference in CFU/ml and transformation efficiency values was due to the different amounts of gDNA used. There was minimal growth on the negative control plate, but these were colonies of Δ*1661*Δ*2432*Δ*2433* that were resistant to hygromycin (Supplementary Figure 1C).

Five colonies from each strain were picked from the plates. Half of the colony was used to inoculate cultures for freezer stocks while the other half was used for small-scale gDNA extraction. The extracted gDNA was used to confirm the complement derivatives by PCR. Two primer pairs were used to confirm the complement strains, BS1+L2 and BS2+L4. The wild type strain was used as a negative control. The expected band sizes for BS1+L2 and BS2+L4 were 282 bp and 320 bp respectively (Figure 3.5A). For the confirmation of Δ*1661*Δ*2432*Δ*2433::1661*, there was an unexpected band in the wild type lane, but this was deemed to be non-specific binding as a band of the same size appeared in lanes of the complement strains (Figure 3.5B). The expected bands were obtained for BS1+L2 for each of the five colonies as well as for BS2+L4 (Figure 3.5A). There was a faint band in the negative control lane for BS2+L4, which was due to contamination in the primer stock (Figure 3.5B). However, the use of BS1+L2 was sufficient enough to confirm that the strains were indeed complements (Figure 3.5B). A similar result was seen in the confirmation of Δ*1661*Δ*2432*Δ*2433::2432* (Figure 3.5C) and Δ*1661*Δ*2432*Δ*2433::2433* (Figure 3.5D).

B



A

Expected sizes	
Primer pair	**Expected size (bp)**
L2+BS1	282
L4+BS2	320

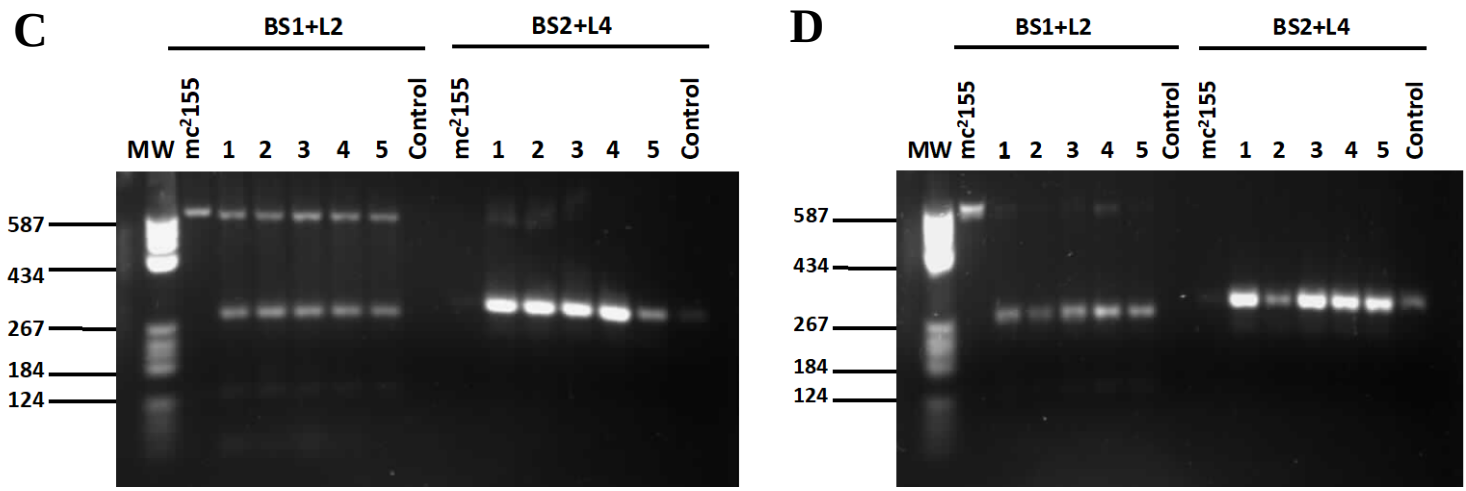


Figure 3. 5:Confirmation of complement strains in *Msmeg* by PCR. Five colonies from each complement strain were confirmed by PCR using two primer pairs, BS1+L2 and BS2+L4. The expected band sizes for each primer pair are indicated in a table (A). The agarose gel of the PCR products of Δ*1661*Δ*2432*Δ*2433::1661* (B), Δ*1661*Δ*2432*Δ*2433::2432* (C) and Δ*1661*Δ*2432*Δ*2433::2433* (D) are shown. *Mc²155* was used as a negative control. Another negative control of dH_2O in the place of gDNA was also included.

3.6 There was no significant difference in the MIC values for Rifampicin, Vancomycin and Meropenem between wild type, the triple mutant and complement strains in *Msmeg*

To determine if there was a change in susceptibility to RIF, Vancomycin and Meropenem between the complement derivatives, triple mutant and wild type strains, a micro-broth dilution assay was performed to determine the MIC_{90}. The plates are shown in the Appendix, Supplementary Figure 2D. The MIC_{90} for wild type was 5.83, 0.41 and 21,33 for RIF, Vancomycin and Meropenem respectively (Table 3.3). For RIF, the triple mutant and complement derivative strains the MIC remained unchanged at 4.17 µg/ml (Table 3.3). The compliment derivative strains, Δ*1661*Δ*2432*Δ*2433::2432* and Δ*1661*Δ*2432*Δ*2433::2433*, had an MIC_{90} of 0.12 µg/ml for Vancomycin while the triple mutant and the wild type strain had the same MIC_{90} of 0.41 µg/ml (Table 3.3). The complement strain Δ*1661*Δ*2432*Δ*2433::1661* had an MIC_{90} of 0.39 µg/ml for Vancomycin (Table 3.3). The triple mutant and the complement strains, Δ*1661*Δ*2432*Δ*2433::1661* and Δ*1661*Δ*2432*Δ*2433::2432* had an MIC of 16 µg/ml while Δ*1661*Δ*2432*Δ*2433::2433* had and MIC of 13.33 for Meropenem (Table 3.3).

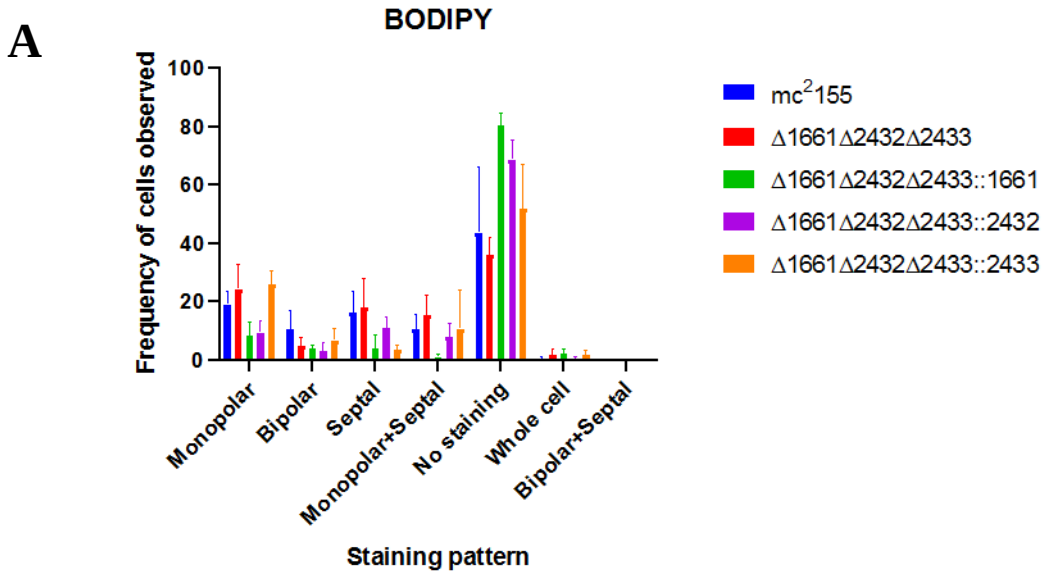
Table 3. 3: Minimum inhibitory concentration of antibiotics in *Msmeg* derivative strains

*All MICs reported in µg/ml

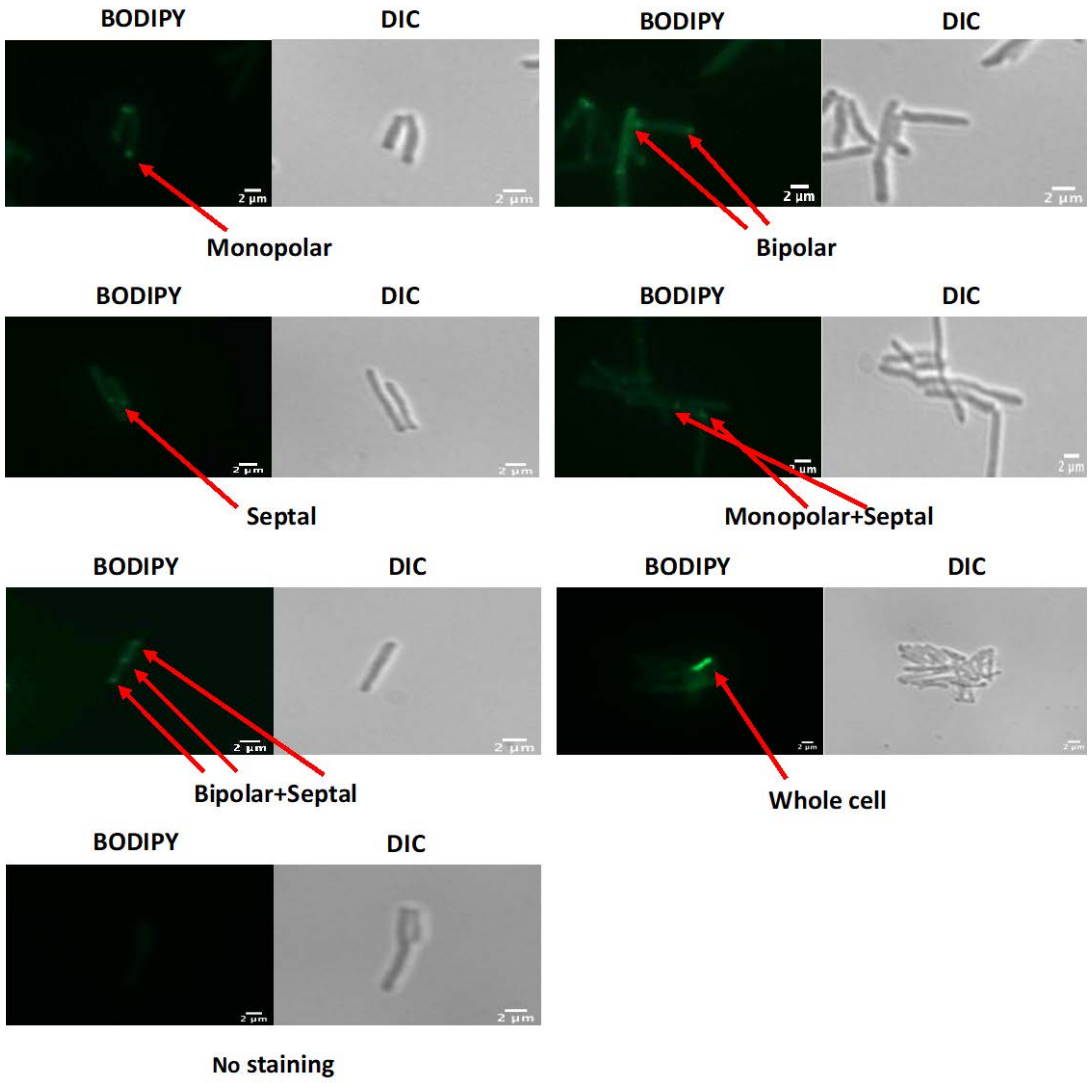
Antibiotic	Expected MIC	mc²155	Δ1661Δ2432Δ2433	Δ1661Δ2432Δ2433 ::1661	Δ1661Δ2432Δ2433 ::2432	Δ1661Δ2432Δ2433 ::2433
Rifampicin	8-25	5,83	4,17	4,17	4,17	4,17
Vancomycin	8	0,41	0,41	0,39	0,12	0,12
Meropenem	5	21,33	16	16	16	13,33

3.7 There was no significant difference in the PG biosynthesis or cross-linking patterns, as observed by fluorescent vancomycin, between the wild type, triple mutant strains as well as the complement derivative strains in *Msmeg*

There was a difference in Vancomycin MIC between the wild type and triple mutant strain, although, this difference was not significant. BODIPY Vancomycin was incorporated into the PG layer of the *Mmseg* strains to observe if there were any changes in PG biosynthesis or cross-linking patterns. A hundred cells per biological repeat for each strain were observed, according to section 3.10, and their staining patterns noted. No significant difference in the staining patterns were observed between the different strains (Figure 3.6A and B). Interestingly, it was noted that a portion of the complemented derivatives and triple mutant strain displayed polar budging (Figure 3.6C). These cell phenotypes were a small proportion and completely absent in the wild type strain (Figure 3.5D).



B


BODIPY
DIC
Monopolar
BODIPY
DIC
Bipolar
BODIPY
DIC
Septal
BODIPY
DIC
Monopolar+Septal
BODIPY
DIC
Bipolar+Septal
BODIPY
DIC
Whole cell
BODIPY
DIC
No staining

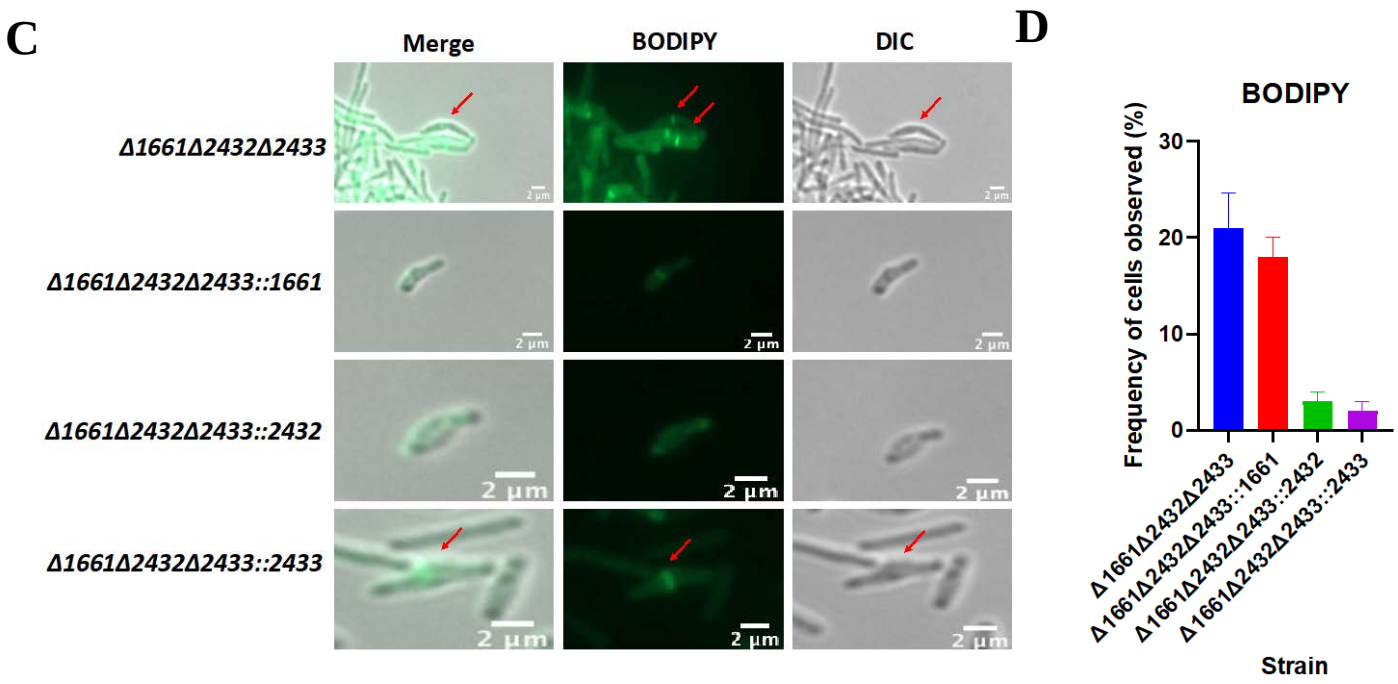


Figure 3. 6: BODIPY Vancomycin staining of wild type, triple mutant, and the complement strains in *Msmeg*. The staining pattern of the wild type, triple mutant and complement strains were observed (A). The microscopy images are provided (B). A portion of the mutant and complement strains had polar bulging (C) and the frequency of cells was recorded (D). Where multiple cells are present the bulging cells are indicated by a red arrow.

3.8 There was no difference between the MICs of Augmentin in the wild type and mutant strains in *Msmeg* and *Mtb*

To determine the concentration of Augmentin to be used in the exposure of the transposon mutagenesis library, a mirco-broth dilution assay was performed. Experiments were performed in triplicate with six biological repeats. Liquid media and DMSO diluted in liquid media were used as controls. The MIC_{90} was determined from each plate (Supplementary Figure 1D). As expected, the plates that only had clavulanate present did not produce an MIC for *Msmeg* and *Mtb* (Table 3.4 and 3.5). Clavulanate is a ß-lactamase inhibitor and not an antibiotic, therefore, will not result in the killing of bacteria. The amoxicillin MIC_{90} in *Mtb* was found to be 7,8 µg/ml (Table 3.5) and 125 µg/ml in *Msmeg* (Table 3.4). While the Augmentin MIC_{90} was found to be 0,024 µg/ml in *Mtb* (Table 3.5) and 7,8 µg/ml (Table 3.4) in *Msmeg*. There was no difference in the MIC_{90} between wild type and the mutant strains for Augmentin, Amoxicillin and Clavulanate for *Msmeg* and *Mtb*. However, the study conducted by Mishra *et al.* (2017) showed that all three DD-Cpases in *Mtb* had altered expression levels in response to Augmentin.

Therefore, PG biosynthesis and crosslinking was interrogated to determine if there was an observable change on a cellular level that would have been missed by the MICs.

Table 3. 4: Minimum inhibitory concentration of Augmentin in *Msmeg*

Antibiotic	Expected MIC	Reference	mc^2155	Δ1661Δ2432Δ2433
Clavulanate	0	-	0	0
Amoxicillin	100	Mishra et al., 2017	125	125
Augmentin	-	-	7,8	7,8

*All MICs reported in µg/ml

Table 3. 5: Minimum inhibitory concentration of Augmentin in *Mtb*

Antibiotic	Expected MIC	Reference	H37Rv	Δ*dacB1*Δ*dacB2*
Clavulanate	0		0	0
Amoxicillin	8	Mishra et al., 2017	7,8	7,8
Augmentin	-		0,024	0,024

*All MICs reported in µg/ml

3.9 There was no significant difference in the cell length and PG biosynthesis between wild type and the triple mutant in *Msmeg* when exposed to Augmentin

To determine if there was a change in cell length and staining pattern between mc^2155 and the Δ*1661*Δ*2432*Δ*2433* mutant in *Msmeg*, cells were exposed to Augmentin (at 0.5x MIC) and stained with TADA (an FDAA). *Msmeg* cultures were split in half; half of the cells were exposed to Augmentin and the other half were not. An unlabeled control was also used for each batch of cells. The length and staining patterns of a hundred cells per biological repeat were recorded. There was no significant difference in cell length between cells that were exposed to Augmentin versus those that were not (Figure 3.7A). There was also no significant difference in cell length between the two strains (Figure 3.7A). No difference in staining pattern was observed between cells that were exposed to Augmentin and those that were not (Figure 3.7B). No significant difference in the staining pattern between strains was noted (Figure 3.7B).

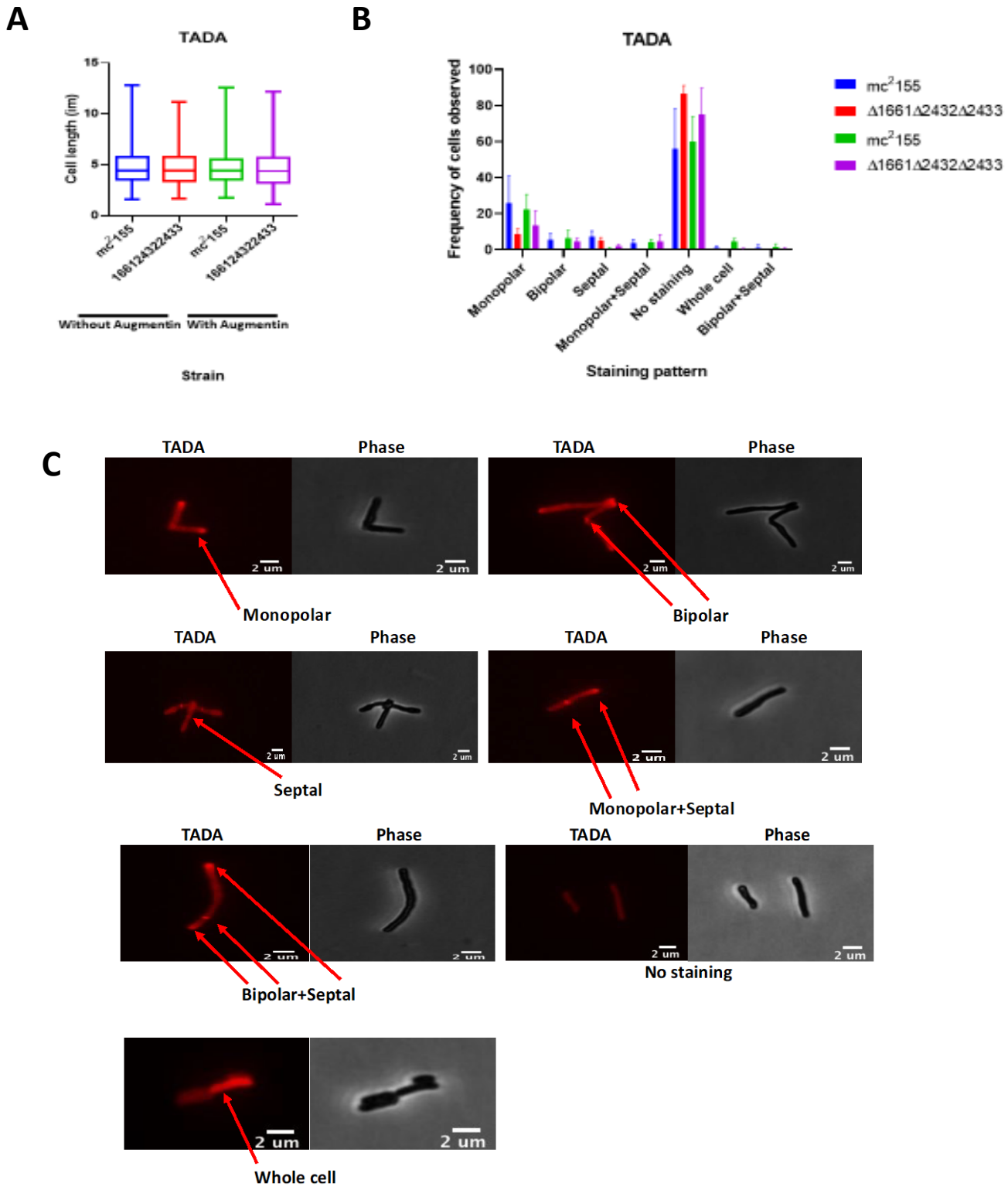
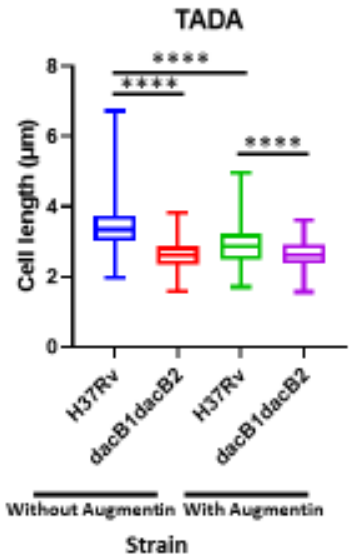


Figure 3. 7: Cell length and staining pattern of *Msmeg* cells observed under a fluorescent microscope. The cell length of a hundred cells per biological repeat were noted (A) as well as their staining pattern (B). Cells exposed to Augmentin are in green and purple for wild type and the triple mutant, respectively, while those that were not exposed are shown in red (*mc²155*) and blue *(Δ1661Δ2432Δ2433*). The microscopy images explaining the staining patterns observed are provided (C).

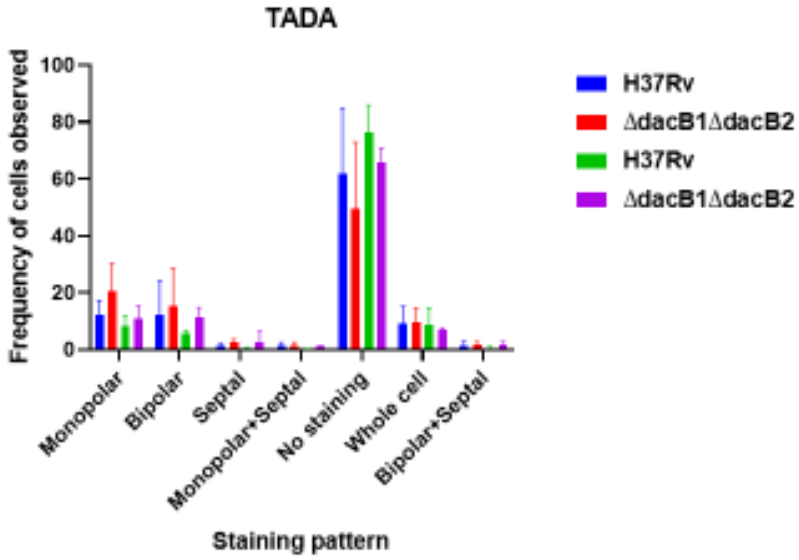
3.10 There was a significant difference in the cell length between *H37Rv* and Δ*dacB1*Δ*dacB2* in *Mtb* but no difference in staining pattern was noted

To determine if there was a change in cell length and staining pattern between *H37Rv* and Δ*dacB1*Δ*dacB2* mutant in *Mtb*, cells were exposed to Augmentin (0.5x MIC) and stained with TADA. *Mtb* cultures were split in half; half of the cells were exposed to Augmentin and the remaining half was not. An unlabeled control was also used for each batch of cells. The length and staining of a hundred cells per biological repeat were recorded. There was a significant difference in cell length ($p < 0.0001$) between the wild type and double mutant strain when exposed to Augmentin (Figure 3.8A). Similarly, a difference in cell length was observed in the absence of Augmentin (Figure 3.8A). *H37Rv* cells that were exposed to Augmentin are longer in length ($p<0.0001$), then those that were not, while no significant difference between the treated and untreated Δ*dacB1*Δ*dacB2* cells was observed (Figure 3.8A). No significant difference was observed in the staining pattern between wild type and the double mutant strains. There was no difference in the staining pattern between cells exposed to Augmentin and those that were not (Figure 3.8B). Microscopy images to describe the staining patterns are provided in Figure 3.8C. *H37Rv* cells appeared to be longer in length than Δ*dacB1*Δ*dacB2* cells.

A



B



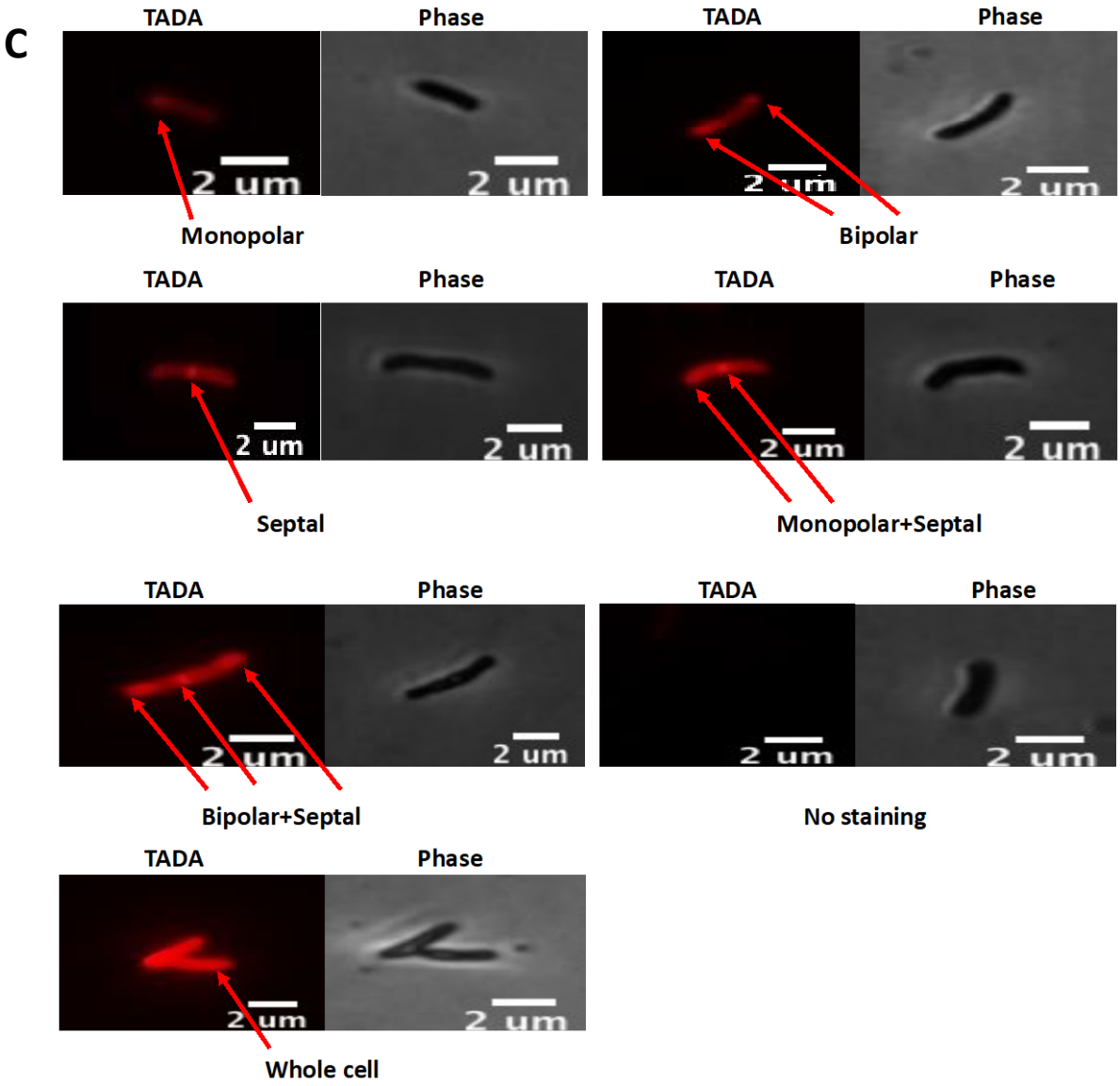


Figure 3. 8: Cell length and staining pattern of *Mtb* cells observed under a fluorescent microscope. The cell length of a hundred cells per biological repeat were noted (A) as well as their staining pattern (B). Cells exposed to Augmentin are in green and purple for wild type and the double mutant, respectively, while those that were not exposed are shown in red (*H37Rv*) and blue *(ΔdacB1ΔdacB2*). The microscopy images for the cells exposed to Augmentin (C) and those that were not (D) is shown.

3.11 Bulking up of øMycoMarT7 mycobacteriophage stock for maximal viral titre (PFU/ml) and library construction

The MIC for Augmentin has been established and can be used in the exposure of the transposon mutagenesis library. Various mycobacterial phage stocks were prepared according to section 4.2.1 to transduce *Mtb* strains in order to create a transposon mutagenesis library. This was done multiple times and the various phage stocks mixed together in order to obtain a PFU/ml of approximately 10^{10}, as anything lower would not be able to generate a transposon mutagenesis library of a CFU/ml of 10^5 or higher. It was also noted that if the mycobacterial phage stock was stored at 4ºC for a long period the PFU/ml would start to decrease. An example of a high mycobacterial phage stock (~10^{11} PFU/ml) is shown in Figure 3.9.

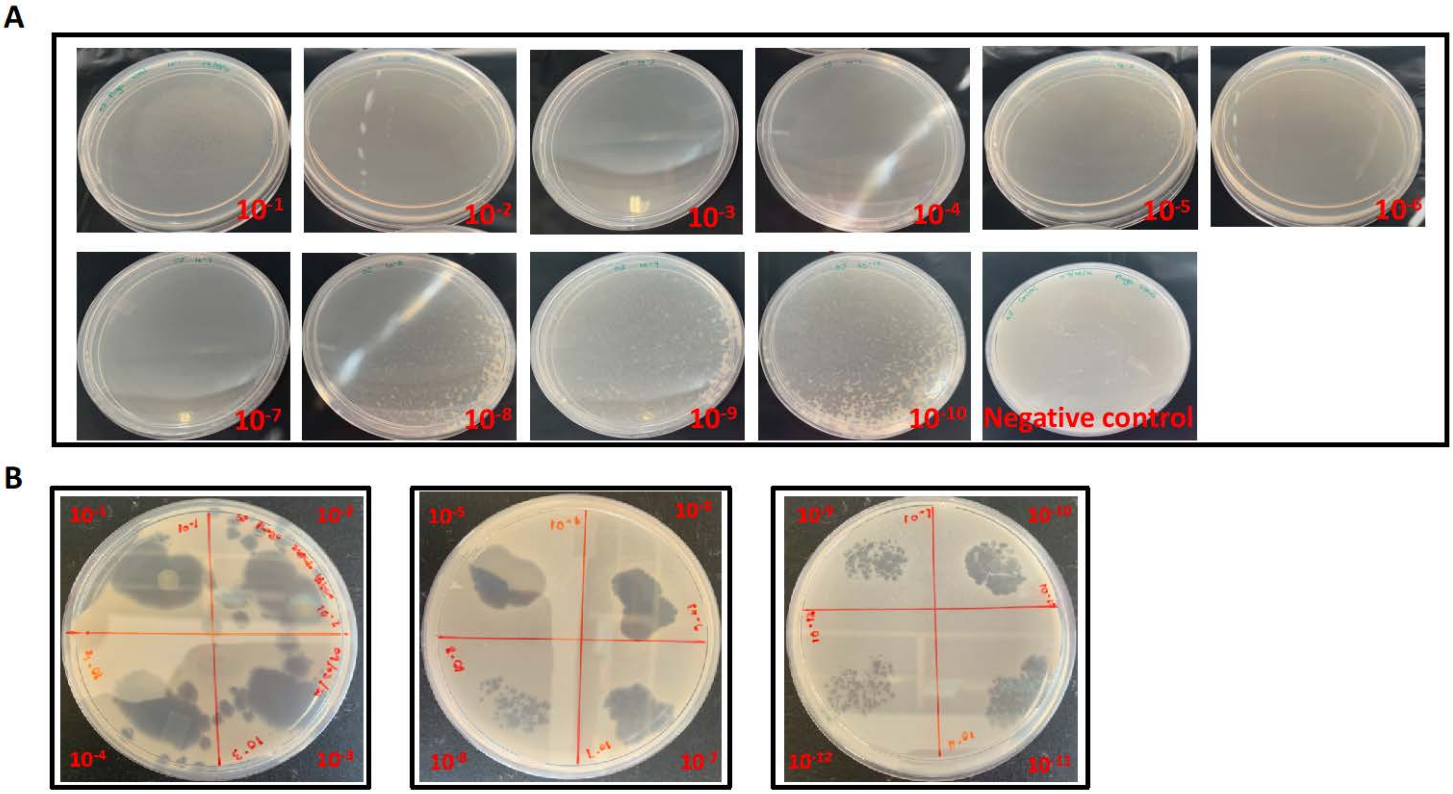


Figure 3. 9: High titer øMycoMarT7 phage stock. øMycoMarT7 phage stock was prepared and the PFU/ml determined (A). A spot test of the øMycoMarT7 phage stock was done in order to determine the PFU/ml of the combined phage stock (B). The øMycoMarT7 phage stock was deemed to be adequate enough for mycobacterial transductions.

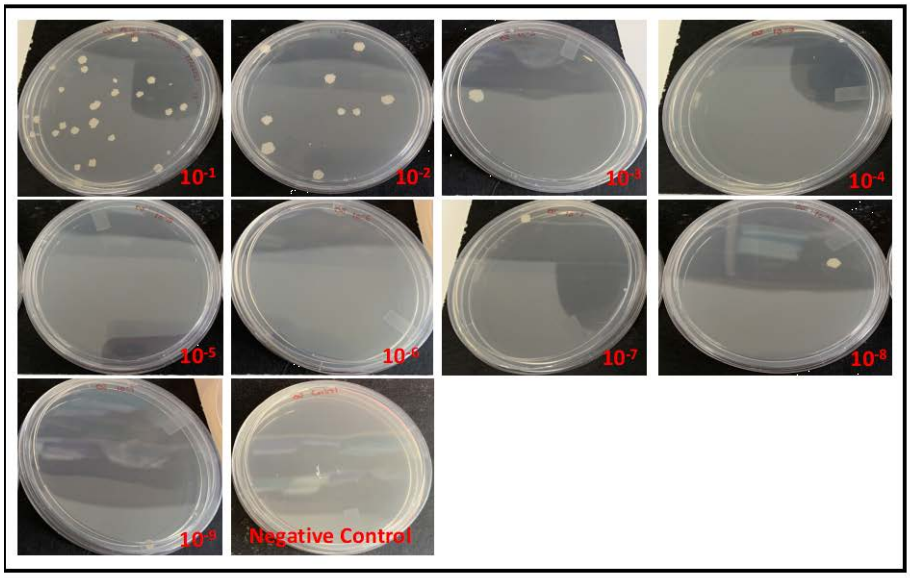
3.12 Transposon mutagenesis library in *Mtb* strains was deemed to have inadequate library/genome coverage

A transposon mutagenesis library in *Mtb* strains was generated according to section 4.2.3. Initially the method used was according to Griffin, et al. (2011) but the CFU/ml of the phage stock was too low to send for NGS (Table 3.6). An adequate transposon library with sufficient coverage has CFU/ml of 10^5. Therefore, transductions were performed in *Msmeg* to perfect the technique before trying again in *Mtb*. When transposon mutagenesis was performed in *Msmeg*the dilution series did not work as expected. Colonies formed on plates from 10^{-1} to 10^{-3} and then again on 10^{-7} and 10^{-8} (Figure 3.10A). This result was unexpected and the CFU/ml could not be determined. This was repeated twice more with a similar result (Supplementary Figure 2E). It was possible that the ratio of mycobacterial cells to mycobacterial phage stock was wrong. Therefore, the ratio of phage stock to cells was adjusted to 1:1, 1:0.5 and 1:0.1 and transposon mutagenesis performed again in *Msmeg*, according to Griffin, et al. (2011; Figure 3.9B; Supplementary Figure 3E). There was no significant difference in the CFU/ml between the different ratios used. It was decided that the method should be changed. The new method, according to Majumdar, *et al*. (2017), was performed several times in *Mtb* with a small adjustment to the method each time. However, the CFU/ml of the transposon mutagenesis library remained low (plates are shown in Supplementary Figure 4E). Therefore, the CFU/ml of the transposon mutagenesis library was deemed inadequate for sufficient coverage.

Table 3. 6: CFU/ml of transposon mutagenesis libraries in *Mtb* and the methods used

Date	H37Rvs (CFU/ml)	ΔdacB1ΔdacB2 (CFU/ml)	Method	Adjustment
01/12/20	$1{,}65x10^4$	$2{,}06x10^4$	Griffin, *et al.*, 2011	No adjustment
02/12/20	$2{,}95x10^3$	$8{,}2x10^3$	Griffin, *et al.*, 2011	Increased PFU/ml of phage stock
27/05/21	No growth	No growth	Griffin, *et al.*, 2011	Plated same day instead of overnight incubation at 80ºC
10/06/21	$2{,}41x10^4$	$1{,}62x10^4$	Majumdar, *et al*. 2017	No adjustment
17/06/21	$8{,}2x10^3$	$7{,}5x10^3$	Majumdar, *et al*. 2017	Incubated with phage stock for 20 hrs
12/08/21	No growth	$1{,}02x10^4$	Majumdar, *et al*. 2017	Incubated PBS+Tween80 and MP Buffer at 37ºC overnight
26/08/21	$3{,}45X10^4$	$1{,}10x10^4$	Majumdar, *et al*. 2017	Increased OD_{600} of *Mtb* cultures to 1
29/09/21	$1{,}15x10^3$	$6{,}2x10^3$	Majumdar, *et al*. 2017	2 ml of phage stock used
22/10/21	No growth	No growth	Majumdar, *et al*. 2017	Prepared fresh mycobacterial phage stock and used same day as transductions

A



B

Mycobacterial transductions at various ratios of cells to phage stock	
Ratio (phage stock: *Msmeg* cells)	**CFU/ml**
1:1	$5.1x10^3$
1:0.5	$3x10^3$
1:0,1	$1,05x10^3$

Figure 3. 10: Mycobacterial phage transductions in *Msmeg*. A transposon mutagenesis library was generated in *Msmeg* (A) but the CFU/ml could not be determined. The ratio of øMycoMarT7 to *Msmeg* cells was adjusted and transposon mutagenesis in *Msmeg* performed again (B). There was no significant difference between the CFU/ml between the different ratios used.

A low CFU/ml is indicative of a low rate of transposon insertion or genome coverage. There are potential reasons for this, including the high GC content of *Mtb*, but it was decided that this library would not be sent for seqeuncing. The reason for this decision is that the essential genes identified by sequencing could be as a result of a lack of insertions and not because the gene was essential. The focus of this study shifted to identififying a novel mycobacterial phage from soil.

3.13 Mycobacterial phage isolation from soil

øMycoMarT7 was not performing at an optimal level. The focus of this study therefore shifted to the identification of a new mycobacterial phage that could infect TB and replace *Himar1* gene with *Himar5*. This was achieved by purifying approximately 150 soil samples, from various parts of Gauteng, and testing for mycobacterial phage activity according to section 4.3.1. øMycoMarT7 was used as a positive control for plaque identification. Three mycobacterial phages were identified and two were able to be regrown and bulked up according to section 4.2.3 (Figure 3.11A). Soil samples that contained no mycobacterial phage are shown in Supplementary Figure 5E. The mycobacterial phages were used to make stocks and a PFU/ml of 10^5 was used to test for lytic activity in *Mtb*. The two mycobacterial phages were tested for lytic activity in *Mtb* using the traditional method of mycobacterial phage stock preparation (Figure 3.11B). One was able to form plaques in *Mtb*. This mycobacterial phage was named øIPJ3107 and is henceforth referred to as such.

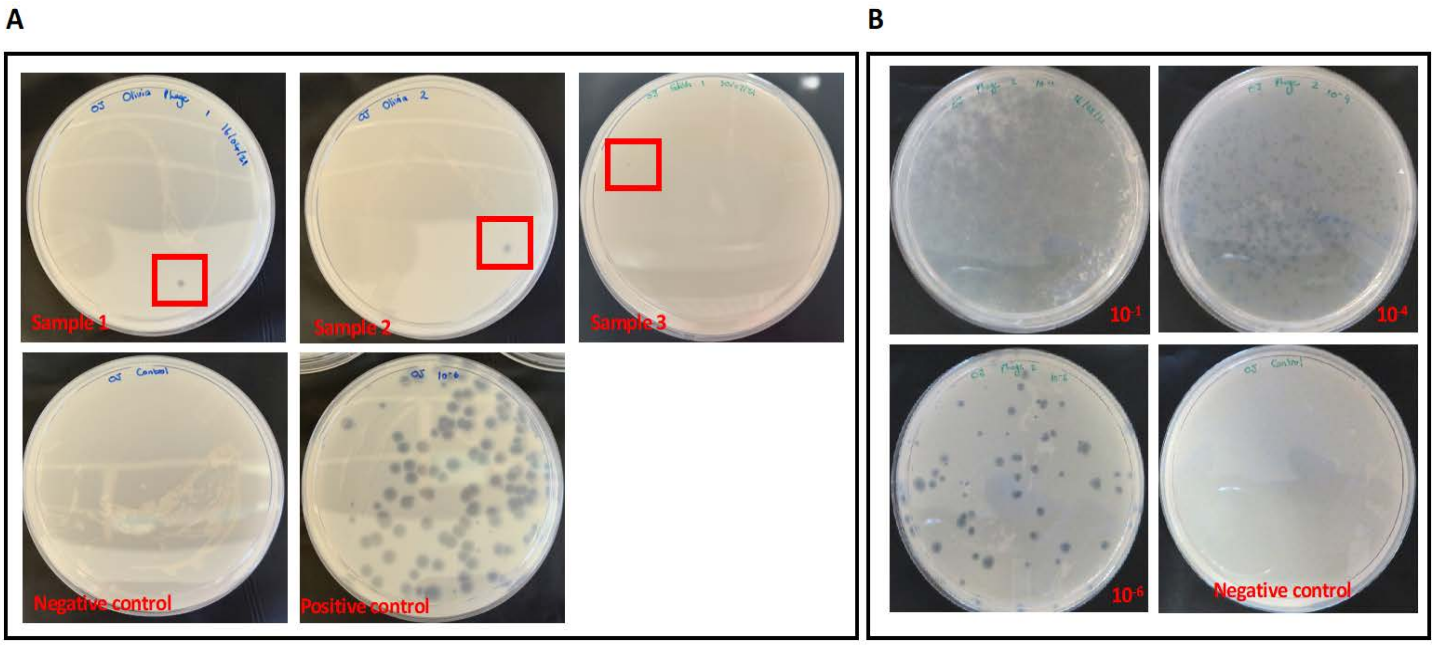


Figure 3. 11: Mycobacterial phage isolation from soil. Approximately 150 samples of soil were tested for mycobacterial phage activity. Three mycobacterial phages were successfully isolated (A). The plaque formation of the mycobacterial phages is highlighted by the red box. øMycoMarT7 was used as a positive control to identify successful plaque formation. A sample that contained no mycobacterial phage was used as a negative control. The two mycobacterial phages that were able to be regrown were tested for lytic activity in *Mtb* and one was able to form plaques (B).

3.14 øIPJ3107 forms larger plaques and is shorter in length and diameter compared to øMycoMarT7

A comparison between plaque formation at various temperatures was made between øMycoMarT7 and øIPJ3107. This was achieved by comparing the size and shape of the plaques formed. Mycobacterial phage stocks were prepared, and plates incubated at varying temperatures. As expected øMycoMarT7 only formed plaques at 30ºC (Figure 3.12A). øIPJ3107 formed plaques at 30ºC, 37ºC and even at 42ºC (Figure 3.12A). The size and length of plaques (visible clearing on top agar plates) was compared at 30ºC (Figure 3.12B). Plaque size and length is a measure of virulence in bacteriophages. øIPJ3107 formed significantly larger plaques ($p < 0.0001$) than øMycoMarT7.

A spot test was done to determine the PFU/ml of each of the mycobacterial phage stocks that would be sent for TEM (Supplementary Figure 7E). TEM analysis revealed that øIPJ3107 is 58.17 nm in diameter and 119.20 nm in length, while øMycoMarT7 is 59.19 nm and 230.64 nm in diameter and length, respectively (Figure 3.12C). Additional TEM images are provided in Supplementary Figure 8E. The significant difference in plaque length, as well as length and diameter between øIPJ3107 and øMycoMarT7, suggests that øIPJ3107 is more virulent than øMycoMarT7.

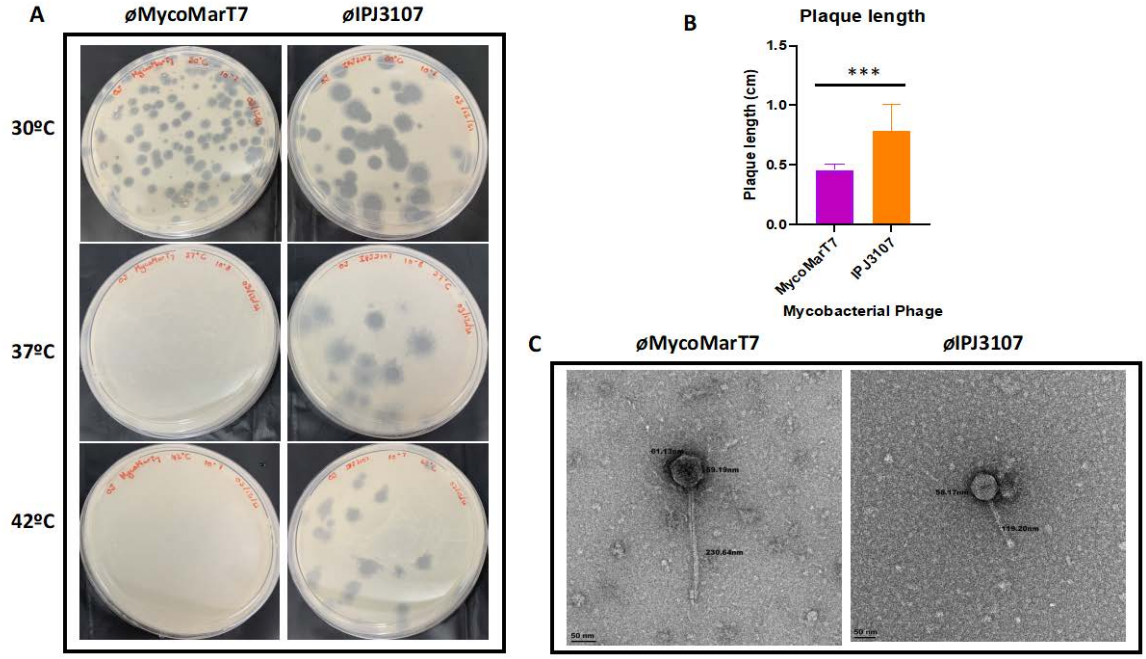


Figure 3. 12: øIPJ3107 plaque formation and TEM analysis in comparison to øMycoMarT7. Plaque formation was compared between the mycobacterial phages at 30ºC, 37ºC and 42ºC (A). Plaque length was measured and recorded at 30ºC (B). øIPJ3107 is significantly longer in length than øMycoMarT7. TEM analysis revealed that øMycoMarT7 is longer in both diameter and length than øIPJ3107.

3.15 Next generation sequencing analysis

3.15.1 The sequence data of øIPJ3107 was of a high quality

The quality of the extracted gDNA of øIPJ3107 was assessed by agarose gel electrophoresis, with øMycoMarT7 gDNA used as a quality control. The solid band produced by øIPJ3107 matches that of øMycoMarT7 and is indicative of gDNA of a high quality (Supplementary Figure 9E). The FastQC report revealed that the sequencing data was of a high quality. The quality score of the per base sequences were all in the green zone, which is indicative of very good quality calls (Supplementary Figure 10EA). The per sequence quality score had one solid peak meaning that the sequences have universally high-quality values (Supplementary Figure 10EB). According to the per base sequence content there was a high GC content present in the sequencing reads and was further confirmed by the per GC content (Supplementary Figure 10EC and D). Typically, there would be no difference between the different bases of the sequencing run but this was not of a concern as mycobacterial phages are known to have a high GC content. If the sequencer is unable to make a base call it will replace the base with an N and the percentage of this is summarized in the per base N content. The report revealed that this did not happen, and the base calling software was able to interpret the data well (Supplementary Figure 10EE). The length of the sequence fragments varied in length which is typical of PacBio® HiFi and the library had a low level of duplication, which indicates a very high level of coverage of the target sequence (Supplementary Figure 10EF). The library was not as diverse as expected as there were several overrepresented sequences. There was no adaptor content present in the sequencing data (Supplementary Figure 10EG).

3.15.2 øIPJ3107 is a novel mycobacterial phage that is classified under subcluster A1

The Quast report revealed that øIPJ3107 has a genome (present here as two contigs) of 50k bp in length with a GC content of 65.07%. There was a balance in length between the two contigs (57 666 bp). øIPJ3107 resembled genomes of various mycobacterial phages as well as mycobacterial viruses (listed in Supplementary Table 1E) and two unclassified taxids. The mycobacterial phages identified were all of subcluster A1, except for TM4, which belongs to subcluster K2. The genome of øIPJ3107 was annotated using Prokka and 155 hypothetical proteins were identified (Supplementary Table 2E). Approximately 95 of these proteins were classified as hypothetical proteins, 5 were unknown and 55 were able to be classified based on similarities to previously annotated mycobacterial phage proteins. The top ten mycobacterial phages that had the most similarity to the hypothetical proteins of øIPJ3107 are listed in Table

3.7. Of these, mycobacterial phages Wheeler, Trouble, HanShotFirst and TM4 were also identified by Kraken2.

Table 3. 7: Top ten mycobacterial phages that are similar to the hypothetical proteins of øIPJ3107

Mycobacterial phage	Subcluster	Frequency of similarity to proteins (%)
Wheeler	A1	23.87
Trouble	A1	20
Violet	A1	19.35
U2	A1	22.58
HanShotFirst	A1	23.23
SarFire	A1	21.94
Bethlehem	A1	19.35
Jasper	A1	18.71
Euphoria	A1	18.71
TM4	K2	50.32

4. Discussion

South Africa has one of the highest burdens of TB worldwide, accounting for an estimated 3.3% of global TB infections (WHO, 2021). Moreover, it is estimated that fifty percent of these individuals infected with TB are co-infected with HIV (WHO, 2021). The high co-infection rate, as well as the emergence of MDR and XDR TB, has necessitated the need for novel drugs and/or targets. A rich source of potential drug targets is the mycobacterial cell wall (Hett & Rubin, 2008). Due to its complex structure, the mycobacterial cell wall is impenetrable to a number of substances, contributing to some level of inherent resistance to certain antibiotics in *Mtb* (Hett & Rubin, 2008). Other antibiotics like fluoroquinolones and rifamycins pass through the cell wall more easily because they are lipophilic (Hett & Rubin, 2008). The PG layer of the cell wall is unique to bacteria and is required for the maintenance bacterial shape and counter-acting of internal osmotic pressure. During growth, the PG layer is constantly remodeled to allow for the insertion of new PG units (Hett & Rubin, 2008). PBPs are enzymes involved in the biosynthesis (via transglycolase and transpeptidase activities) and remodeling (through the hydrolytic activity of endopeptidases and carboxypeptidases) of PG. Although PBPs are a target of ß-lactam antibiotics, the presence of several ß-lactamase homologues renders this class of antibiotics ineffective, via active degradation, in most mycobacterial species. DD-CPases are classified as class C LMW PBPs and are present in high abundance in mycobacteria.

These enzymes cleave the terminal D-amino acid of the stem peptide thereby preventing cross linking of the stem peptide by HMW PBPs (Machowski, *et al*., 2014). Two (*dacB1* and *dacB2*) of the three characterized DD-CPase homologues in *Mtb* are not essential for *in vitro* growth and can be deleted from the genome (Bourai, *et al*., 2012; Machowski, *et al*., 2014). Following exposure to high concentrations of Augmentin, a microarray analysis of the transcriptome of *Mtb* suggested that WhiB4 (a cytoplasmic redox potential and intracellular redox sensor) plays a role in antibiotic tolerance by regulating various genes involved in cell-envelope associated pathways including stress responses, PG biosynthesis and ß-lactamase regulation *(Mishra, et al*., 2017). All three *Mtb* DD-Cpase homologues displayed altered expression levels, i.e., the expression of *dacB1* and Rv3627c was appeared to be induced while *dacB2* was repressed. An analysis into the potential ß-lactamase activity of PBPs in *Mtb* revealed that PBPs are effective in inhibiting several ß-lactams (Kumar, *et al*., 2022). The *Mtb* DD-Cpases were all observed to be inherently resistant to ß-lactams. These observations led us to hypothesize that in a DD-Cpase mutant background (i.e., simultaneous deletion of *dacB1* and *dacB2* in *Mtb*), the strain would either be more susceptible to β-lactams via the inability to properly sense the antibiotic or a disruption in the recruitment of proteins recruited following antibiotic sensing. In order to test this hypothesis, we attempted to use a transposon mutagenesis screen in the mutant strain following exposure to Augmentin. Two strains were used in this study *Msmeg* and *Mtb*. *Msmeg* is a non-pathogenic relative of *Mtb* and is typically used as a model organism to give insight into the genes and behavior of *Mtb*. The double mutant in *Mtb* is equivalent to the triple mutant in *Msmeg* and experiments were conducted in both strains to allow for a comparison to be made.

In order to assess whether the simultaneous deletion of two of the three DD-Cpase homologues in *Mtb* was associated with altered susceptibility to cell-wall targeting antibiotics, two previously constructed mutant mycobacterial strains were used in this study (described above). In both cases, the wild-type strains containing no gene deletions served as controls. The MICs of first line chemotherapy as well as other cell wall targeting antibiotics were determined. There was no statistically significant difference in the MIC_{90} values obtained between the wild type and mutant strains for both *Msmeg* and *Mtb* in response to cell wall targeting antibiotics vancomycin, meropenem and augmentin. In a recent study conducted by Kumar *et. al*, (2022) the ß-lactamase activities of all PBPs in *Mtb* were investigated by a ß-lactam hydrolysis assay, nitrocefin hydrolysis assay and BOCILLIN FL fluorescence inhibition assay. The HMW PBPs *PonA1* and *PonA2*, which were typically thought to only have transglycosylase and

transpeptidase activities, hydrolyzed penicillins and carbapenems more effectively than BlaC which was characterized as the main ß-lactamase in *Mtb*. In addition, HMW PBPs were two times more effective at hydrolyzing penicillins and carbapenems than LMW PBPs. This could potentially explain why no difference was observed in the MICs between the mutant and wild type strains of *Mtb*. It is a possibility that a similar mechanism of ß-lactamase activity is occurring in *Msmeg*, potentially explaining why there was no MIC_{90} difference observed between the wild type and triple mutant strains to ß-lactams.

When considering the susceptibility profiles of these strains to the first-line drug to treat TB (i.e., rifampicin), there was a significant difference in the MIC_{90} between the wild type and triple mutant strain in *Msmeg*. The triple mutant was two-fold more susceptible (as evidenced by a lower MIC_{90} value) relative to the wild type. Typically, resistance to RIF has been characterized by mutations in one of three loci in the *rpoB* gene (Piddock, *et al*., 2000). However, there have also been documented cases of RIF resistant *Mtb* strains that lack mutations in the *rpoB* gene, suggesting that RIF resistance could possibly be mediated by another mechanism (Piddock, *et al*., 2000). The mycobacterial cell wall is composed of multiple layers and is impenetrable to a number of substances resulting in it being a natural source of antibiotic tolerance (Piddock, *et al*., 2000). A possible explanation for the differences observed in the RIF MIC_{90} values for *Msmeg* could be a weakening of the cell wall in Δ1661Δ2432Δ2433 due to altered PG cross-linking, which inadvertently causes an increased uptake of RIF into the cell. This can be proven by an ethidium bromide diffusion assay. In an *ami1*mutant background there was enhanced diffusion of ethidium bromide in comparison to wild type *Msmeg* (Senzani, *et al*., 2017). This substantiated the increased susceptibility of the mutant strain to antibiotics. In contrast, there was no difference observed between the *Mtb* strains to first line drug chemotherapy.

We next assessed changes in susceptibility to vancomycin which directly targets PG cross-linking. Vancomycin irreversibly binds to terminal D-alanyl D-alanine in the penta-peptide sidechain of PG, ultimately leading to the prevention of the synthesis and polymerization of NAM and NAG (Lee, *et al*., 2019). A four-fold differences in the susceptibility profiles was observed for *Msmeg* but these were not statistically significant. However, the difference was quite large and warranted further exploration. For this reason, individually complimented derivatives of the triple mutant containing one of the three *Msmeg* DD-CPase homologues were generated. The MIC_{90} values for vancomycin, RIF and meropenem were determined similarly.

However, when the experiments were repeated, a discrepancy between the MIC_{90} values obtained for the triple mutant and wild type strains was observed from this set of data. There was a two-fold increase in the RIF and meropenem MIC_{90} values and there was a five-fold decrease in the vancomycin MIC_{90} value. In order to troubleshoot this observation, we referred to the literature. Typically, the MIC_{90} values for rifampicin, vancomycin and meropenem against mycobacterial strains range between 8-25 µg/ml and 5-8 µg/ml and 4-8 µg/ml, respectively. Therefore, the first set of experiments was correct and suggest that the discrepancy could have been due to an error in the preparation of the antibiotics

Despite not detecting any significant changes in the antibiotic susceptibility profiles, we were curious to determine whether PG biosynthesis was affected. In order to explore this, we used a fluorescent vancomycin to serve as a proxy for newly synthesized PG (Plocinski, *et al*., 2013). This experiment was not performed in *Mtb* as there was no change in the vancomycin MIC_{90} value. There were no changes in the staining pattern between the different *Msmeg* strains. Staining was primarily observed at one pole (monopoloar) and could be explained by the presence of *dacB*. When *dacB* was repressed with tetracycline and stained with BODIPY-Vancomycin there was a decrease in bipolar staining and an increase in monopolar staining in comparison to wild type (Ealand, *et al*., 2019). About 21% of the cells in the triple mutant strain displayed bulging and this phenotype was completely absent from the wild type strain. In order to ascribe the bulging phenotype to one of the DD-Cpase homologues in *Msmeg*, the complimented derivatives were then assessed following staining with fluorescent vancomycin under similar conditions. The bulging phenotype was seen in the complement homologues primarily in Δ1661Δ2432Δ2433::1661 (about 18% of cells displayed bulging). It can be concluded that this phenotype was not a result of the BODIPY-Vancomycin stain. The swollen regions of these cells were predominantly at the polar regions, which was associated with distinct vancomycin staining. This was to be expected as mycobacteria extend from the poles (Joyce, *et al*., 2012, Odermatt, *et al*., 2020, Hett & Rubin, 2008). This bulging phenotype was not unique to our study. When *PonA1* was overexpressed in *Msmeg* a bulging phenotype was observed primarily at the poles (Kieser, *et al*., 2015). This phenotype remained when an inactive form of *PonA1* was overexpressed. This data suggested that *PonA1* promotes pole elongation in mycobacteria and interacts with other factors to achieve this (Kieser, *et al*., 2015). In a study conducted by Plocinski, *et al* (2013), *CwsA* (a small membrane protein involved in cell wall synthesis) was overexpressed. *CwsA* has been previously shown to interact with *CrgA* and *Wag1* to ensure optimal septal and polar PG synthesis as well as co-ordination with FtsZ-

catalysed cell division. *CwsA* is required for regulated cell wall synthesis and maintenance of cell shape and likely interacts with and/or regulates other cell wall enzymes including PBPs (Plocinski, *et al*., 2013). It is possible that the DD-Cpases in *Msme*g could possibly be interacting and/or regulating other cell wall remodeling enzymes in a similar way to *PonA1* and the *CwsA-CrgA-Wag1* interaction complex but this requires further investigation.

We next sought to determine the MIC_{90} value of Augmentin for *Mtb* as this value was to be used when exposing our transposon mutagenesis library to Augmentin. As with other experiments this was conducted in *Msmeg* as well. No significant differences in the MIC_{90} of Augmentin between the mutant and wild type strains in *Msmeg* and *Mtb* were observed in our study However, DD-Cpases in *Mtb* have previously been shown to have altered expression levels in response to Augmentin (Mishra, *et al*., 2017). Therefore, we sought to investigate potential defects in the cell wall due to altered PG biosynthesis and/or processing following deletion of DD-Cpase genes that were not possible to identify using the micro-broth dilution assays. To do this, we used an FDAA probe (i.e., TADA) as a proxy for nascent PG in the cell wall. TADA is a monopeptide FDAA that incorporates into the D-amino acid backbone of bacteria and is representative of remodeled PG (Kuru, *et al*., 2015). Following the staining, under standard laboratory conditions and exposure to Augmentin, of all mycobacterial strains tested in this study staining was observed to be monopolar, bipolar, septal, monopolar, and septal, bipolar, and septal as well as whole cell. There was no significant difference between the staining patterns observed between the wild type and mutant strains of both mycobacterial species. However, staining was primarily observed at one pole (monopolar) in *Msmeg* and a similar ratio of monopolar and bipolar in *Mtb*. This suggested that combinatorial deletion of DD-CPase genes had no significant effect on PG remodeling or uptake of the probe. There is a dipeptide probe (AlkDada) available that is incorporated into nascent PG (that is un-crosslinked) and is representative of newly synthesized PG (Siegrist, *et al*., 2013; Papadupoulos, *et al*., 2021). It would have been useful to use this probe to create a full picture of the biosynthesis and remodeling of PG in these mycobacterial mutant strains, but it was not available in the laboratory and due to time constraints could not be ordered.

Despite the lack of observable difference in staining patterns, cell lengths appeared to be affected following deletion of DD-Cpases in *Mtb*. The wild type strain (H37Rv) was significantly longer than Δ*dacB1*Δ*dacB2*, which suggested a possible defect in growth or polar extension rates. In contrast, no differences in cell length were observed between the wild type

and triple mutant strains in *Msmeg*. Our polar extension phenotype observed in the *Mtb* mutant strain was supported in the literature because it has previously been demonstrated in other bacterial species that LMW PBPs may be involved in other cellular processes and the regulation of other cell wall enzymes (Hett & Rubin, 2008). In other bacterial species such as *E. coli*, a stable complex formed between recombinant forms of Slt70 (a transglycosylase), PBP3 (a transpeptidase) and PBP 7/8 (a DD-endopeptidase) that was able to synergistically hydrolyze PG (Hett & Rubin, 2008; Romeis & Holtje, 1994). Furthermore, a previous unpublished MSc study from our lab (P. Mashilo, 2018), showed that the *Msmeg* homologues of FtsI (PBP3) and *PonA1* were able to bind to the hydrolase domain of MSMEG_2433 and MSMEG_6113 (*dacB*), which are homologues of *dacb1* and *dacB2* in *Mtb*. FtsI forms part of a multiprotein interaction complex (FtsI-FtsW-FtsZ) thought to regulate the initiation of septation (Datta, *et al*., 2006). *PonA1* is a HMW PBP and is essential for growth in *Mtb* via various cellular processes including polar growth and maintenance of cell shape and length (Kieser, *et al*., 2015).

To identify genes that become conditionally essential in a DD-Cpase mutant background exposed to Augmentin we sought to create a transposon mutagenesis library in *Mtb*. The øMycoMarT7 mycobacteriophage has been used successfully to identify essential genes in mycobacteria (Sassetti, *et al*., 2001; Sassetti & Rubin, 2003; Griffin, *et al*., 2011; Kieser, *et al*., 2015; Zhang, *et al*., 2020). In this study we attempted to identify conditionally essential genes in a DD-Cpase mutant background exposed to Augmentin. Despite trying various optimization approaches to improve the genome coverage in the library - including changes to incubation time of øMycoMarT7 stock with *Mtb* wild type and mutant strains, pre-warming reagents and the amount of mycobacterial phage stock added to cell cultures - it remained consistently low CFU/ml (less than a CFU/ml of ~10^5). This indicated a low frequency of insertions into the genome. Adequate genome coverage is vital as genes with a lack of insertions will be deemed essential under the experimental conditions tested. Therefore, poor coverage could lead to ambiguity in gene essentiality.

The protocol initially used was developed by Griffin, *et al*. (2011) and Sassetti, *et al*. (2001). A newer protocol developed by Majumdar, *et al*. (2017) was also used to improve genome coverage in the library. The main difference between the two protocols was a change in the incubation period with the mycobacterial phage stock. Griffin, *et al*. (2011) incubated for three hours, whereas Majumdar, *et al*. (2017) incubated overnight and eliminated a freezing step

before plating to allow for enhanced recovery. Both methods were extensively tested in *Msmeg* before being applied in *Mtb*. Overall, both approaches failed to produce adequate gene coverage and the reason for this remains unclear. A possible causation of this is the mycobacteriophage stock we received may have had a reduced ability to insert transposons in *Mtb*, potentially the result of numerous passages. Therefore, we sought to identify a novel mycobacterial phage whose genome could be modified to include the *Himar5* gene, which has been shown to have an increased insertion rate compared to *Himar1*, potentially producing libraries with a higher transposon coverage and an increased specificity in identifying essential genes. It has been proven in the literature that a transposon mutagenesis library of a higher coverage leads to increased specificity in the identification of essential genes. In a study conducted by Patil, *et al*. (2021) they were able to produce transposon mutagenesis libraries that ranged from 67.1% to 69.6% genome coverage, which was two percent higher than any other transposon mutagenesis library previously reported. This allowed for the essentiality of 13 new coding sequences to be determined as well as 26 RNAs (Patil, *et al*., 2021).

In this study, approximately 150 damp soil samples were purified and tested for mycobacterial phage activity. Damp soil is the ideal environment for mycobacterial phages as established by various other studies (Miller, *et al*., 2019, Ali & Kotturi, 2018, Fullner & Hatfull, 1997). From these samples, a novel mycobacterial phage, named øIPJ3107, was identified. The protocols used to isolate this mycobacterial phage have been previously established. Briefly, *Msmeg* (strain mc^2155 used) was used as a host to propagate the mycobacteriophage (Bajpai, *et al*., 2018). Using this method, Bajpai *et al*. (2018) were able to identify 17 mycobacterial phages, which is evidence of the methods ability to successfully isolate mycobacterial phages.

The lytic activity of øIPJ3107 was tested by infecting two different mycobacterial species via plaque formation, which suggested that it was able to infect both *Msmeg* and *Mtb*. Relative to the original mycobacteriophage used in this study (i.e., øMycoMarT7), øIPJ3107 produced larger plaques which suggests that it is more virulent. A comparison between the temperature sensitivity of øMycoMarT7 and øIPJ3107 was conducted at 30°C, 37°C and 42°C. As expected øMycoMarT7 only formed plaques at 30°C (Sassetti, *et al*., 2001). Interestingly, øIPJ3107 was able to form plaques up to 42°C. This shows that it is quite robust. In addition, its ability to form plaques at these various temperatures will aid in making this mycobacteriophage temperature sensitive. The method used to achieve this is discussed in section 8.3 (Future studies). The ability to successfully extract øIPJ3107 gDNA using the Wizard DNA Extraction

kit indicates that it has dsDNA. There are three annotated families of bacteriophages, namely: *Siphoviridae, Myoviridae* and *Podoviridae* (Hatfull, 2018). Mycobacteriophages have been found to be only *Siphoviridae* and *Myoviridae*. *Siphoviridae* family is characterized by long non-contractile tails, while phages belonging to the *Myoviridae* family have short contractile tails (Hatfull, 2018). The TEM imaging revealed that øIPJ3107 is 58.17 nm in diameter and 119.20 nm in length which is indicative of it belonging to the short-tailed *Siphoviridae* family.

The next step was to sequence the genome of øIPJ3107 using PacBio® HiFi. The quality of the sequencing data was assessed using FastQC and deemed to be of a high quality. The genome was annotated by Inqaba Biotech and its quality confrmed by Quast. Mycobacteriophages are placed into clusters based on genome similarity and the location of genes in their DNA (Pope, *et al*., 2015). A Kraken2 BLAST search revealed that øIPJ3107 shares sequence similarity with multiple other identified mycobacterial phage species that all belonged to sub-cluster A1 (except for one). This means that øIPJ3107 very likely belongs to sub-cluster A1. The genome of sub-cluster A1 mycobacterial phages encodes a lysis system that is typically located upstream of the virion structural genes (Hatfull, 2018). This was the case for øIPJ3107 which encoded an LysinA (an endolysin) and Lysin B (serine-esterase). LysinA is believed to play a role in the regulation of lysis, while LysinB encodes for an esterase which will cleave the mycolic acid layer of the cell wall (promoting efficient lysis) (Hatfull, 2018). These proteins had similarity to those found in mycobacteriophages øtTrouble and øWheeler, both of which belong to sub-cluster A1.

Interestingly, most mycobacterial phages belonging to sub-cluster A1 are not able to infect *Mtb* and mainly mycobacterial phages that have this ability are mainly found in sub-cluster A2, A3 and K (Hatfull, 2018). This could potentially explain the similarities found in the genomes of øIPJ3107 and øTM4. øTM4 is a dsDNA-tailed mycobacterial phage that belongs to cluster K (Ford, et al., 1998). øTM4 is widely used as a mycobacterial shuttle phasmid that encodes proteins with similarity to haloperoxidases, glutaredoxins and the WhiB family of transcriptional regulators (Ford, *et al*., 1998). øIPJ3107 possesses a protein that shares is of sequence similarity with the WhiB family. This is of particular interest to this study as WhiB4 was found to play a role in antibiotic tolerance through the regulation of various genes including the DD-Cpases in *Mtb* (Mishra, *et al*., 2017).

5. Conclusion, limitations, and future studies

5.1 Conclusion

DD-Cpases are not essential for *in-vitro* growth but there is a considerable amount of knowledge to be gained about their function in response to antibiotic exposure and remodeling the PG layer of the mycobacterial cell wall. The results obtained from this study are suggestive of DD-Cpases having a role in ß-lactamase activity and possibly interacting with other cell wall remodeling enzymes to achieve this. However, there is no concreate evidence for this and further research will be required. In summary, our research showed an increased susceptibility of the wild type and triple mutant strains in *Msmeg* to RIF. The literature suggests a weakening of the mycobacterial cell wall due to the decrease in DD-Cpases available for remodeling as a possible cause of this. However, there was no significant difference in the MIC_{90} values between the wild type and mutant strains in both mycobacterial species. A recent study suggests that LMW PBPs with DD-Cpase activity in *Mtb* have inherent resistance to ß-lactam antibiotics. In addition to this, cells displaying polar bulging were noted when the wild type, triple mutant and complemented derivatives of *Msmeg* were probed with fluorescent Vancomycin. The bulging is suggestive of a cell wall synthesis and cell division defect as vancomycin binds to the terminal D-alanine in the pentapeptide chain (a substrate for DD-Cpases) A significant difference in cell length was observed in the *Mtb* strains. In a previous study conducted in our laboratory it was observed that homologues of the DD-Cpases in *Msmeg* bind to enzymes involved in cell division and growth. It is possible that a similar interaction could be occurring in *Mtb*, which is resulting in unregulated growth and division, due to the decrease in DD-Cpase activity in the mutant strains. This explains the decrease in cell length observed between the wild type and double mutant strains. Phenotypic and genomic characterization of our novel mycobacterial phage øIPJ3107 revealed that it likely belongs to the *Siphoviridae* family and is classified under sub-cluster A1. øIPJ3107 has the typical genome of mycobacterial phages classified in this sub-cluster and has the ability to infect *Mtb*. øIPJ3107 also forms large plaques (indicative of a high virulence) at varying temperatures (i.e., it is quite robust), which makes it an ideal candidate for use as a molecular tool.

5.2 Limitations of this study

A significant limitation of this study was the inability to produce a transposon mutagenesis library with adequate genome coverage to proceed with our intended project objectives. Due to this, we were unable to identify conditionally essential genes in the DD-Cpase mutant background for *Mtb* or to test the hypothesis of this study. We could have requested a new mycobacterial phage stock from the original author, but due to time constraints it would not have arrived in time. Nevertheless, we sought to address this limitation by identifying a novel mycobacteriophage from soil, in order to eventually manipulate it as a molecular tool for library construction. The ultimate goal is to introduce the *Himar5* mariner gene into the genome of this novel phage as well as make it temperature sensitive to create transposon mutagenesis libraries of a higher coverage. We also observed discordant results between the 'equivalent' strains in *Msmeg* and *Mtb*, indicating that, although, *Msmeg* can give some insight into the roles of the genes of *Mtb*, they are different organisms and *Msmeg* may not always serve as an accurate model for *Mtb*.

5.3 Future studies

Future work will include using a mutagenesis approach to create a temperature sensitivity in øIPJ3107. This is important in order to be able to create a mycobacterial phage stock at 30ºC (form plaques) and create a transposon mutagenesis library at 37ºC (form colonies). A standard protocol will be utilized to mutagenize øIPJ3107 stocks (10^9PFU/ml) with hydroxylamine under conditions that will yield 0.1% viable surviving phages (Bardarov, *et al*., 1997). These mycobacteriophages will then be plated on a lawn of stationary phase *Msmeg* mc^2155 (OD_{600} of 2.5) and incubated at 30°C (to ensure that plaques will be able to form at this temperature). These phages will be harvested, and the process repeated at 42°C (to ensure that it is able to grow at higher temperatures). The clones that grow will then be tested for plaque formation at 30°C, 37°C and 42°C and those that only grow at 30°C and 37°C will be selected for. Thereafter, the *Himar5* mariner gene will be introduced. The *Himar5* gene will be provided by GenScript. Standard protocols are available for the cloning and transformation methods needed in order to achieve this (Sambrook, *et al*., 1989; Rubin, *et al*., 1999). The next step would then be to test the infectivity of øIPJ3107 in *Msmeg*, by generating a transposon mutagenesis library in *Msmeg* to ensure it is able to generate a transposon mutagenesis library of 10^5 CFU/ml or higher.

In addition to what needs to be performed to prepare øIPJ3107 as a molecular tool for the creation of transposon mutagenesis libraries, a more in-depth annotation into the genome of øIPJ3107 is required. This work will involve formal phylogenetic and taxonomic classification of this novel mycobacterialphage to confirm that it is a member of the *Siphoviridae* family and thus classified under sub-cluster A1. This hypothesis is currently being addressed in a manuscript preparation preliminarily entitled “Genomic and phenotypic analysis of the novel mycobacteriophage øIPJ3107”.

6. References

Akerley, B. J. *et al*., 2002. A genome-scale analysis for identification of genes required for growth or survival of *Haemophilus influenza*. *PNAS*, 99(2), pp. 966-971.

Alam, G.-H.*et al*., 2018. Peptidoglycan precursor synthesis along the sidewall of pole-growing mycobacteria. *eLIFE*, Volume 7, p. e37243.

Aldridge, B. B. *et al*., 2012. Asymmetry and Aging of Mycobacterial Cells Lead to Variable Growth and Antibiotic Susceptibility. *Science*, Volume 335, pp. 100-104.

Ali, A.K. and Kotturi, H., 2018. Isolation of Four Mycobacteriophages from Oklahoma Soil and Testing Their Infectivity Against Mycobacterium abscessus. In Proceedings of the Oklahoma Academy of Science, Volume 98, pp. 112-117.

Bajpai, U. *et al*., 2018. Isolation and characterization of bacteriophages from India, with lytic activity against *Mycobacterium tuberculosis*. *Canadian Journal of Microbiology*, Volume 64, pp. 483-491.

Bardarov, S. *et al*., 1997. Conditionally replicating mycobacteriophages: A system for transposon delivery to *Mycobacterium tuberculosis*. *Microbiology*, Volume 94, pp. 10961-10966.

Basta, L. A. B. *et al*., 2015. Loss of a Functionally and Structurally Distinct ld-Transpeptidase, LdtMt5; Compromises Cell Wall Integrity in *Mycobacterium tuberculosis*. *Journal of Biological Chemistry*, 290(42), pp. 25670-25685.

Botella, H. *et al*., 2017. Distinct Spatiotemporal Dynamics of Peptidoglycan Synthesis between *Mycobacterium smegmatis* and *Mycobacterium tuberculosis*. *Microbiology*, 8(5), pp. e01183-17.

Bourai, N., Jacobs, W. R. J. & Narayanan, S., 2012. Deletion and overexpression studies on DacB2, a putative low molecular mass penicillin binding protein from *Mycobacterium tuberculosis* H37Rv. *Microbial Pathogenesis*, 52(2), pp. 109-116.

Brown, J., Pirrung, M. & McCue, L. A., 2017. FQC Dashboard: integrates FastQC results into a web-based, interactive, and extensible FastQ quality control tool. *Bioinformatics*, 33(19), pp. 3137-3139.

Caminero, J. A. *et al*., 2010. Best drug treatment for multidrug-resistant and extensively drug-resistant tuberculosis. *The Lancet*, Volume 10, pp. 621-629.

Chamber, H. F. *et al*., 1995. Can Penicillins and other ß-Lactam Antibiotics Be Used To Treat Tuberculosis? *Antimicrobial Agents and Chemotherapy*, 39(12), pp. 2620-2624.

Cohen, A., Mathiasen, V. D., Schon, T. & Wesje, C., 2019. The global prevalence of latent tuberculosis: a systematic review and meta-analysis. *European Respiratory Journal*, 53 (3), pp. 1-14.

Cole, S. *et al*., 1998. Deciphering the biology of *Mycobacterium tuberculosis* from the complete genome sequence. *Nature*, Volume 393, pp. 537-544.

Crick, D. C., Mahapatra, S. & Brennan, P. J., 2011. Biosynthesis of the arabinogalactan-peptidoglycan complex of *Mycobacterium tuberculosis*. *Glycobiology*, 11(9), pp. 107-118.

Datta, P. *et al*., 2006. Interaction between FtsW and penicillin-binding protein 3 (PBP3) directs PBP3 to mid-cell, controls cell septation and mediates the formation of a trimeric complex involving FtsZ, FtsW and PBP3 in mycobacteria. *Molecular Microbiology*, 62(6), pp. 1655-1673.

DeFalun, M. F. & Paul, J. H., 1996. Hoeschst 33258* staining of DNA in agarose gel electrophoresis. *Journal of Microbiological Methods*, Volume 5, pp. 265-270.

Ealand, C. S., Asmal, R., Mashigo, L. C. L. & Kana, B. D., 2019. Characterization of putative DD-carboxypeptidase-encoding genes in *Mycobacterium smegmatis*. *Scientific Reports*, 9(5194), pp. 1-11.

Egan, A. J. F., Errington, J. & Vollmer, W., 2020. Regulation of peptidoglycan synthesis and remodelling. *Nature Reviews*, Volume 18, pp. 446-460.

Ford, M. E., Stenstrom, C., Hendrix, R. W. & Hatfull, G. F., 1998. Mycobacteriophage TM4: genome, structure and gene expression. *Tubercle and Lung Disease*, 79(2), pp. 63-73.

Frirdich, E. and Gaynor, E.C., 2013. Peptidoglycan hydrolases, bacterial shape, and pathogenesis. Current opinion in microbiology, 16(6), pp.767-778.

Garcia-Heredia, A. et al., 2018. Peptidoglycan precursor synthesis along the sidewall of pole-growing mycobacteria. Elife, 7, p.e37243.

Geissendorfer, M. & Hillen, W., 1990. Regulated expression of heterologous genes in *Bacillus subtilis* using the Tn10 encoded tet regulatory elements. *Applied Microbiology and Biotechnology*, Volume 33, pp. 657-663.

Ghodh, A., Chowdhury, C. & Nelson, D. E., 2008. Physiological functions of D-alanine carboxypeptidases in *Escherichia coli*. *Trends in Microbiology*, 16(7), pp. 309-317.

Griffin, J. E. *et al*., 2011. High-Resolution Phenotypic Profiling Defines Genes Essential for Mycobacterial Growth and Cholesterol Catabolism. *PLoS Pathogens*, 7(9), p. e1002251.

Gupta, R. *et al*., 2010. The Mycobacterium tuberculosis protein LdtM2 is a non-classical transpeptidase required for virulence and resistant to amoxicillin. Nature Medicine, Volume 16, pp. 466-469.

Gurevich, A., Saveliev, V., Vyahhi, N. & Tesler, G., 2013. QUAST: Quality assessment tool for genome assemblies. *Bioinformatics*, 29(6), pp. 1072-1075.
Guzman, L.-M., Belin, D., Carson, M. J. & Beckwith, J., 1995. Tight Regulation, Modulation and High-Level Expression by Vectors Containing the Arabinose PBAD promoter. *Journal of Bacteriology*, 177(14), pp. 4121-4130.
Hatfull, G. F., 2018. Mycobacteriophages. *Microbiology*, 6(5), pp. doi:10.1128/microbiolspec.GPP3-0026-2018.
Henderson, T. A., Templin, M. & Young, K. D., 1995. Identification and Cloning of the Gene Encoding Penicillin-Binding Protein 7 Escherichia coli. *Journal of Bacteriology*, 177(8), pp. 2074-2079.
Hett, E. C., Chao, M. C. & Steyn, A. J., 2007. A partner for the resuscitation-promoting factors of Mycobacterium tuberculosis. *Molecular Microbiology*, 66(3), pp. 658-668.
Hett, E. C. & Rubin, E. J., 2008. Bacterial Growth and Cell Division: a Mycobacterial Perspective. *Microbiology and Molecular Biology Reviews*, 72(1), pp. 126-156.
Hugonnet, J.-E. & Blanchard, J. S., 2007. Irreversible Inhibition of the Mycobacterium tuberculosis ß-lactamase by Clavulanate. *Biochemistry*, 46(43), pp. 11998-12004.
Ji, Y. *et al*., 2001. Identification of Critical Staphylococcal Genes Using Conditional Phenotypes Generated by Antisense RNA. *Science*, Volume 293, pp. 2266-2269.
Johnson, M. *et al*., 2008. NCBI BLAST: a better web interface. *Nucleic Acids Research*, Volume 36, pp. W5-W9.
Joshi, M. & Deshpande, J., 2010. Polymerase chain reaction: methods, principles and application. *International Journal of Biomedical Research*, 2(1), pp. 81-97.
Joyce, G. *et al*., 2012. Cell Division Site Placement and Assymetric Growth in Mycobacteria. *PLoS ONE*, 7(9), p. e44582.
Kieser, K. J. *et al*., 2015. Phosphorylation of the Peptidoglycan Synthase PonA1 Governs the Rate of Polar Elongation in Mycobacteria. *PLoS*, 11(6), p. e1005010.
Kieser, K. J. & Rubin, E. J., 2014. How sisters grow apart: mycobacterial growth and division. *Nature Reviews*, Volume 12, pp. 550-562.
Kong, K.-F., Schneper, L. & Mathee, K., 2010. Beta-lactam antibiotics: from antibiosis to resistance and bacteriology. *Apmis*, 118(1), pp. 1-36.
Kumar, G. *et al*., 2022. Penicillin Binding Proteins and ß-Lactamases of Mycobacterium tubeculosis: Reexamination of the Historical Paradigm. *mSphere*, 7(1), pp. e00039-22.

Kuru, E. *et al*., 2015. Synthesis of fluorescent D-amino acids (FDAAs) and their use for probing peptidoglycan synthesis and bacterial growth in situ. *Nature Protocol*, 10(1), pp. 33-52.

Lee, T., Pang, S., Abraham, S. & Coombs, G. W., 2019. Antimicrobial-resistant CC17 Enterococcus faecium: The past, the present and the future. *Journal of Global Antimicrobial Resistance*, Volume 16, pp. 36-47.

Machowski, E. E., Senzani, S., Ealand, C. & Kana, B. D., 2014. Comparative genomics for mycobacterial peptidoglycan remodelling enzymes reveals extensive genetic multiplicity. *BMC Microbiology*, 14(74), pp. 1-12.

MacNeil, A., Glaziou, P., Sismanidis, C., Maloney, S. and Floyd, K., 2019. Global epidemiology of tuberculosis and progress toward achieving global targets—2017. Morbidity and Mortality Weekly Report, 68(11), p.263.

Maitra, A. *et al*., 2019. Cell wall peptidoglycan in *Mycobacterium tuberculosis*: An Achilles' heel for the TB-causing pathogen. *FEMS Microbiology Reviews*, 43(5), pp. 548-575.

Mallick, S. *et al*., 2019. Role of *Escherichia coli* endopeptidases and DD-carboxypeptidases in infection and regulation of innate immune response. *Microbes and Infection*, 21(10), pp. 464-474.

Majumdar, G., Mbau, R., Singh, V., Warner, D.F., Dragset, M.S. and Mukherjee, R., 2017. Genome-wide transposon mutagenesis in Mycobacterium tuberculosis and Mycobacterium smegmatis. In In vitro mutagenesis (pp. 321-335). Humana Press, New York, NY.

Martinelli, D. J. & Pavelka, M. S. J., 2016. The RipA and RipB Peptidoglycan Endopeptidases are Individual Non-essential to *Mycobacterium smegmatis*. *Journal of Bacteriology*, 198(9), pp. 1464-1475.

Maurice, C. F., Bouvier, R. d. W. & Bouvier, T., 2013. Linking the lytic and lysogenic bacteriophage cycles to environment conditions, host physiology and their variability in coastal lagoons. *Environmental microbiology*, 15(9), pp. 2463-2475.

McDonough, K., Krees, Y. & Bloom, B. R., 1993. Pathogenesis of Tuberculosis: Interaction of *Mycobacterium tuberculosis* with Macrophages. *Infection and Immunity*, 61(7), pp. 2763-2773.

Meberg, B. M., Paulson, A. L., Priyadarshini, R. & Young, K. D., 2004. Endopeptidase Penicillin-Binding Protein 4 and 7 Play Auxiliary Roles in Determining Uniform Morphology of *Escherichia coli*. *Journal of Bacteriology*, 186 (24), pp. 8326-8336.

Meniche, X. *et al*., 2014. Subpolar addition of new cell wall is directed by DivIVA in mycobacteria. *PNAS*, 111(31), pp. E3243-E3251.

Mishra, S. *et al*., 2017. Efficacy of B-lactam/B-lactamase inhibitor combination is linked to WhiB4-mediated changes in redox physiology of Mycobacterium tuberculosis. *eLIFE*, Volume 6, p. E25624.

Mitchison, D. A., 1985. The action of anti-tuberculosis drugs in short-course chemotherapy. *Tubercle*, 66(3), pp. 219-225.

Murphy, S. G. *et al*., 2019. Endopeptidase Regulation as a Novel Function of the Zur-Dependent Zinc Starvation Response. *Microbiology*, 10(1), pp. e02620-18.

Nakamura, H. & Funahashi, J., 2013. Electroporation: Past, present and future. *Development, Growth and Differentiation*, Volume 55, pp. 15-19.

Nelson, D. E. & Young, K. D., 2000. Penicillin Binding Protein 5 Affects Cell Diameter, Countour and Morphology of Escherichia coli. *Journal of Bacteriology*, 182(6), pp. 1714-1721.

Odermatt, P.D. et al., 2020. Overlapping and essential roles for molecular and mechanical mechanisms in mycobacterial cell division. Nature physics, 16(1), pp.57-62.

Onyebujoh, P. *et al*., 2005. Treatment of tuberculosis: present status and future prospects. *Bulletin of the World Health Organization*, Volume 83, pp. 857-865.

Pandey, S. D. *et al*., 2020. MSMEG_2432 of *Mycobacterium smegmatis* mc2155 function enzyme that exhibits DD-carboxypeptidase and ß-lactam activities. *Microbiology*, Volume 166, pp. 546-553.

Patil, S., Palande, A., Lodhiya' Pandit, A. & Mukherjee, 2021. Redefining genetic essentiality in Mycobacterium tuberculosis. *Gene*, Volume 765, p. 145091.

Patru, M.-M. & Pavelka, M. S. J., 2010. A role for the Class A Penicillin-Binding Protein PonA2 in the survival of *Mycobacterium smegmatis*. *Journal of Bacteriology*, 192(12), pp. 3043-3054.

Pedersen, L. B., Murray, T., Popham, D. L. & Peter, S., 1998. Characterization of dacC, which encodes a new Low-Molecular-Weight Penicillin-Binding Protein. *Journal of Bacteriology*, 180(18), pp. 4967-4973.

Phillips, J. A. & Ernst, J. D., 2012. Tuberculosis Pathogenesis and Immunity. Annual Review of Pathology: *Mechanisms of Disease*, Volume 7, pp. 353-384.

Piddock, L. J. V., Williams, K. J. & Ricci, V., 2000. Accumulation of rifampicin by *Mycobacterium aurum*, *Mycobacterium smegmatis* and *Mycobacterium tuberculosis*. *Journal of Antimicrobial Chemotherapy*, Volume 45, pp. 159-165.

Plocinski, P. *et al*., 2013. *Mycobacterium tuberculosis* CwsA overproduction modulates cell division and cell wall synthesis. *Tuberculosis*, 93(1), pp. s21-s27.

Poham, D. L. & Setlow, P., 1996. Phenotypes of Bacillus subtilis Mutants Lacking Multiple Class A High-Molecular-Weight Penicillin-Binding Proteins. *Journal of Bacteriology*, 178(7), pp. 2079-2085.
Papadopoulos, A.O. et al.., 2021. Characterisation of a putative M23-domain containing protein in Mycobacterium tuberculosis. PloS one, 16(11), p.e0259181.
Pope, W. H. *et al*., 2015. Whole genome comparison of a large collection of mycobacteriophages reveals a continuum of phage genetic diversity. *eLIFE*, p. e06416.
Raghavendra, T., Patil, S. & Mukherjee, R., 2018. Peptidoglycan in Mycobacteria: Chemistry, biology and intervention. *Glyconjugate*, Volume 35, pp. 421-432.
Rampersad, S. N., 2012. Multiple applications of Alamar Blue as an indicator of metabolic function and cellular health in cell viability asays. *Sensors*, 12(9), pp. 12347-12360.
Rhoads, A. & Au, K. F., 2015. PacBio Sequencing and Its Applications. *Genomics Proteomics Bioinformatics*, Volume 13, pp. 278-289.
Romeis, T. & Holtje, J.-V., 1994. Penicillin-binding protein 7/8 of Escherichia coli is a DD-endopeptidase. *European Journal of Biochemistry*, Volume 224, pp. 597-604.
Rubin, E. J. *et al*., 1999. In vivo transposition of mariner-based elements in enteric bacteria and mycobacteria. *PNAS*, Volume 96, pp. 1645-1650.
Sambrook, J., Fritsch, E. & Maniatis, T., 1989. *Molecular Cloning: A laboratory manual*. 2nd ed. New York: Cold Spring Harbor Lab.
Sassetti, C. M., Boyd, D. H. & Rubin, E. J., 2001. Comprehensive identification of conditionally essential genes in mycobacteria. *PNAS*, 98(22), pp. 12712-12717.
Sassetti, C. M. & Rubin, E. J., 2003. Genetic requirements for mycobacterial survival during infection. *PNAS*, 100(2), pp. 12989-12994.
Sauvage, E. *et al*., 2008. The penicillin-binding proteins: structure and role in peptidoglycan biosynthesis. *FEMS Microbiology Reviews*, 32(2), pp. 234-258.
Seemann, T., 2014. Prokka: rapid prokaryotic genome annotation. *Bioinformatics*, 30(14), pp. 2068-2069.
Senzani, S. *et al*., 2017. An Amidase_3 domain containing N-acetylmuramyl-L-alanine amidase is required for mycobacterial cell division. *Scientific reports*, 7(1140), pp. 1-16.
Schoonmaker, M.K., Bishai, W.R. and Lamichhane, G., 2014. Nonclassical transpeptidases of Mycobacterium tuberculosis alter cell size, morphology, the cytosolic matrix, protein localization, virulence, and resistance to β-lactams. Journal of bacteriology, 196(7), pp.1394-1402.

Sharifzadeh, S., Dempwolff, F., Kearns, D. B. & Carlson, E. E., 2020. Harnessing B-lactam Antibiotics for Illumination of the Activity of Penicillin-Binding Proteins in Bacillus subtilis. *Chemical Biology*, Volume 15, pp. 1242-1251.
Siegrist, S. M. *et al*., 2013. D-Amino Acid Chemical Reporters Reveal Peptidoglycan Dynamics of an Intracellular Pathogen. *ACS chemical biology*, 8(3), pp. 500-505.
Smith, I., 2003. Mycobacterium tuberculosis Pathogenesis and Molecullar Determinants of Virulence. *Clinical Microbiology Reviews*, 3(463-496), p. 16.
Snapper, S., Melton, R., Mustafa, S., Kieser, T., & WR Jr, J., 1990. Isolation and characterization of efficient plasmid transformation mutants of Mycobacterium smegmatis. *Molecular microbiology*, 4(11), 1911-1919.
Somoskovi, A., Parsons, L. M. & Salfinger, M., 2001. The molecular basis of resistance to isoniazid, rifampin and pyrazinamide in Mycobacterium tuberculosis. *Respiratory Research*, 2(3), pp. 164-168.
Sotgiu, G., Goletti, D. & Matteelli, A., 2019. Global tuberculosis prevention: should we start from the beginning? *European Respiratory Journal*, 54(3), pp. 1-4.
Spratt, B. G., 1977. Properties of the Penicillin-Binding Proteins of Escherichia coli K12. *European Journal of Biochemistry*, Volume 72, pp. 341-352.
Sreevatsan, S. *et al*., 1997. Analysis of the oxyR-aphC Region in Isoniazid-Resistant and Susceptible *Mycobacterium tuberculosis* Complex Organisms Recovered from Diseased Humans and Animals in Diverse Localities. *Antimicrobial agents and chemotherapy*, 41(3), pp. 600-606.
Steenken, W., 1935. Lysis of Tubercle Bacilli in Vitro. Proceedings of the Society for Experimental Biology and Medicine, 33(2), pp. 253–255. doi: 10.3181/00379727-33-8330P.
Stone, M. R. L. *et al*., 2018. Fluorescent Antibiotics: New Research Tools to Fight Antibiotic Resistance. *Cell Press Reviews*, 36(5), pp. 523-536.
Tuomanen, E. & Schwartz, J., 1987. Penicillin-Binding Protein 7 and Its Relationship to Lysis of Nongrowing *Escherichia coli*. *Journal of Bacteriology*, 169(11), pp. 4912-4915.
Waxman, D. J. & Strominger, J. L., 1983. Penicillin-Binding Proteins and the mechanism of action of B-lactam antibiotics. *Annual Reviews Biochemistry*, 52(1), pp. 825-869.
WHO, 2021. *Global Tuberculosis Report*. [Online] Available at: https://www.who.int/teams/global-tuberculosis-programme/tb-reports/global-tuberculosis-report-2021

Wilson, W. H., Van Etten, J. L. & Allen, M. J., 2009. The Phycodnaviridae: The Story of How Tiny Giants Rule the World. *Current Topics in Microbiology and Immunity*, Volume 328, pp. 1-42.

Wood, D. E., Lu, J. & Langmead, B., 2019. Improved metagenomic analysis with Kraken2. *Genome Biology*, 20(257), pp. 1-13.

Vollmer, W., Blanot, D. and De Pedro, M.A., 2008. Peptidoglycan structure and architecture. FEMS microbiology reviews, 32(2), pp.149-167.

Zhang, S. *et al.*, 2013. Mutations in panD encoding aspartate decarboxylase are associated with pyrazinamide resistance in *Mycobacterium tuberculosis*. Emerging Microbes and Infections, 2(1), pp. 1-5.